An Analysis of Magnitude Differentiation in Type Ia Supernova

Jake Miller
Mentor: Professor David Cinabro
Wayne State University
Department of Physics and Astronomy

August 31, 2015

Abstract

Milne et al. (2015), hereafter Milne(2015), claims to have observed two distinct sub-groups of Type Ia Supernovas (SNIa). With a diverse sample of 52 SNIa they claim one sub-group is 0.4 mag redder than the other in the ultra-violet (UV) part of the rest frame spectrum at the peak optical brightness of the SNIa light curve. We check this claim with the Sloan Digital Sky Survey Supernova data set (SDSS) as described in Sako et al. (2014). Our preliminary approach here is to measure 16 u-g colors at low redshift and 53 g-r colors at intermediate redshift at optical peak brightness with a sample of securely typed SDSS SNIa light curves. These colors at these red shifts closely correspond to the rest frame U-V color used in Milne(2015). We see no evidence of two SNIa samples in the intermediate redshift g-r color sample, rather seeing a single distribution about 0.2 mag wide.

1 Background

SNIa are extremely important to the study of astronomy. Formed by a white dwarf accreting enough mass to pass the Chandrasekhar limit, these massive explosions briefly outshine their own galaxies, and are among the most energetic phenomena in the universe. Due to the uniform nature of these phenomena, SNIa are useful in determining distances at cosmological scales. This is perhaps their most important trait - their uniformity. However, one paper claims that they are not uniform. A study done by Milne(2015) states that there are in fact two separate groups of SNIa - some that are more "blue" and some that are more "red". The difference manifests itself as two groups in a UV and optical color of about 0.1 mag width, separated by roughly 0.4 mag. These two groups of SNIa also have differing rates, with the redder group being twice as common as the bluer group. The existence of two distinct sub-groups of SNIa would have large implications for astronomy. They are the primary method of measuring distances at cosmological scales and observations of them have led to the discovery and measurement of dark energy. The assumption of SNIa uniformity underlies these studies.

2 Methods

To check the claims of Milne(2015) we use a distinct set of SNIa from the SDSS data. The SDSS does not have the same set of filters as used by Milne thus for a preliminary check we approximate their observations of U-V color in the SNIa rest frame with the SDSS u- and g-filters standing in for U- and V-filters at low redshift and g- and r-filters at intermediate redshifts. The U-filter on the Swift satellite used by Milne(2015) covers the wavelength range of 268-425 nm at full width at half maximum (FWHM) and the Swift V-filter 470-624 nm while the SDSS u-filter covers 320-380 nm, the g-filter 400-535 nm, and the r-filter 540-670 nm. We use a simple formula to determine the proper redshift ranges necessary for our filters to approximate Milne(2015) observations. We take the FWHM wavelengths edges of each filter, and using

$$(\mu_f - \mu s)/\mu s \tag{1}$$

where μf are the SDSS u, g, or r filter we are converting to, and the μs is the Swift U or V filter Milne(2015) uses. We only use the SDSS u- and g- filters to stand in for the Swift U-filter because the data for filters bluer than the g-filter are beyond the redshift limit of 0.4 at which the SDSS no longer detects SNIa. We round up and down to the nearest tenth when determining our redshift ranges. The SDSS u-filter approximates the Swift U-filter in the redshift range of 0¡z¡0.1, labeled "low redshift", while the g-filter does so in the redshift range 0.3¡z¡0.4, labeled "intermediate redshift".

Milne(2015) key observation was in the U-V color and we use the SDSS u-g color at low redshift and the g-r color at intermediate redshift as approximations. We analyze this data with the Supernova Analysis (SNANA) program to access the SNIa light curves, observed filter fluxes versus time, of securely confirmed SNIa. SNANA gives their CID, a unique integer identifier, Modified Julian Date (MJD) in the observer frame, and filter fluxes, photon counts in the filter restricted wavelength ranges. For the low redshift u-g color data we find a small sample of 18 SNe, while our intermediate g-r color data has 63 SNe.

We convert the flux data to magnitudes using

$$Mag = -2.5 \times (\log(FLUX)) + 27.5\ . \tag{2}$$

After finding the magnitudes, we then find the brightest 15 points for each light curve in each filter. We decided upon the top 15 because our relatively simple light curve analysis would often generate obviously incorrect fits when only 5 points were used.

Our light curve magnitude data are analyzed with the gnuplot fitting software. We fit the brightest part of the light-curves to a parabola,

$$f(x) = a(x-d)^2 + m \tag{3}$$

where a is initially 0.0025 and allowed to float; d, the time of peak brightness, is set initially to the average MJD of the 15 observations and is allowed to float; and m, the peak magnitude, is initially set to the average magnitude of the 15 observations and is also allowed to float. This procedure eliminates bias in the fitting. Some example light curve fits are shown in Figure 1, and all are shown in the Appendix.

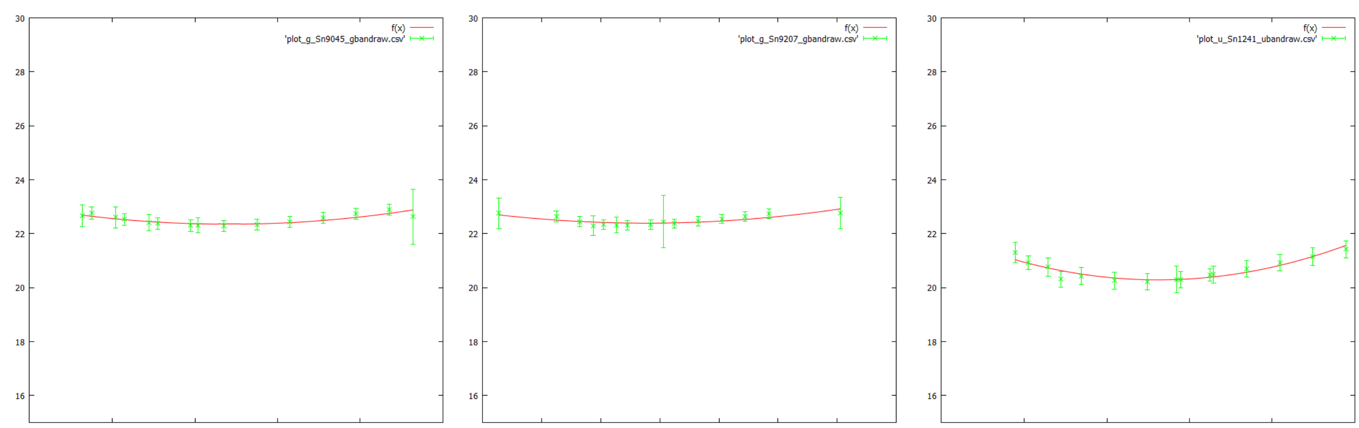

Figure 1: Examples of selected SDSS SNIa light-curves and our fits for the peak magnitude.

We can see that some of the fits are problematic. At this stage our sample size is decreased to 77, as 4 SNIa in the intermediate redshift g-r color sample have fits that give inverted light curves that do not give a peak brightness. These are removed from the data sample. The distributions of the peak u-filter magnitude in the low redshift u-g color sample and the peak g-filter magnitude g-r color sample are shown in Figures 2 and 3 respectively.

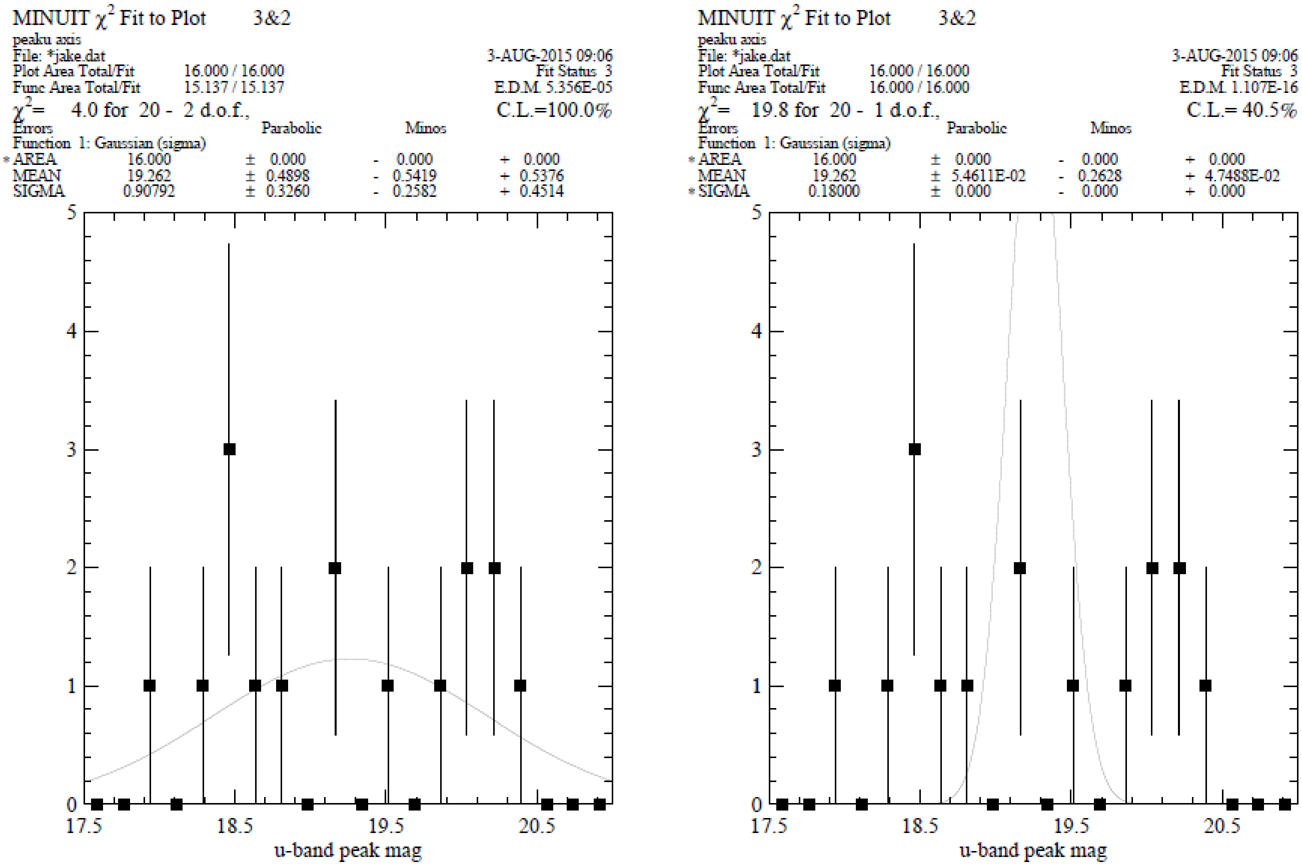

Figure 2: The peak u-filter magnitude distribution in the low redshift u-g color sample.

We already see that the u-g color sample is too small to say anything meaningful about possible sub-samples characterized by their peak brightness in the UV part of spectrum, and see no hint of such a sub-sample in the g-r color sample.

To better compare with Milne(2015) we also compute colors using the SDSS filter set. Milne(2015) found the U-V color at the peak V-band magnitude. To emulate this we find the u-g color at the peak g-filter magnitude at low redshift and g-r color at the peak r-filter magnitude at intermediate redshift. The distribution of these colors can be seen respectively in Figures 4 and 5.

3 Results

The u-g color low redshift sample is simply too small to show the existence of sub-samples. However, the g-r color intermediate redshift samples shows a distribution that is roughly 0.15 mag wide, which directly contradicts Milne(2015)'s claim of two 0.1 mag width distributions with a 0.4 mag width difference. While our results do not support the observation of Milne(2015) this one piece of evidence alone is not enough to conclusively say that Milne(2015) is incorrect. Our methods are very different, but they are suggestive that this deserves further study.

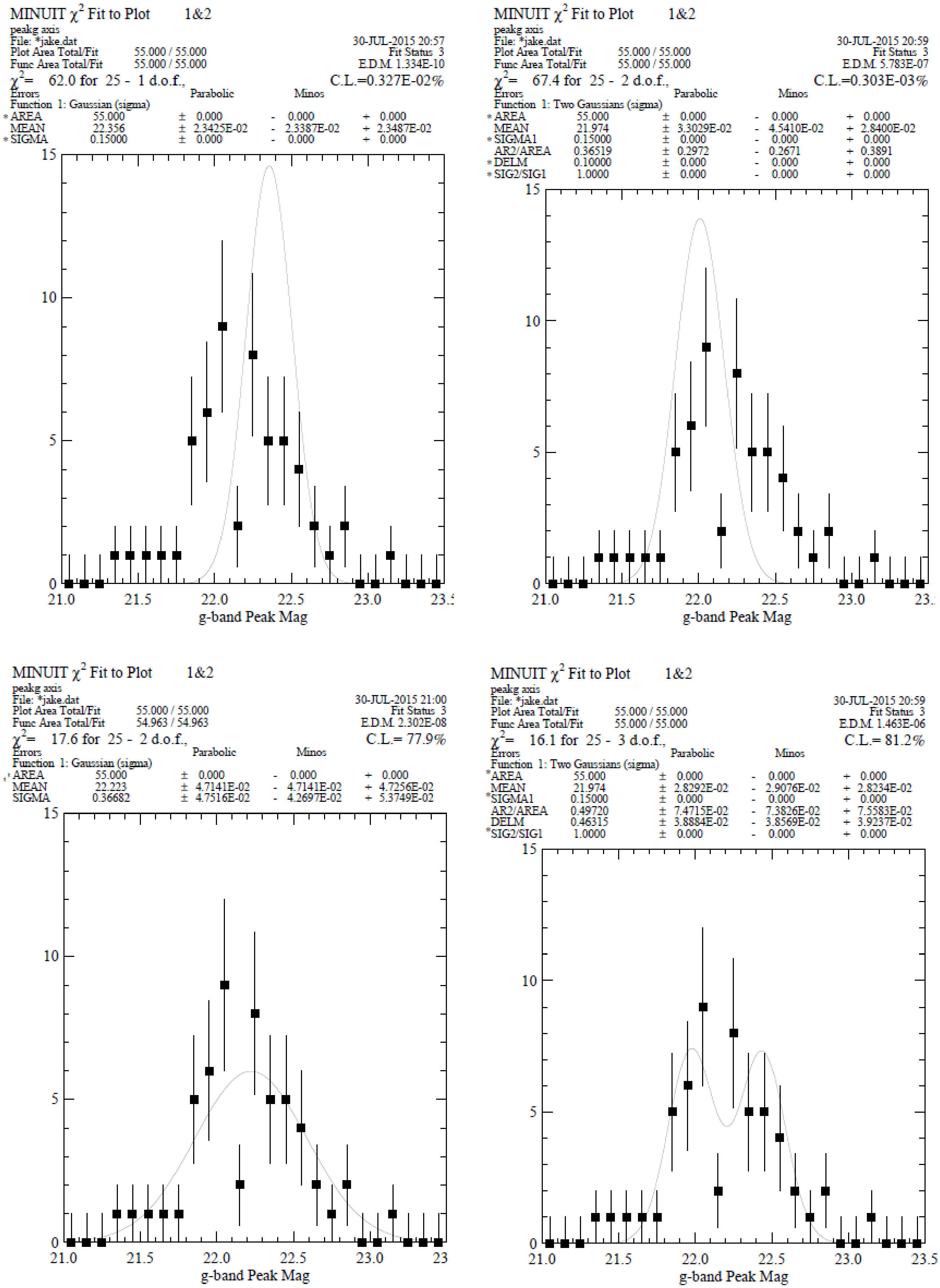

Figure 3: The peak g-filter magnitude distribution in the intermediate redshift g-r color sample. In the upper right the distribution is fit to a single Gaussian with a width fixed at the expected resolution of 0.15 mag; the fit is poor. In the upper left it is fit to two Gaussians with widths fixed to the expected resolution and fits poorly. In the lower right it is fit to a single Gaussian with floating width. In the

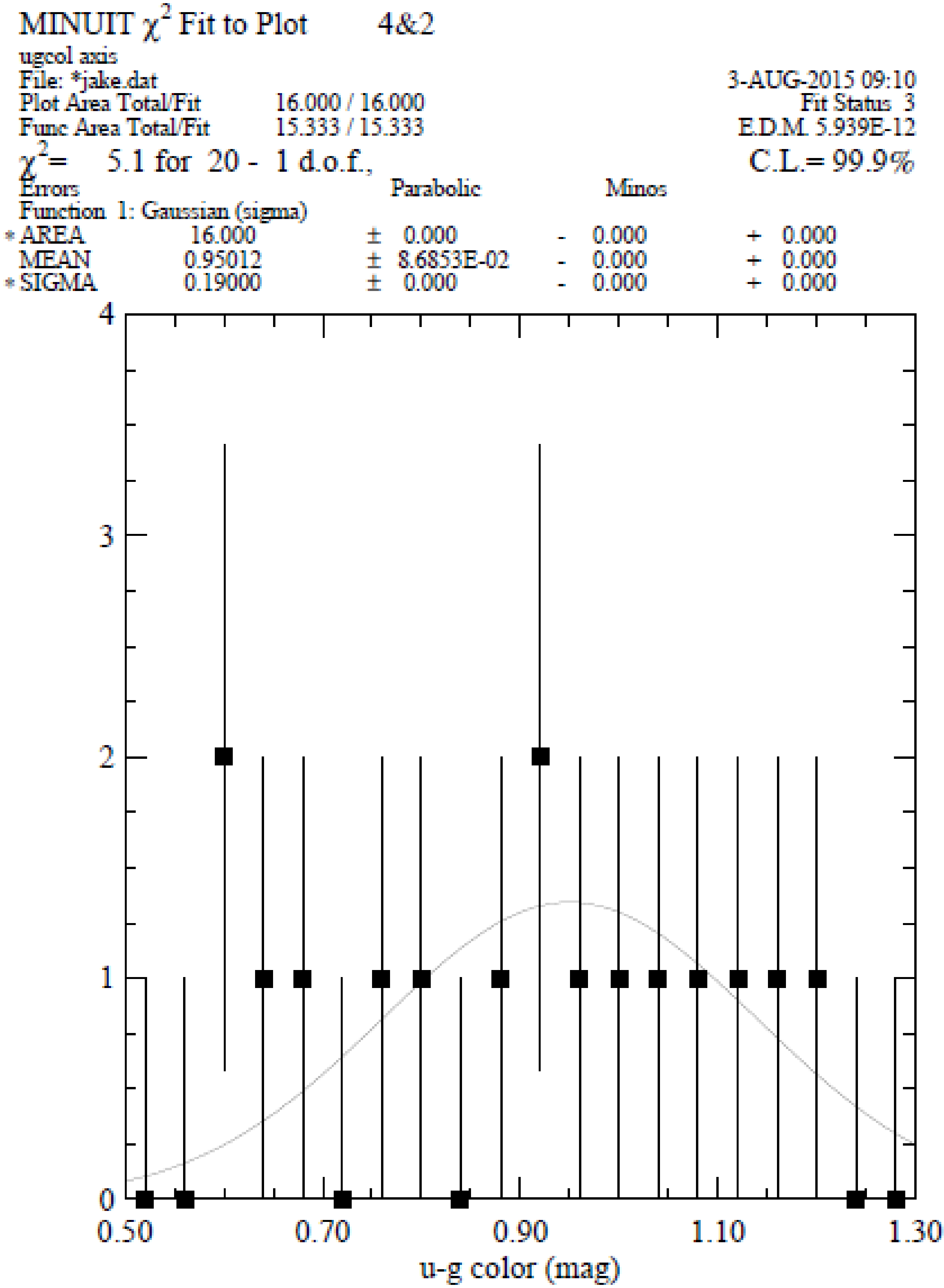

Figure 4: The u-g color for the SDSS u-g color low redshift SNIa sample.

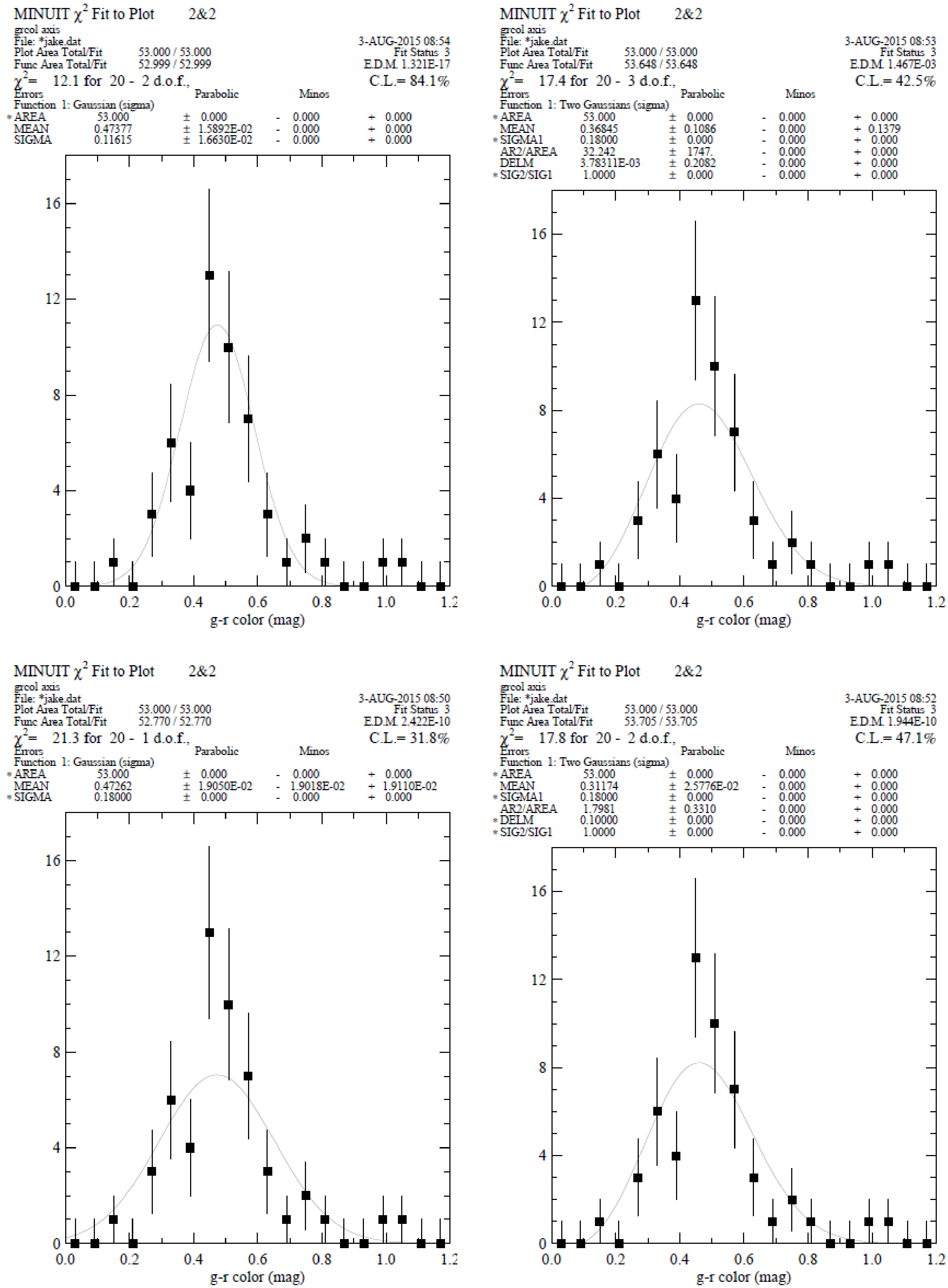

Figure 5: The g-r color for the SDSS g-r color intermediate redshift SNIa sample. The upper right is the best fit to a single Gaussian with floating width. The others are fits to a single or two Gaussians with fixed or floating widths. None of these favor two distinct samples.

Further work would be to do an analysis much more like Milne(2015) with a more sophisticated fit to the observed SDSS SNIa light curves using SNIa light curve fitting programs to extract the U-V color at peak V-band brightness using synthetic photometry.

4 References

Milne et. al. The Changing Fractions of Type Ia Supernova NUV-Optical Subclasses with Redshift The Astrophysical Journal. 803.1 (2015).

Sako et. al. The Data Release of the Sloan Digital Sky Survey-II Supernova Survey arXiv: 1401.3317.

"SNANA: A Public Software Package for Supernova Analysis", Richard Kessler, Joseph P. Bernstein, David Cinabro *et al.*, Publications of the Astronomical Society of the Pacific 121 (2009) 1028-1035.

5 Appendix

Below is a collection of the light curves we analyzed.

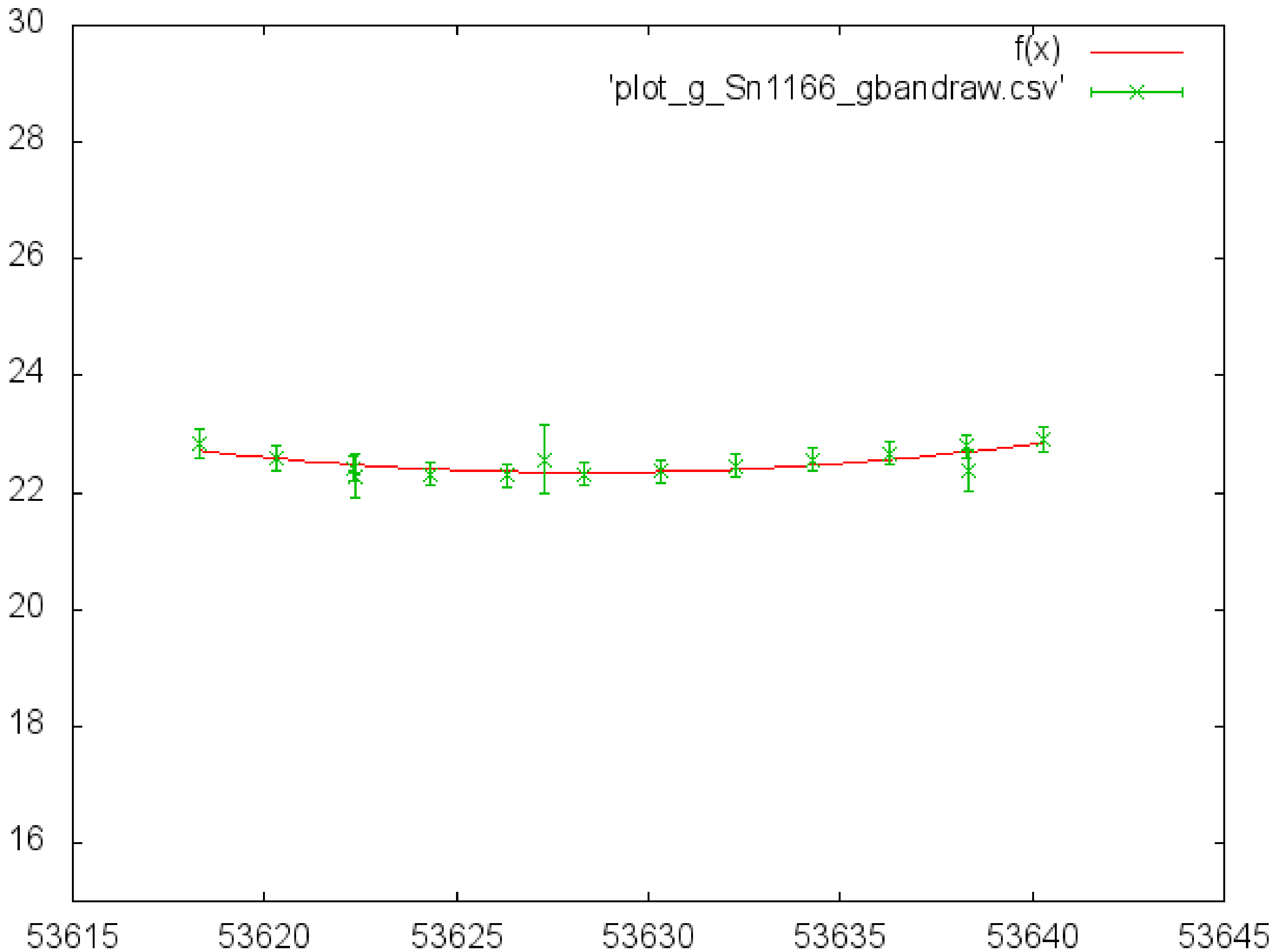

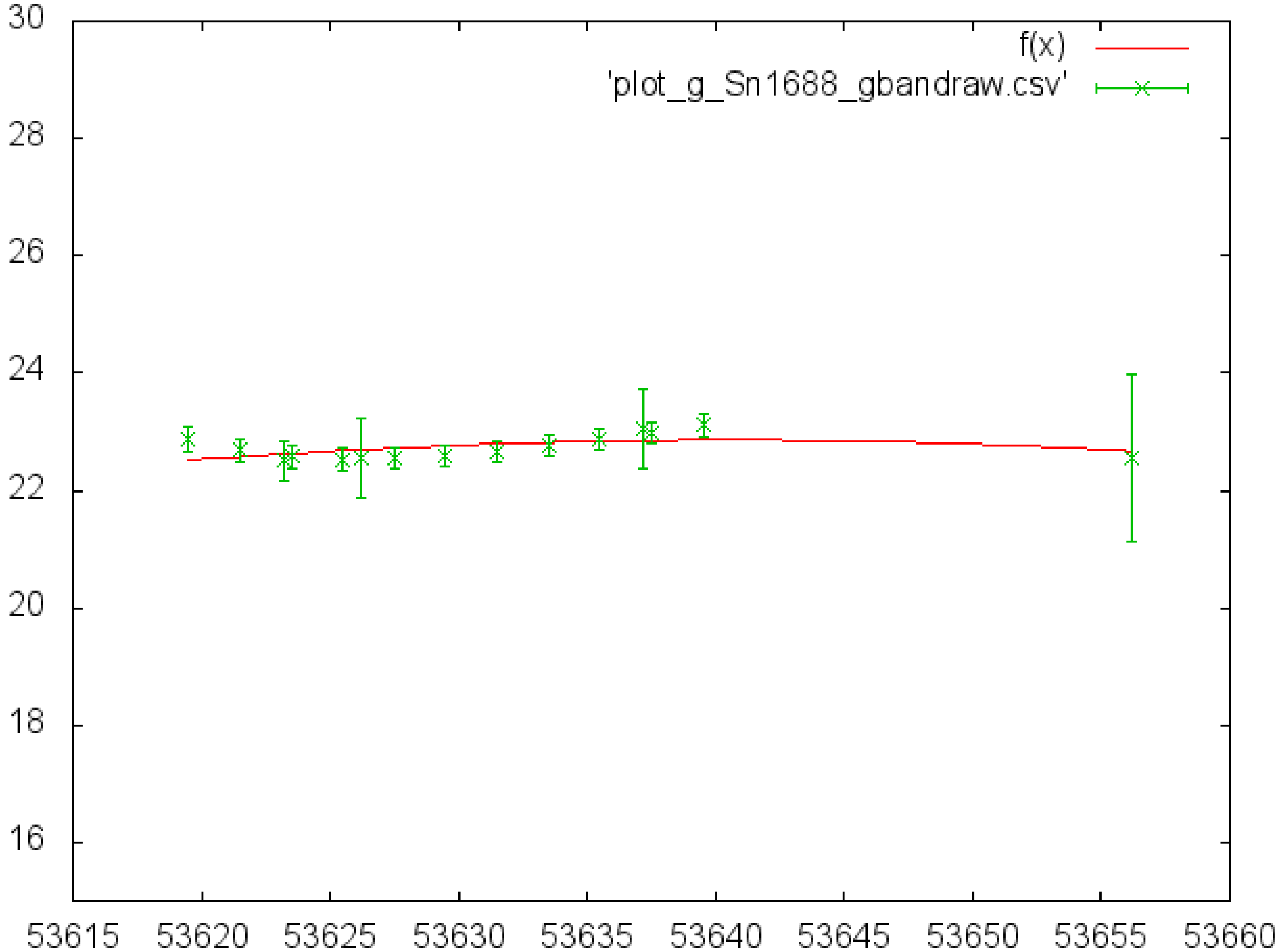

30
28
26
24
22
20
18
16
53615
53620
53625
53630
53635
53640
53645
53650
53655
53660
f(x)
'plot_g_Sn1688_gbandraw.csv'

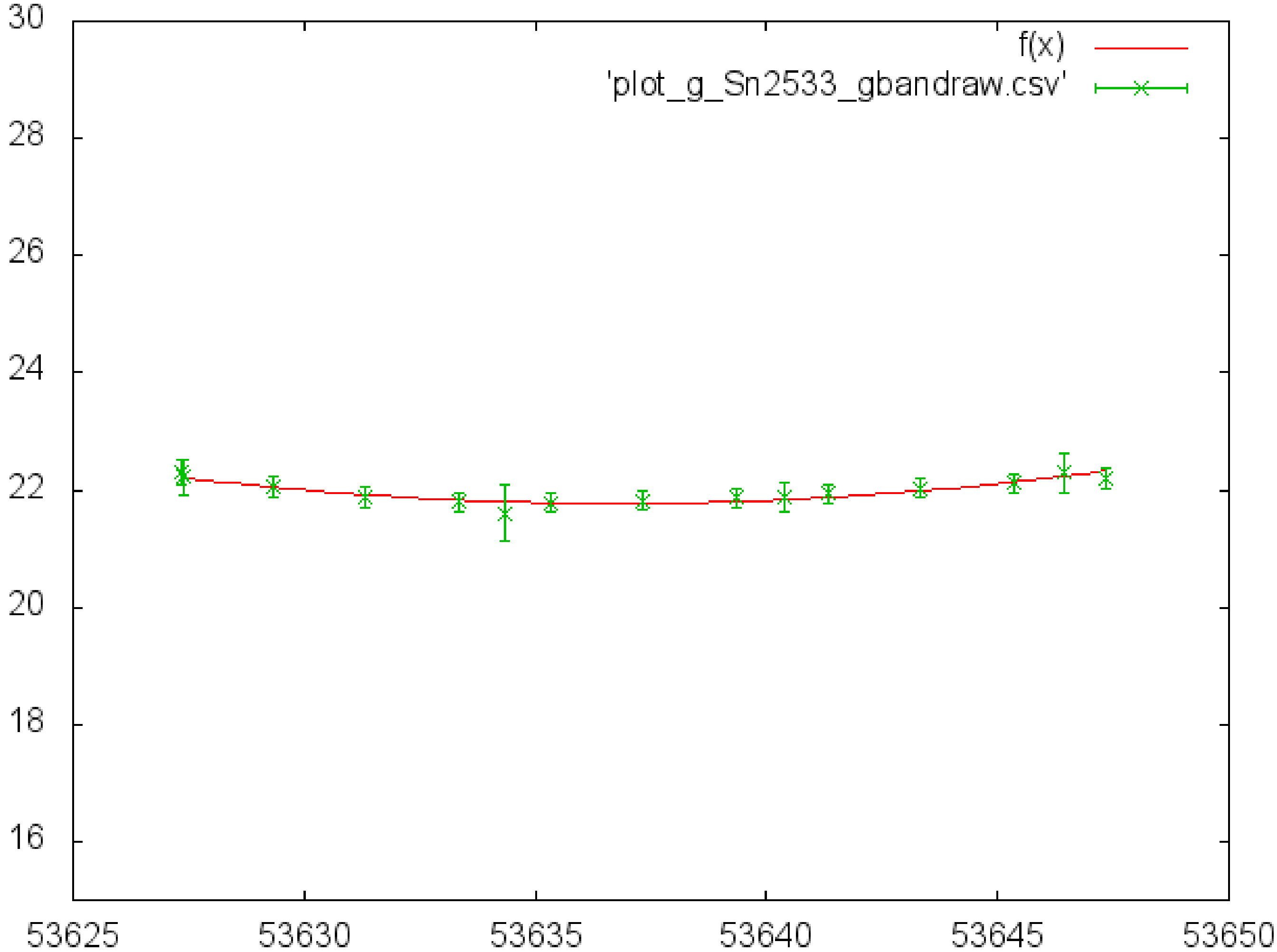
30
28
26
24
22
20
18
16
53625
53630
53635
53640
53645
53650
f(x)
'plot_g_Sn2533_gbandraw.csv'

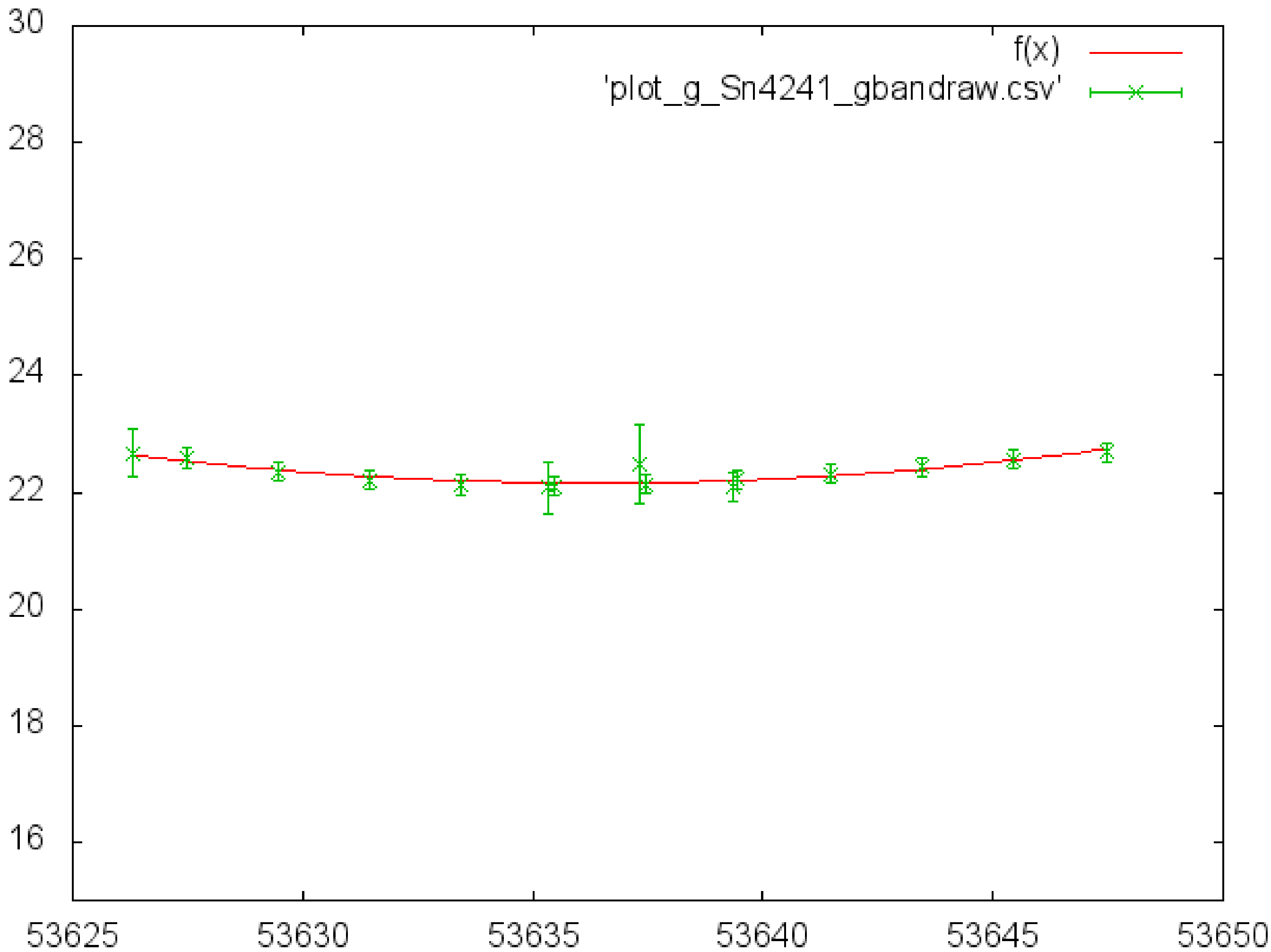
f(x)
'plot_g_Sn4241_gbandraw.csv'
30
28
26
24
22
20
18
16
53625
53630
53635
53640
53645
53650

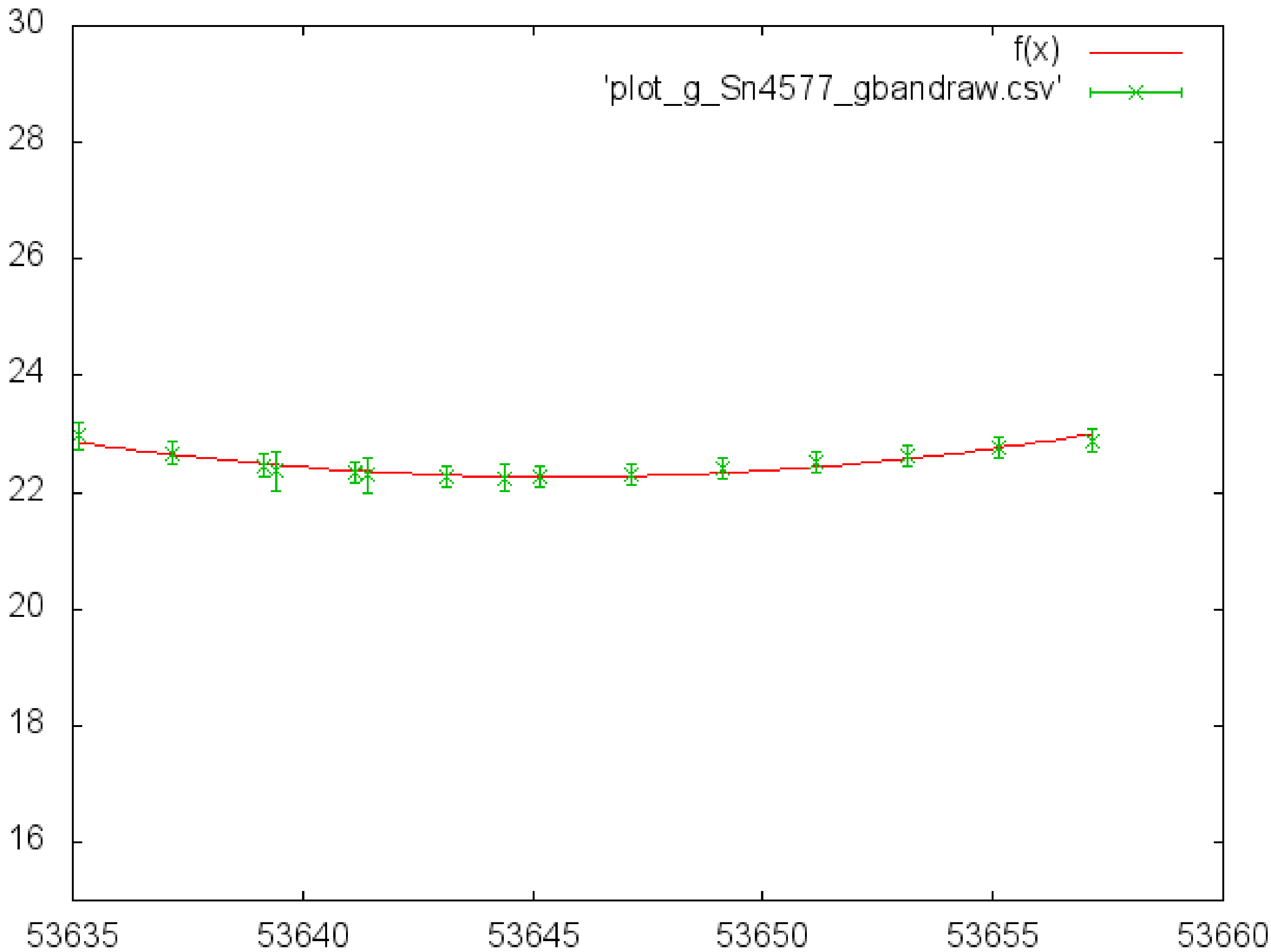

30
28
26
24
22
20
18
16
53635
53640
53645
53650
53655
53660
f(x)
'plot_g_Sn4577_gbandraw.csv'

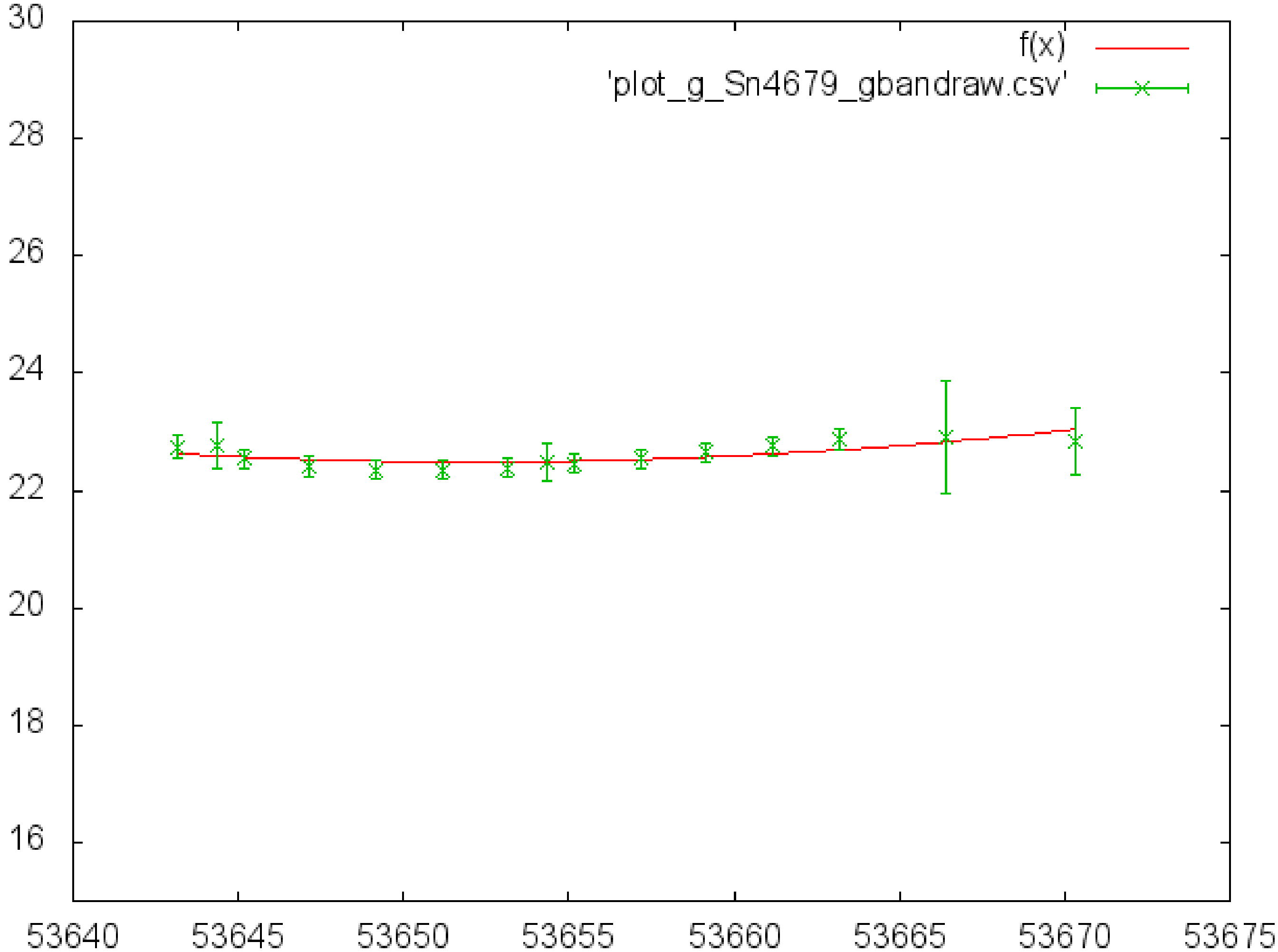

f(x)
'plot_g_Sn4679_gbandraw.csv'
30
28
26
24
22
20
18
16
53640
53645
53650
53655
53660
53665
53670
53675

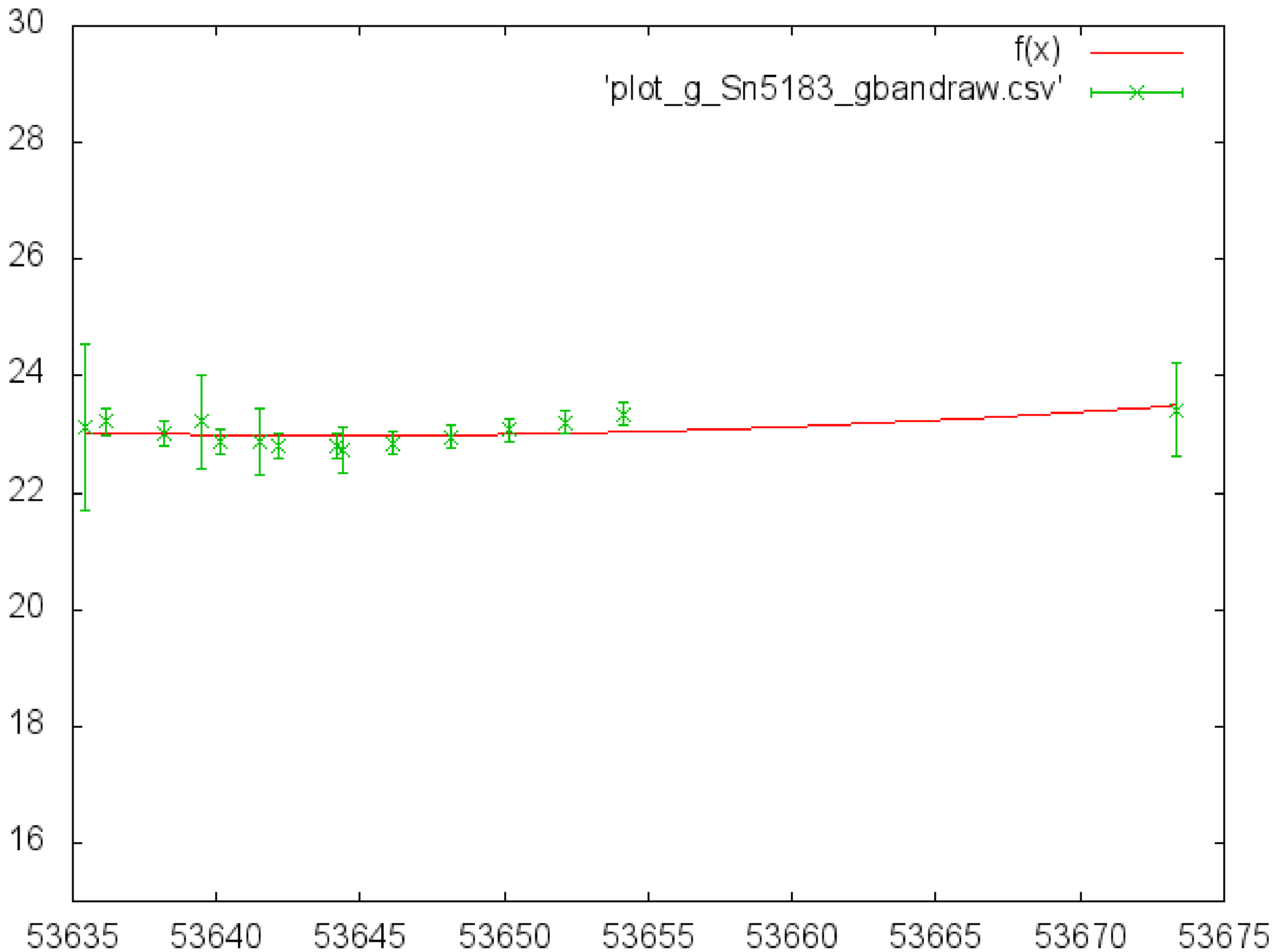

30
28
26
24
22
20
18
16
53635
53640
53645
53650
53655
53660
53665
53670
53675
f(x)
'plot_g_Sn5183_gbandraw.csv'

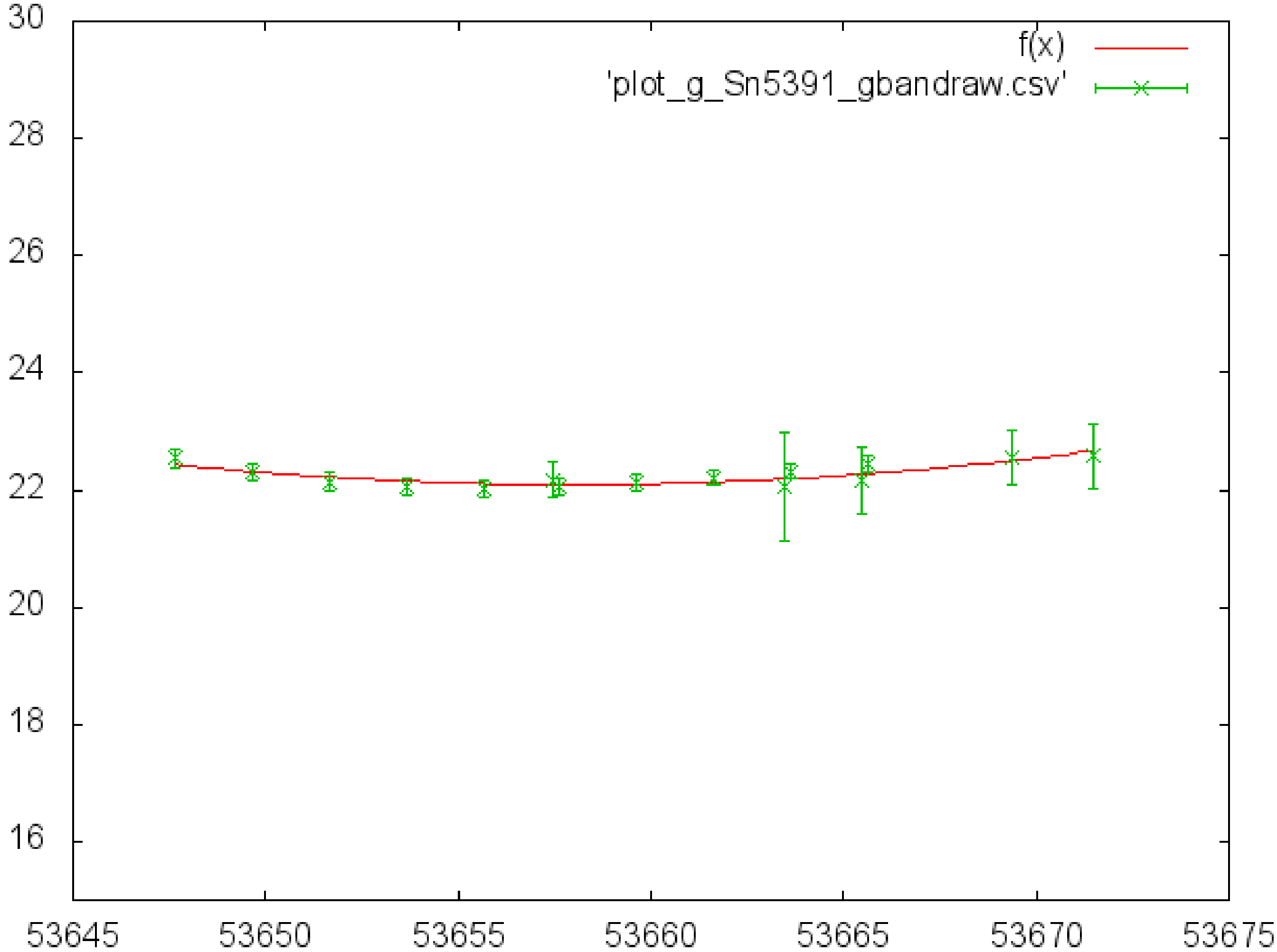

f(x)
'plot_g_Sn5391_gbandraw.csv'
30
28
26
24
22
20
18
16
53645
53650
53655
53660
53665
53670
53675

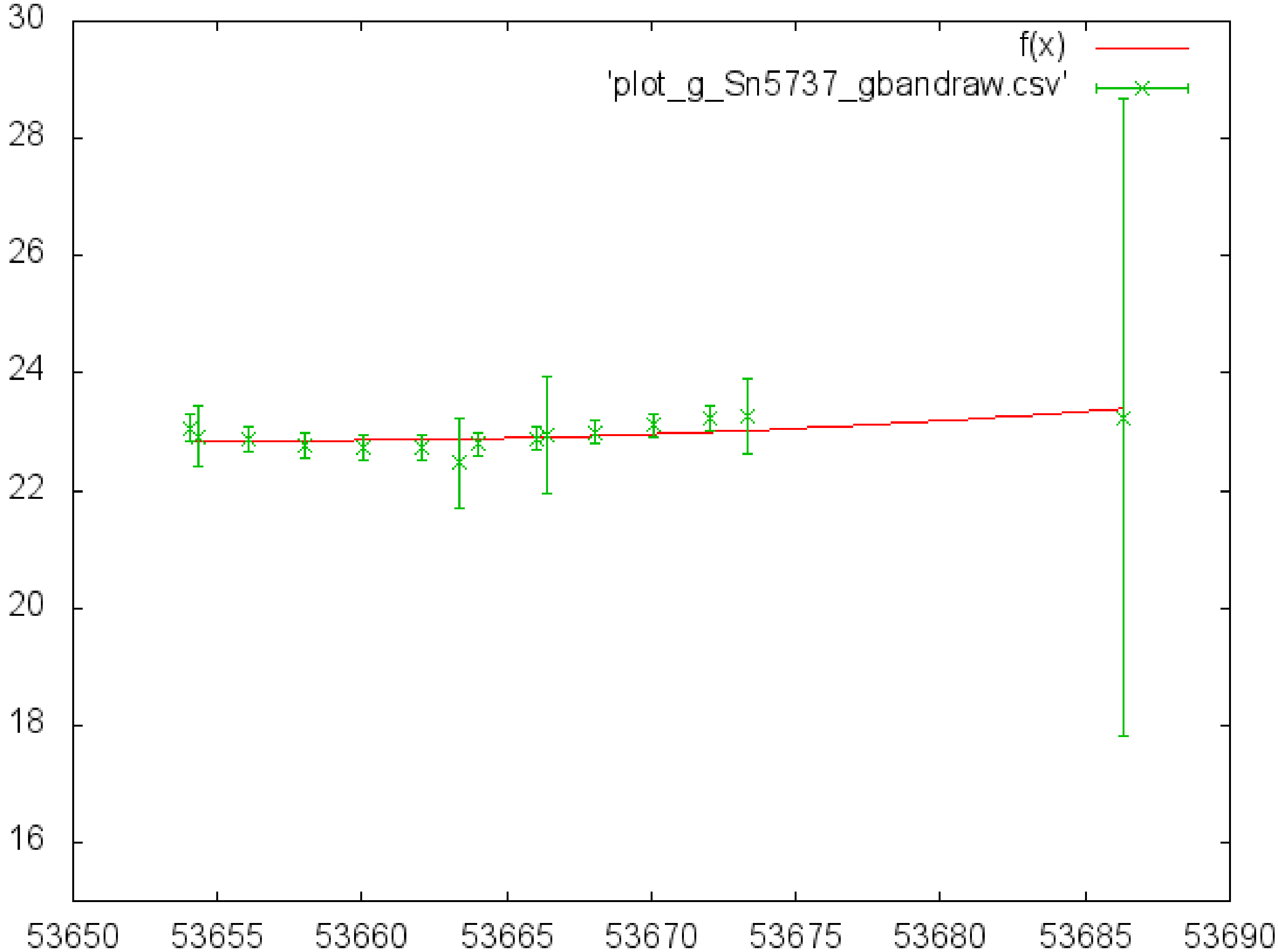

30
28
26
24
22
20
18
16
53650
53655
53660
53665
53670
53675
53680
53685
53690
f(x)
'plot_g_Sn5737_gbandraw.csv'

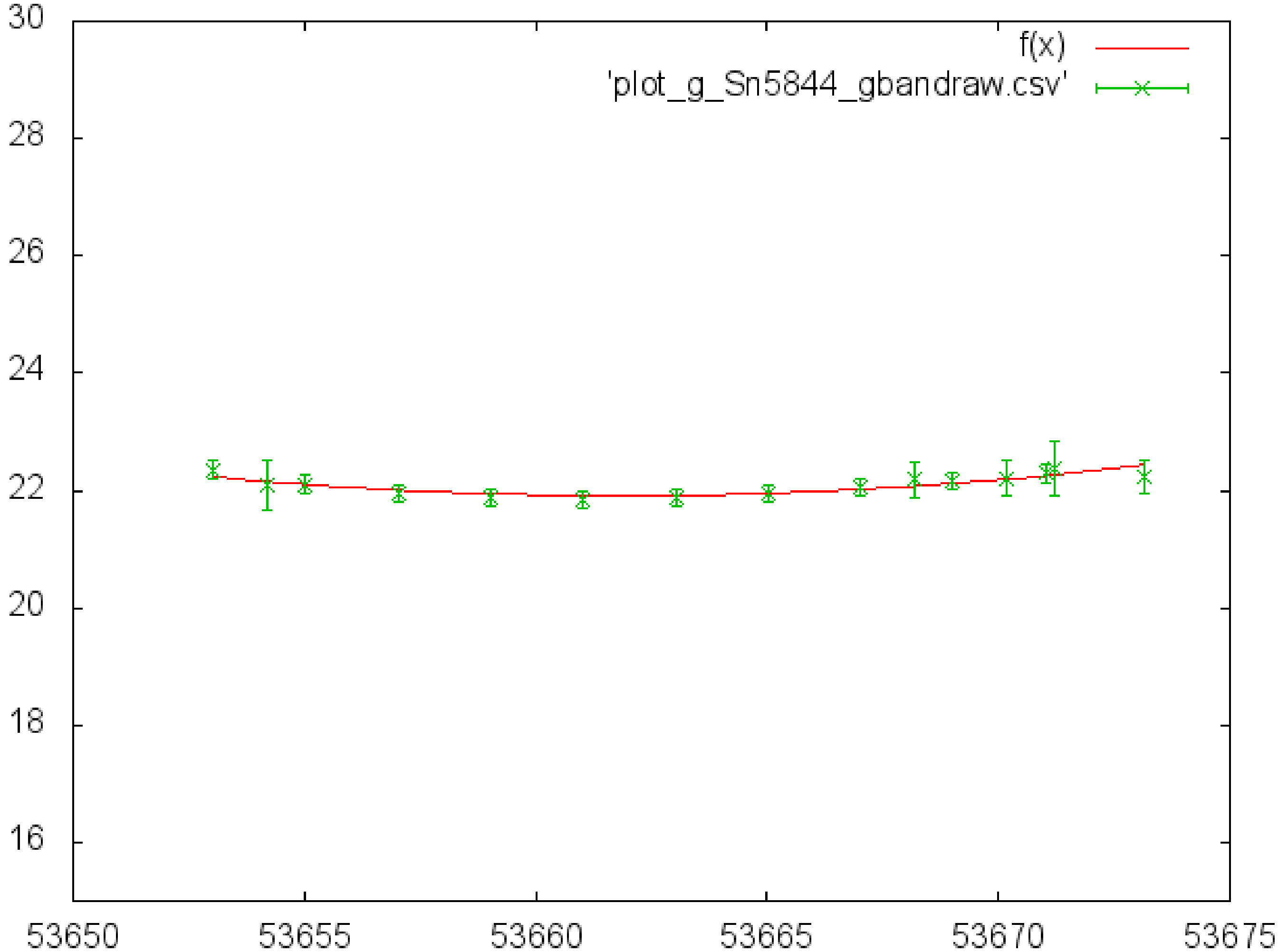
30
28
26
24
22
20
18
16
53650
53655
53660
53665
53670
53675
f(x)
'plot_g_Sn5844_gbandraw.csv'

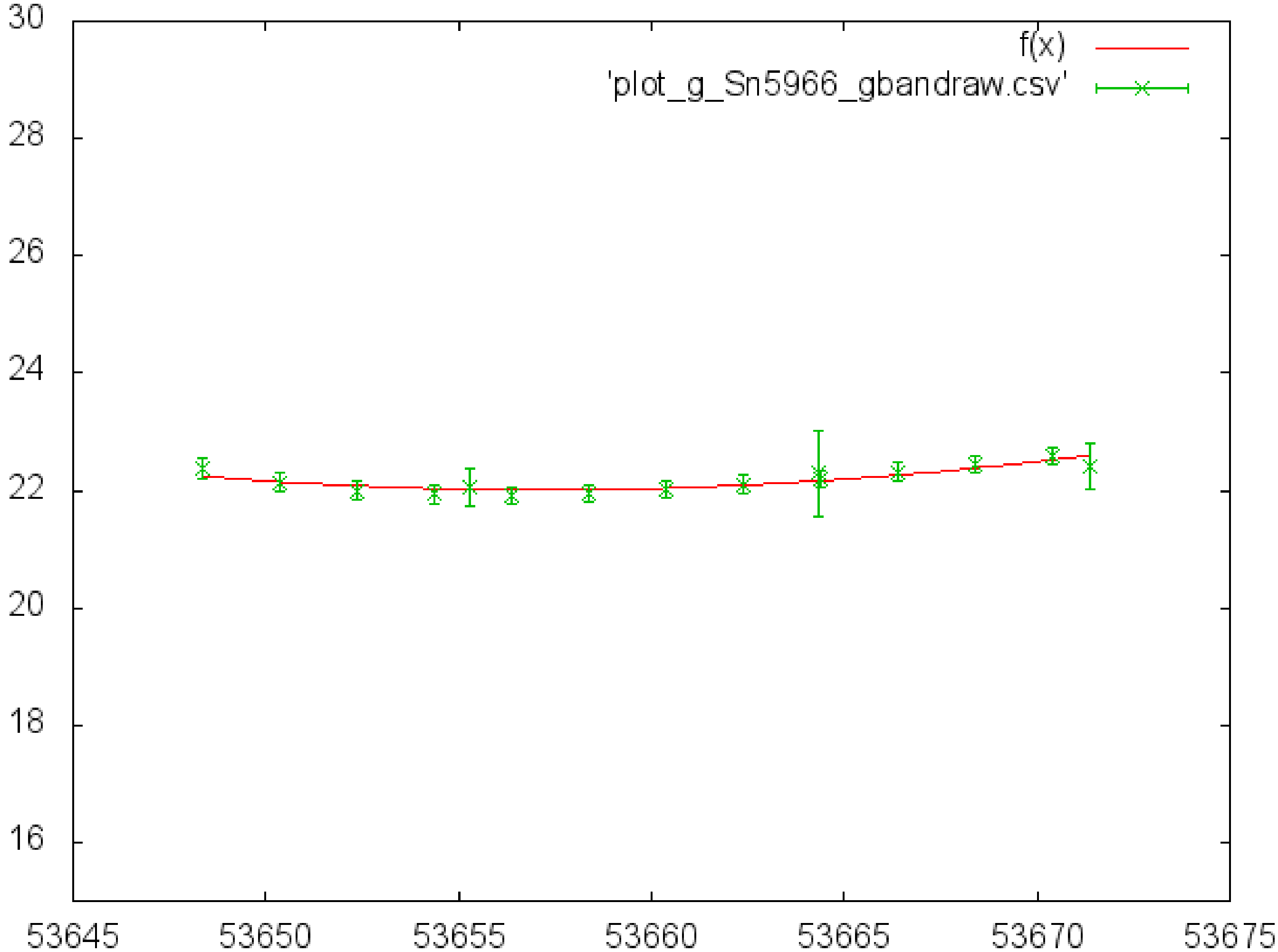
30
28
26
24
22
20
18
16
53645
53650
53655
53660
53665
53670
53675
f(x)
'plot_g_Sn5966_gbandraw.csv'

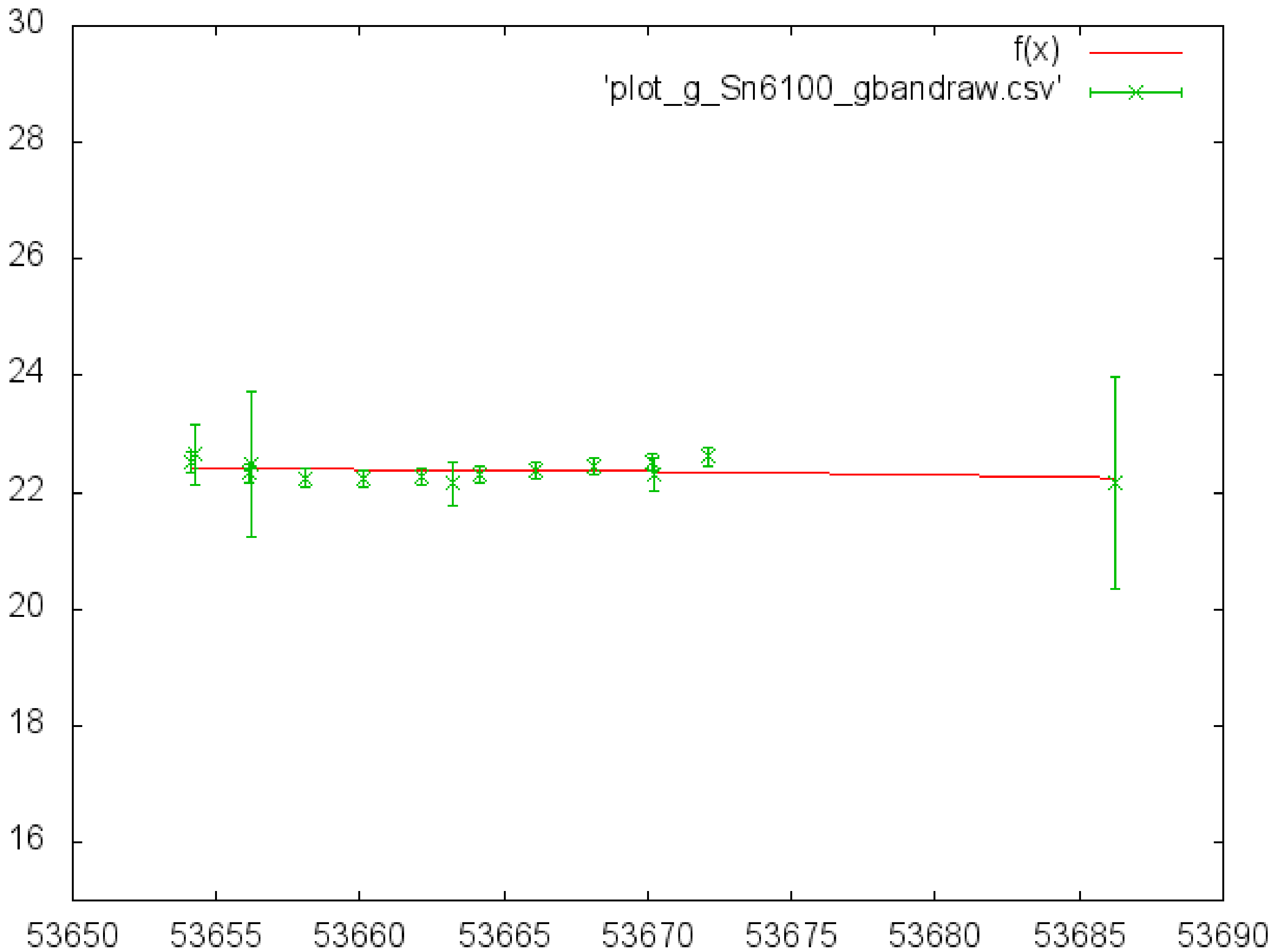
f(x)
'plot_g_Sn6100_gbandraw.csv'
30
28
26
24
22
20
18
16
53650
53655
53660
53665
53670
53675
53680
53685
53690

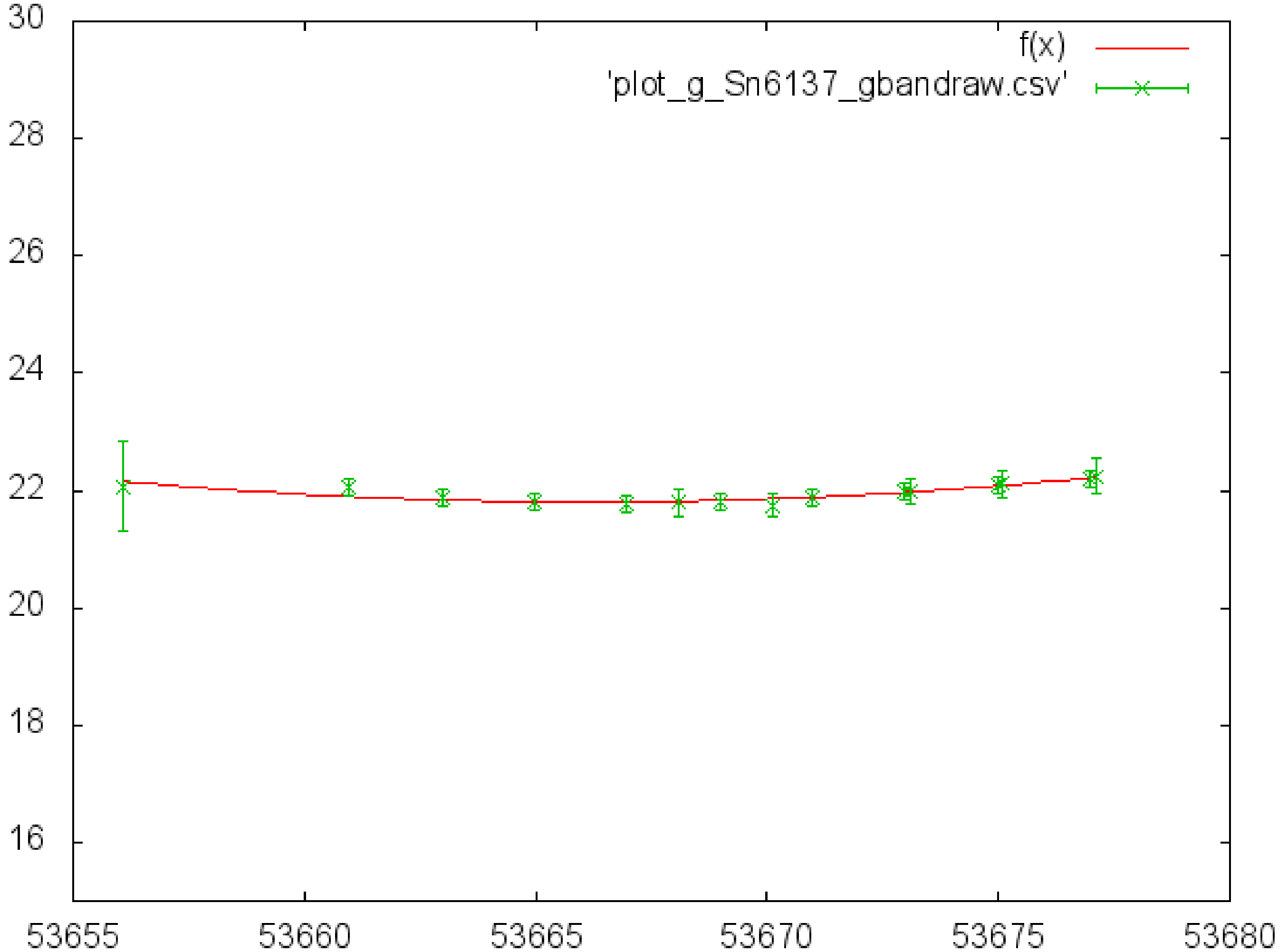

30
28
26
24
22
20
18
16
53655
53660
53665
53670
53675
53680
f(x)
'plot_g_Sn6137_gbandraw.csv'

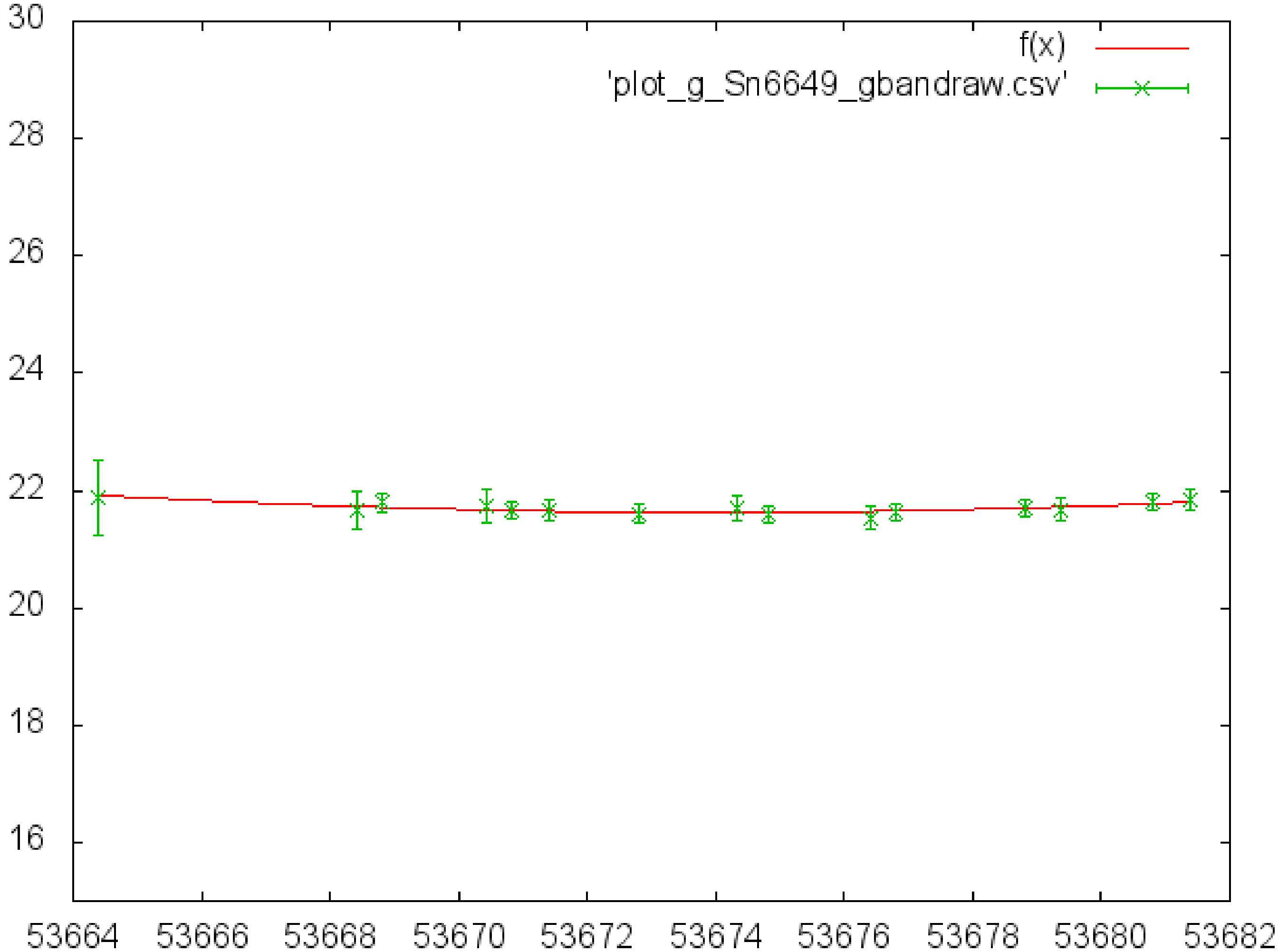
30
28
26
24
22
20
18
16
53664
53666
53668
53670
53672
53674
53676
53678
53680
53682
f(x)
'plot_g_Sn6649_gbandraw.csv'

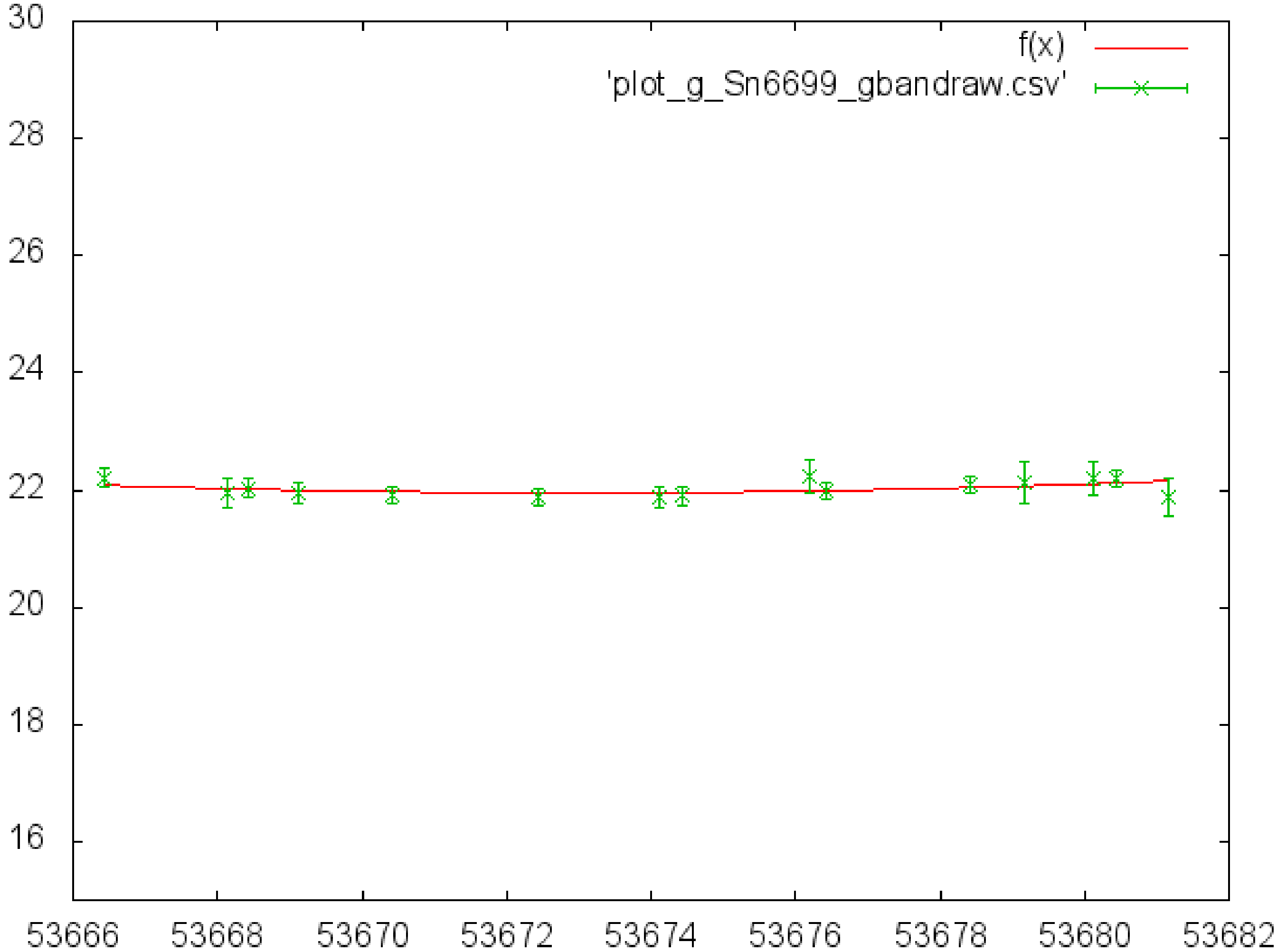

30
28
26
24
22
20
18
16
53666
53668
53670
53672
53674
53676
53678
53680
53682
f(x)
'plot_g_Sn6699_gbandraw.csv'

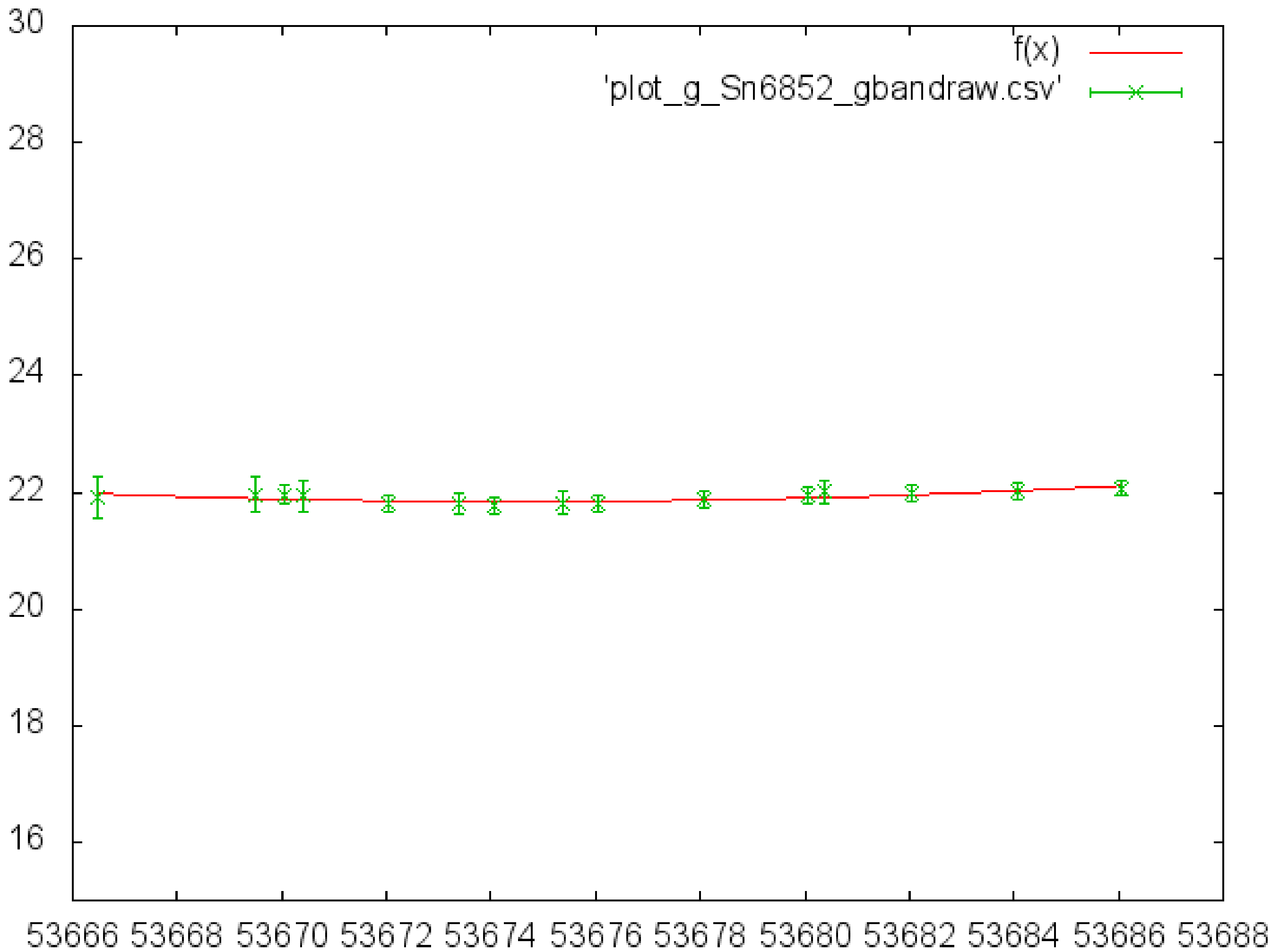
30
28
26
24
22
20
18
16
f(x)
'plot_g_Sn6852_gbandraw.csv'
53666 53668 53670 53672 53674 53676 53678 53680 53682 53684 53686 53688

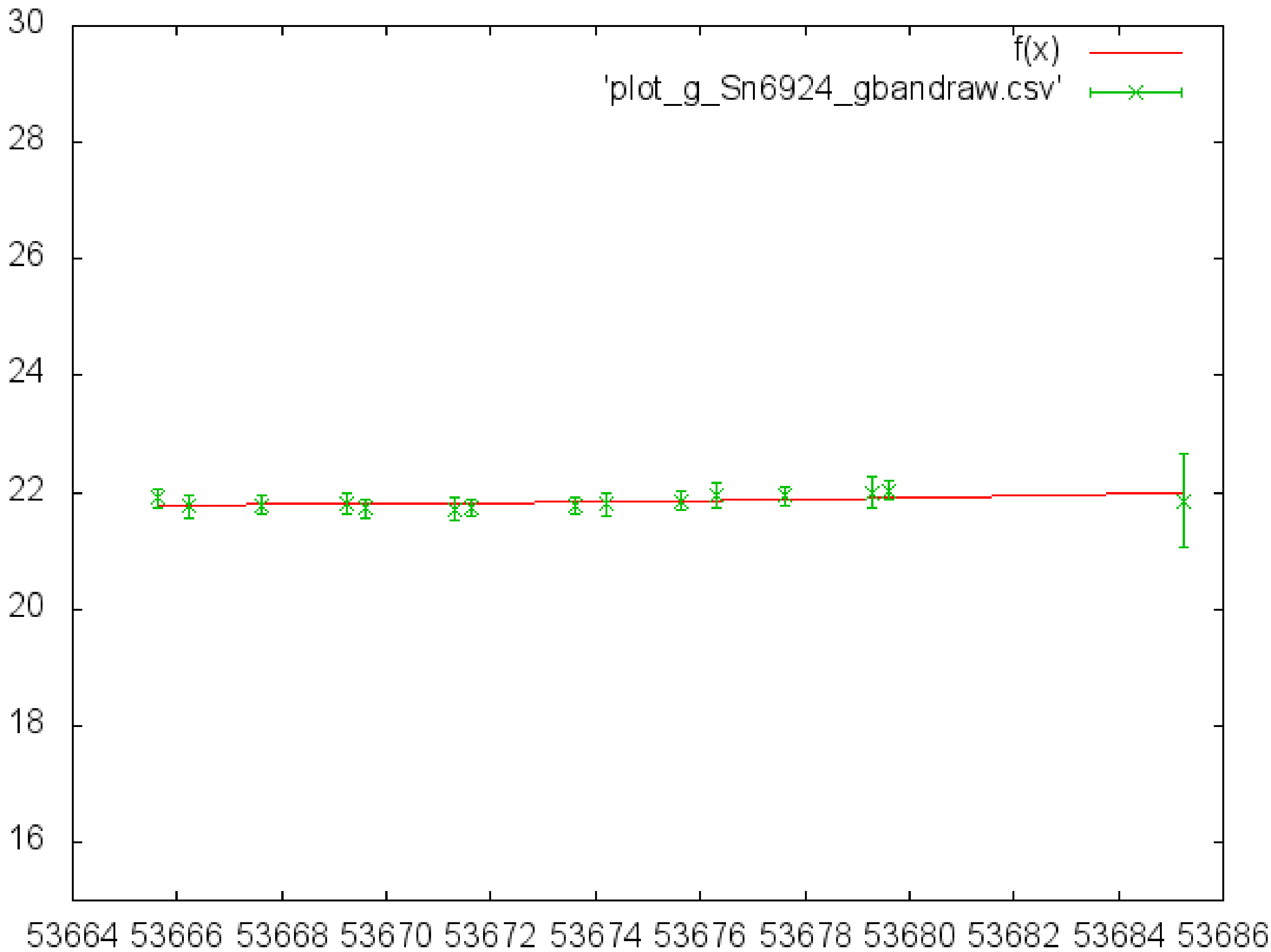

30
28
26
24
22
20
18
16
53664
53666
53668
53670
53672
53674
53676
53678
53680
53682
53684
53686
f(x)
'plot_g_Sn6924_gbandraw.csv'

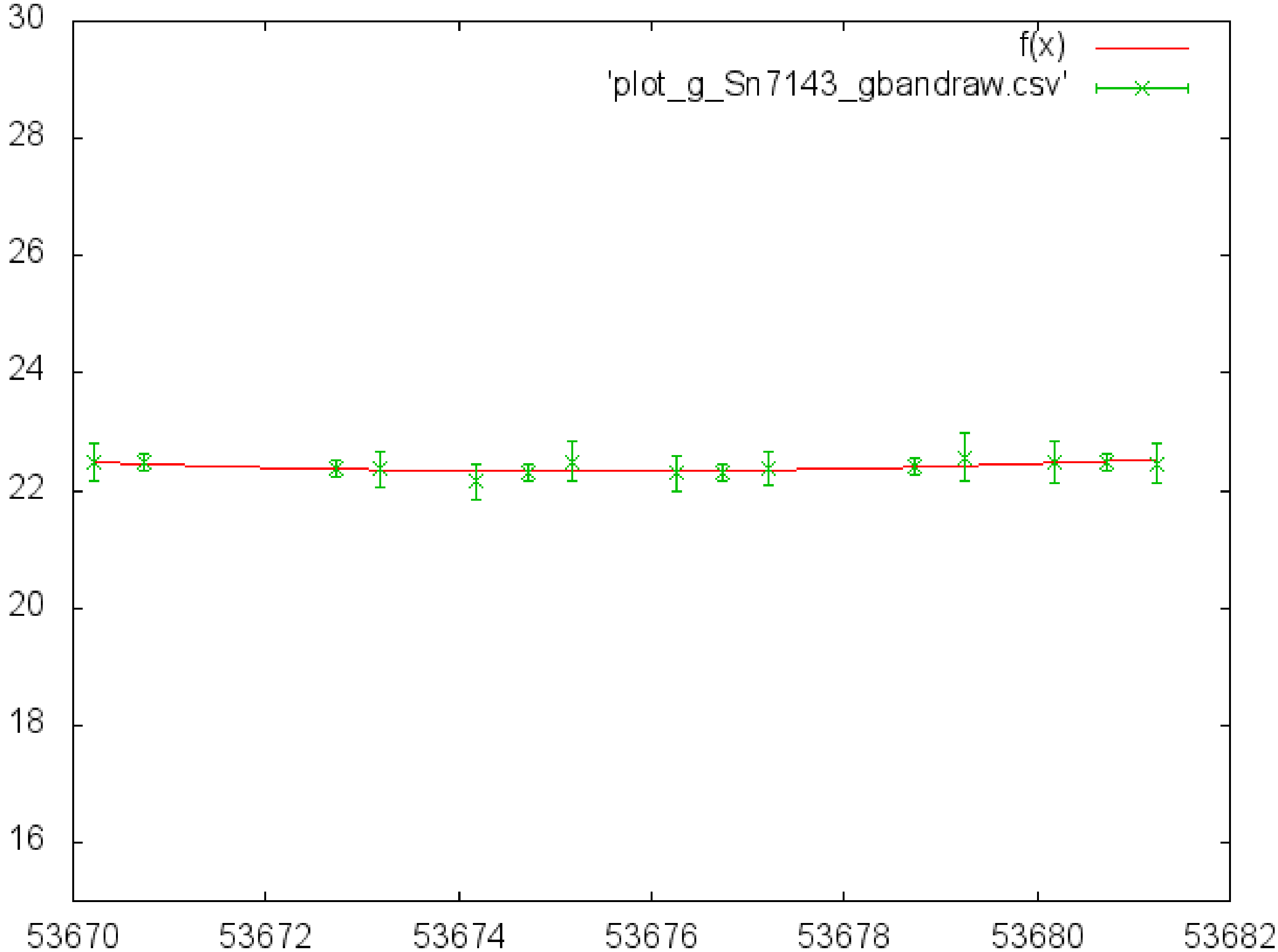

30
28
26
24
22
20
18
16
53670
53672
53674
53676
53678
53680
53682
f(x)
'plot_g_Sn7143_gbandraw.csv'

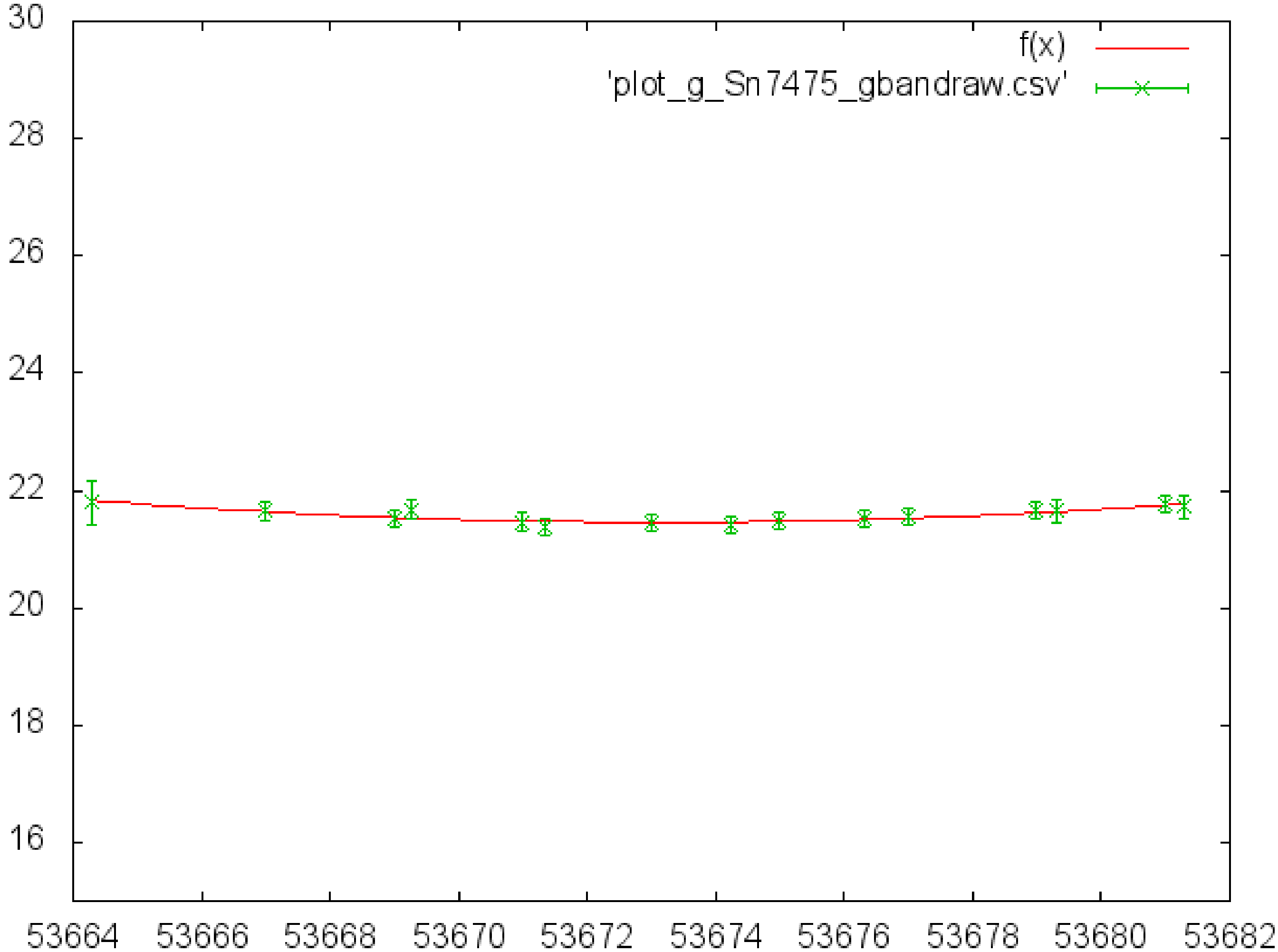

f(x)
'plot_g_Sn7475_gbandraw.csv'
30
28
26
24
22
20
18
16
53664
53666
53668
53670
53672
53674
53676
53678
53680
53682

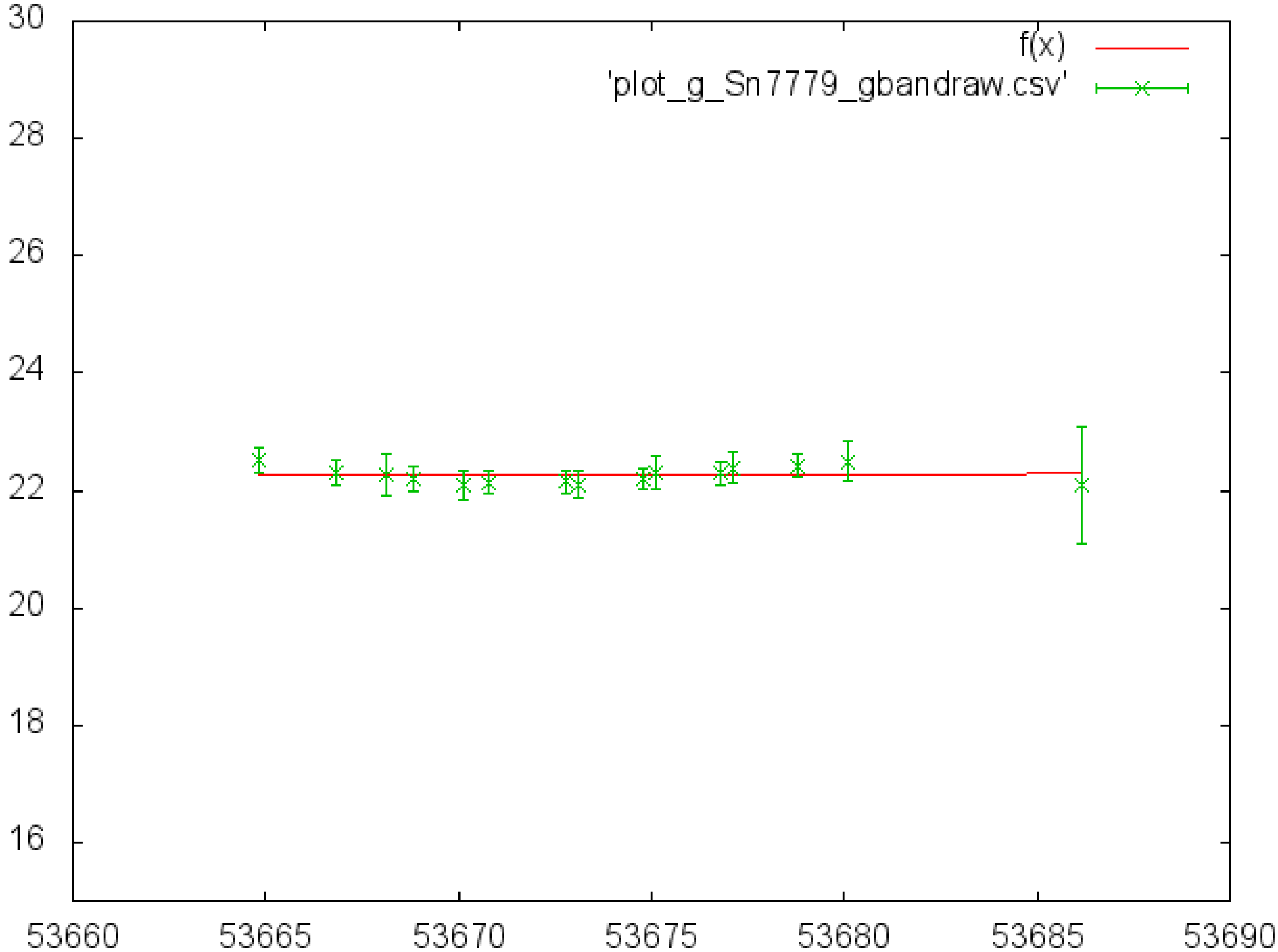

30
28
26
24
22
20
18
16
53660
53665
53670
53675
53680
53685
53690
f(x)
'plot_g_Sn7779_gbandraw.csv'

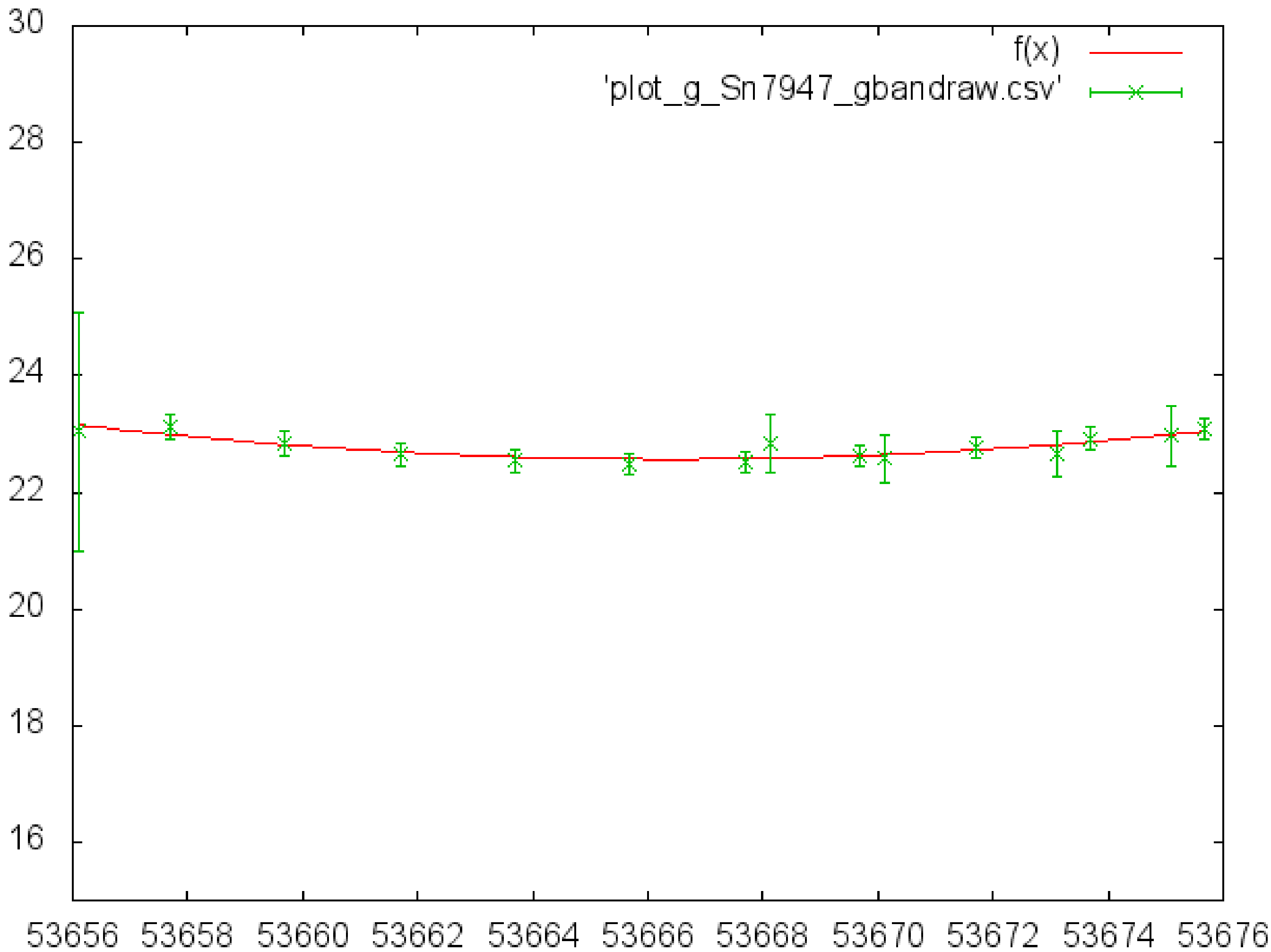
f(x)
'plot_g_Sn7947_gbandraw.csv'
30
28
26
24
22
20
18
16
53656
53658
53660
53662
53664
53666
53668
53670
53672
53674
53676

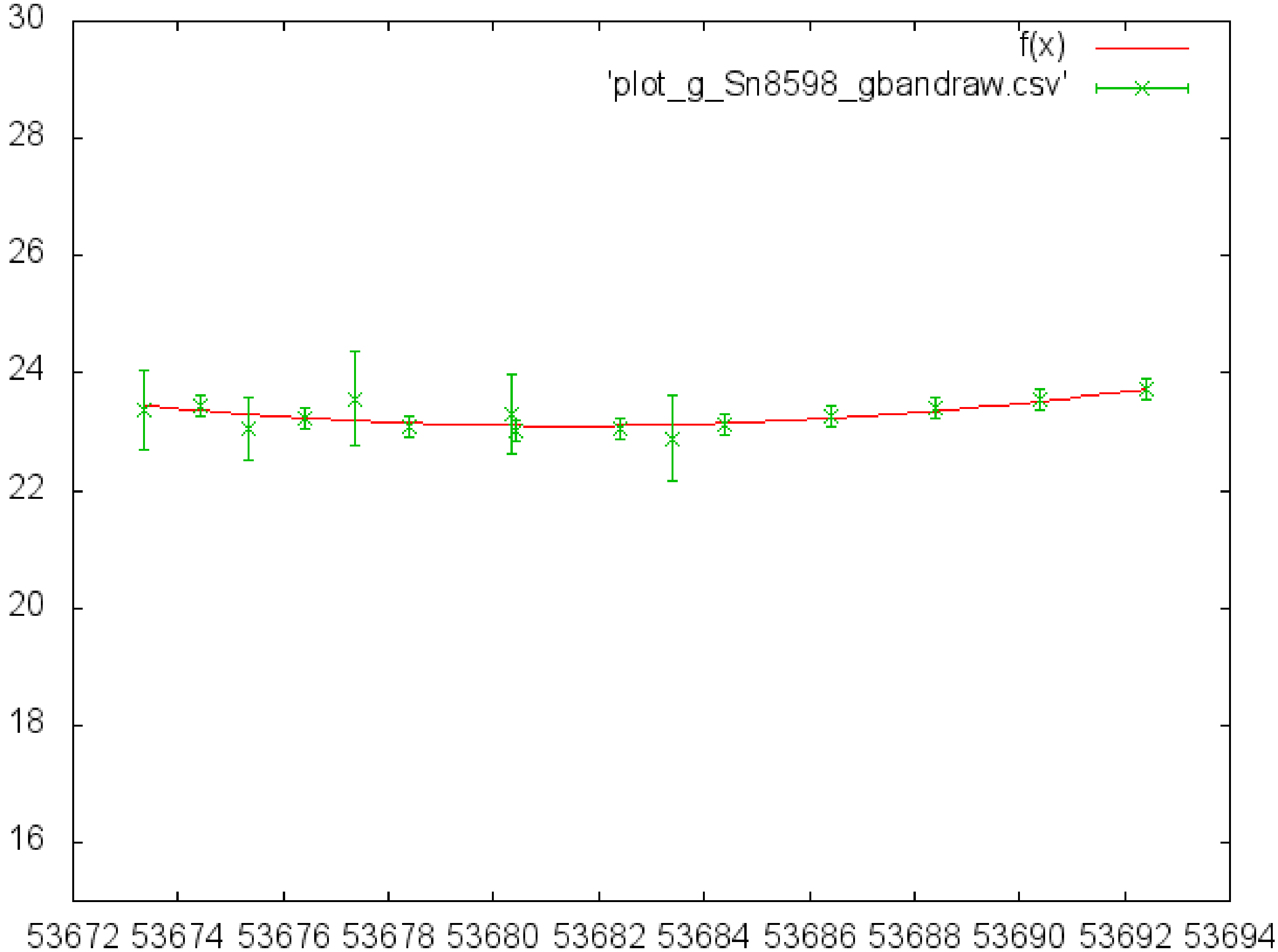
30
28
26
24
22
20
18
16
53672 53674 53676 53678 53680 53682 53684 53686 53688 53690 53692 53694
f(x)
'plot_g_Sn8598_gbandraw.csv'

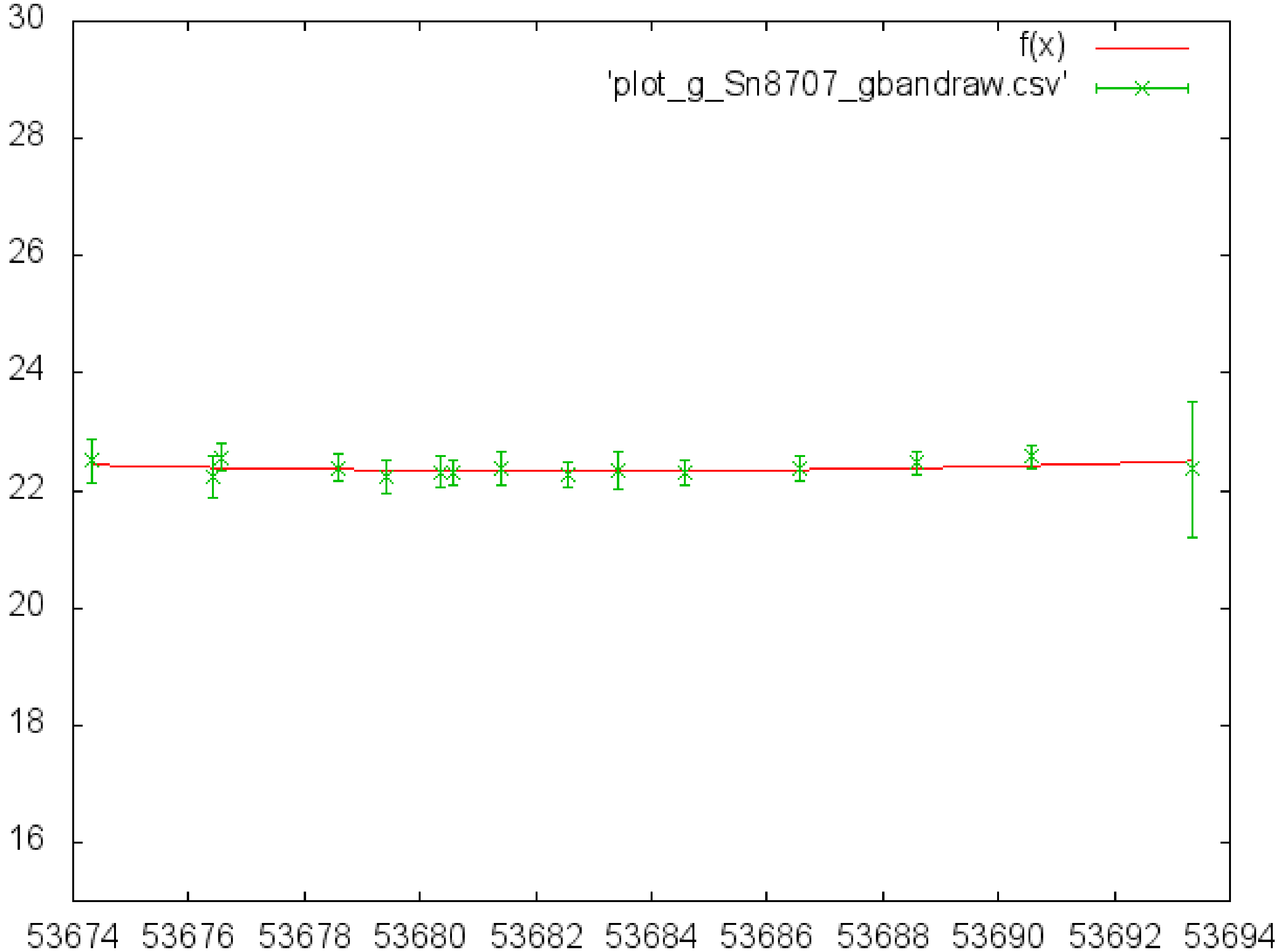
f(x)
'plot_g_Sn8707_gbandraw.csv'
30
28
26
24
22
20
18
16
53674
53676
53678
53680
53682
53684
53686
53688
53690
53692
53694

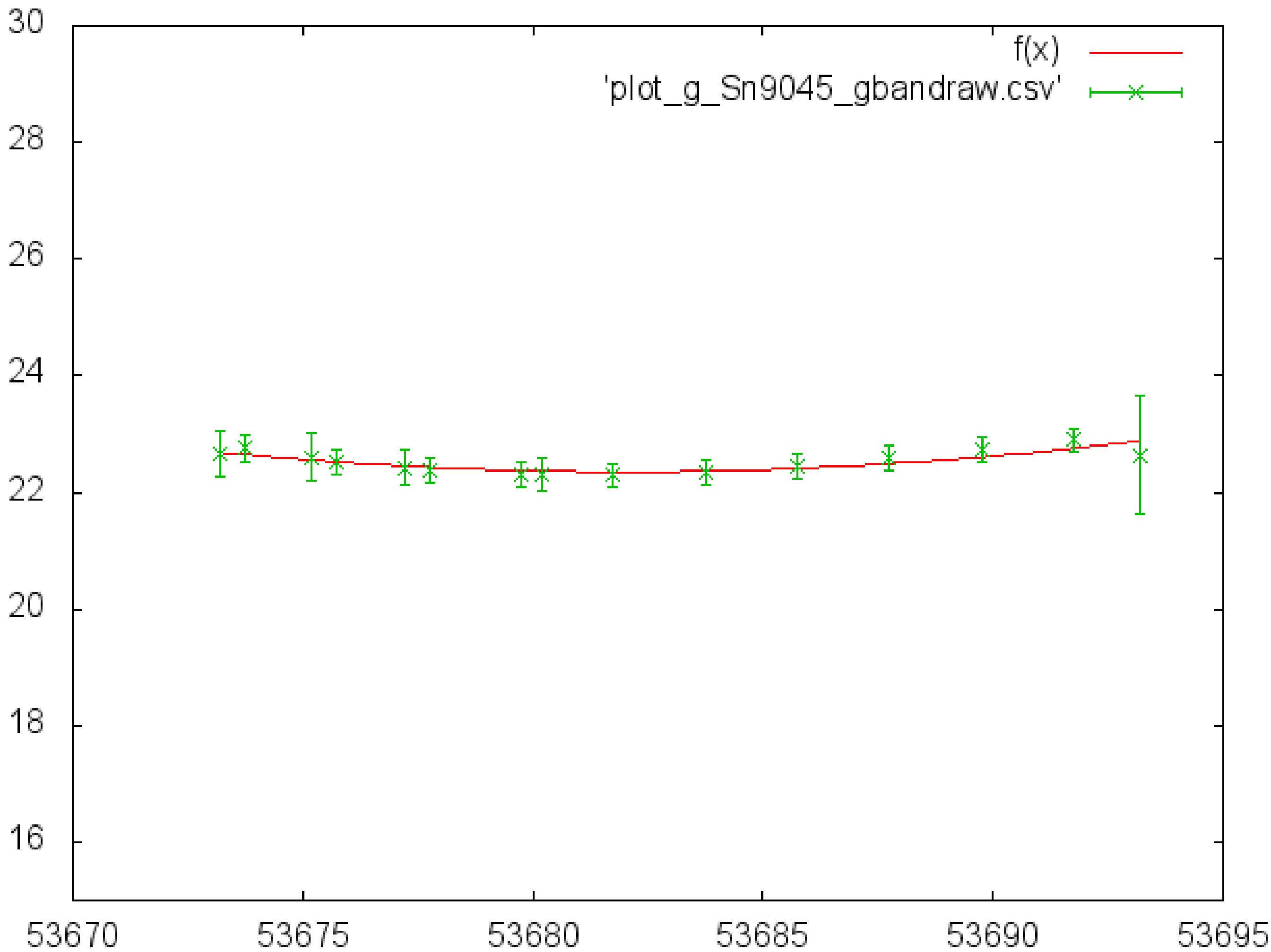
f(x)
'plot_g_Sn9045_gbandraw.csv'
30
28
26
24
22
20
18
16
53670
53675
53680
53685
53690
53695

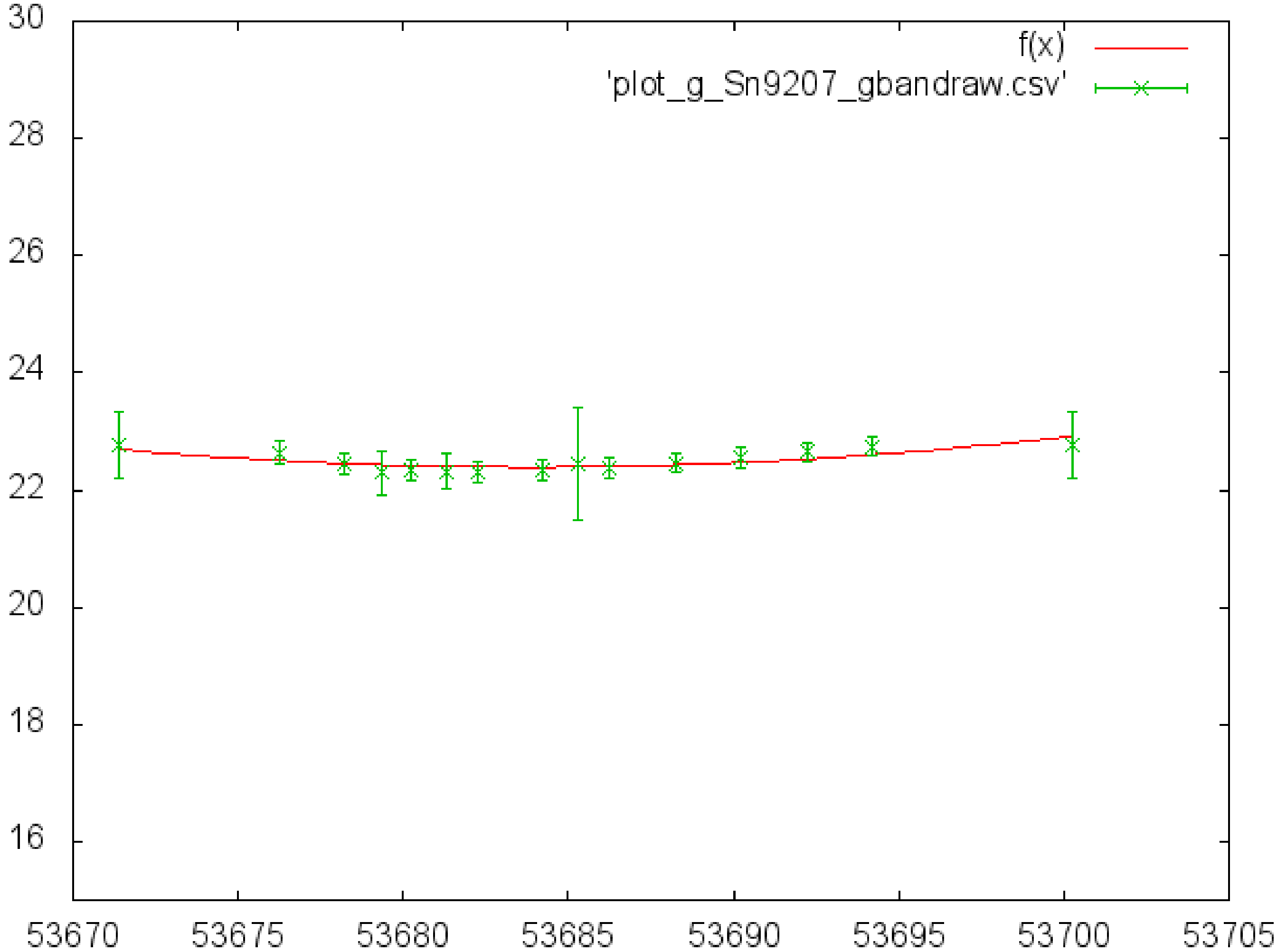

f(x)
'plot_g_Sn9207_gbandraw.csv'
30
28
26
24
22
20
18
16
53670
53675
53680
53685
53690
53695
53700
53705

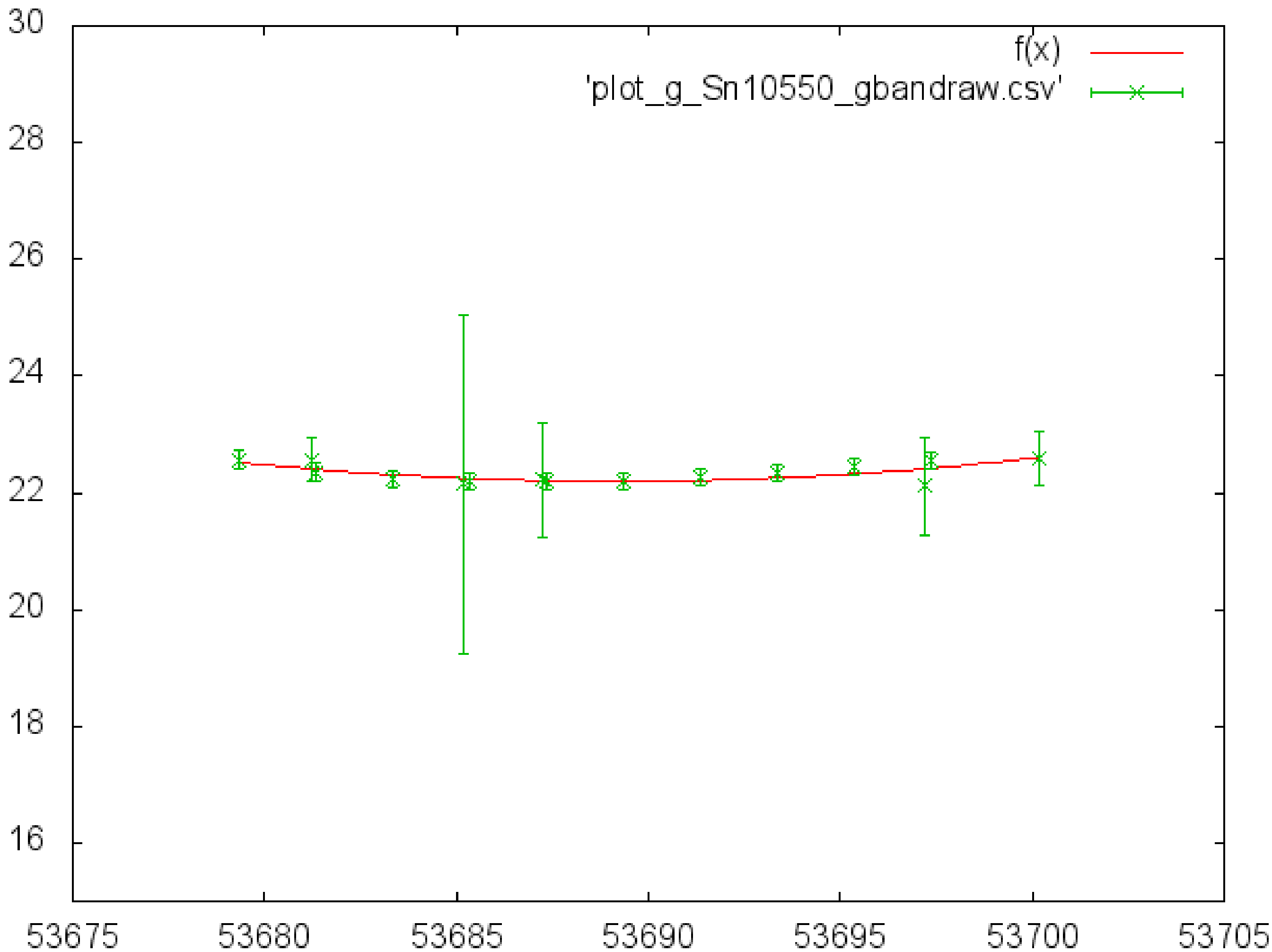

30
28
26
24
22
20
18
16
53675
53680
53685
53690
53695
53700
53705
f(x)
'plot_g_Sn10550_gbandraw.csv'

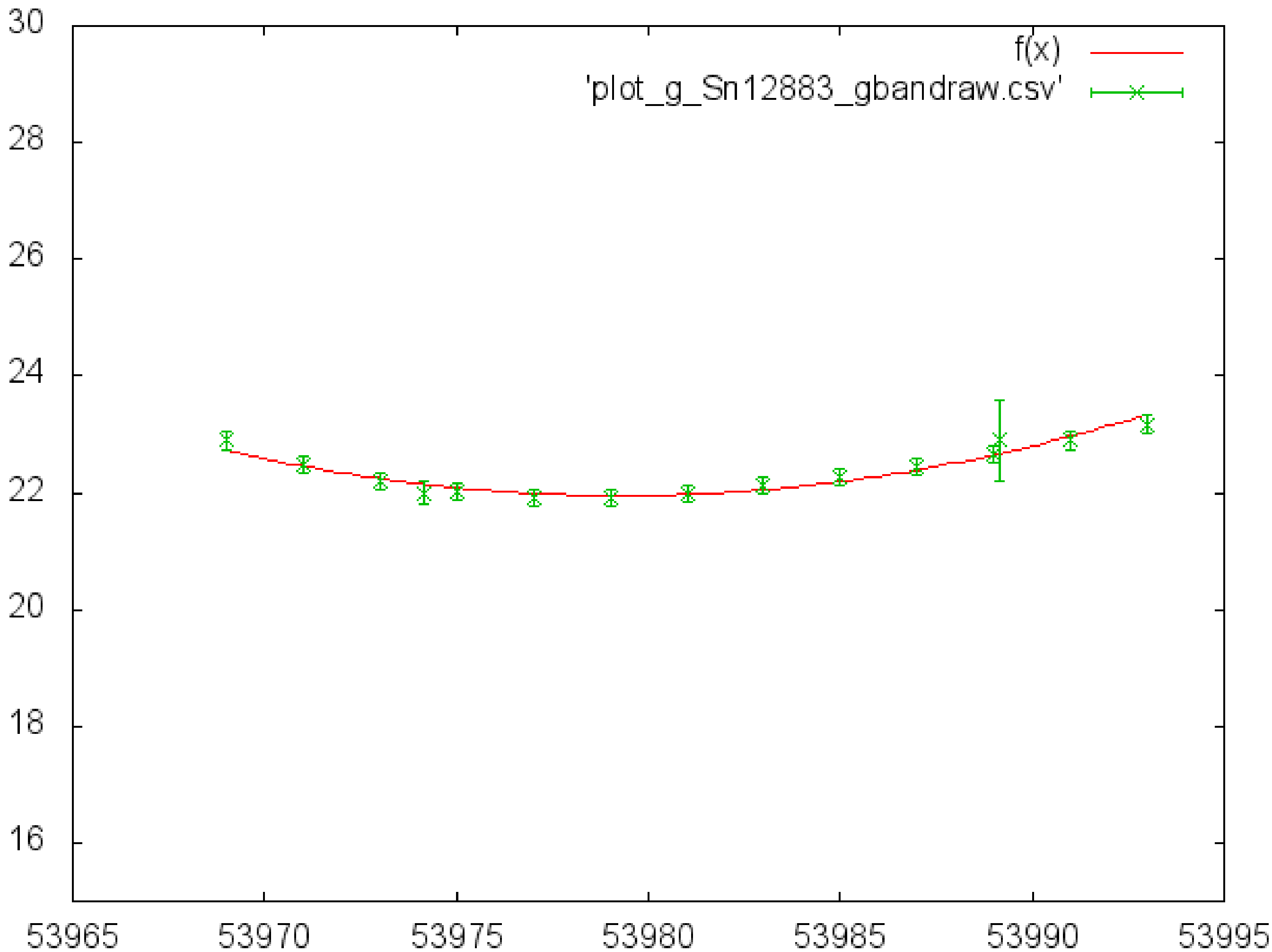

30
28
26
24
22
20
18
16
53965
53970
53975
53980
53985
53990
53995
f(x)
'plot_g_Sn12883_gbandraw.csv'

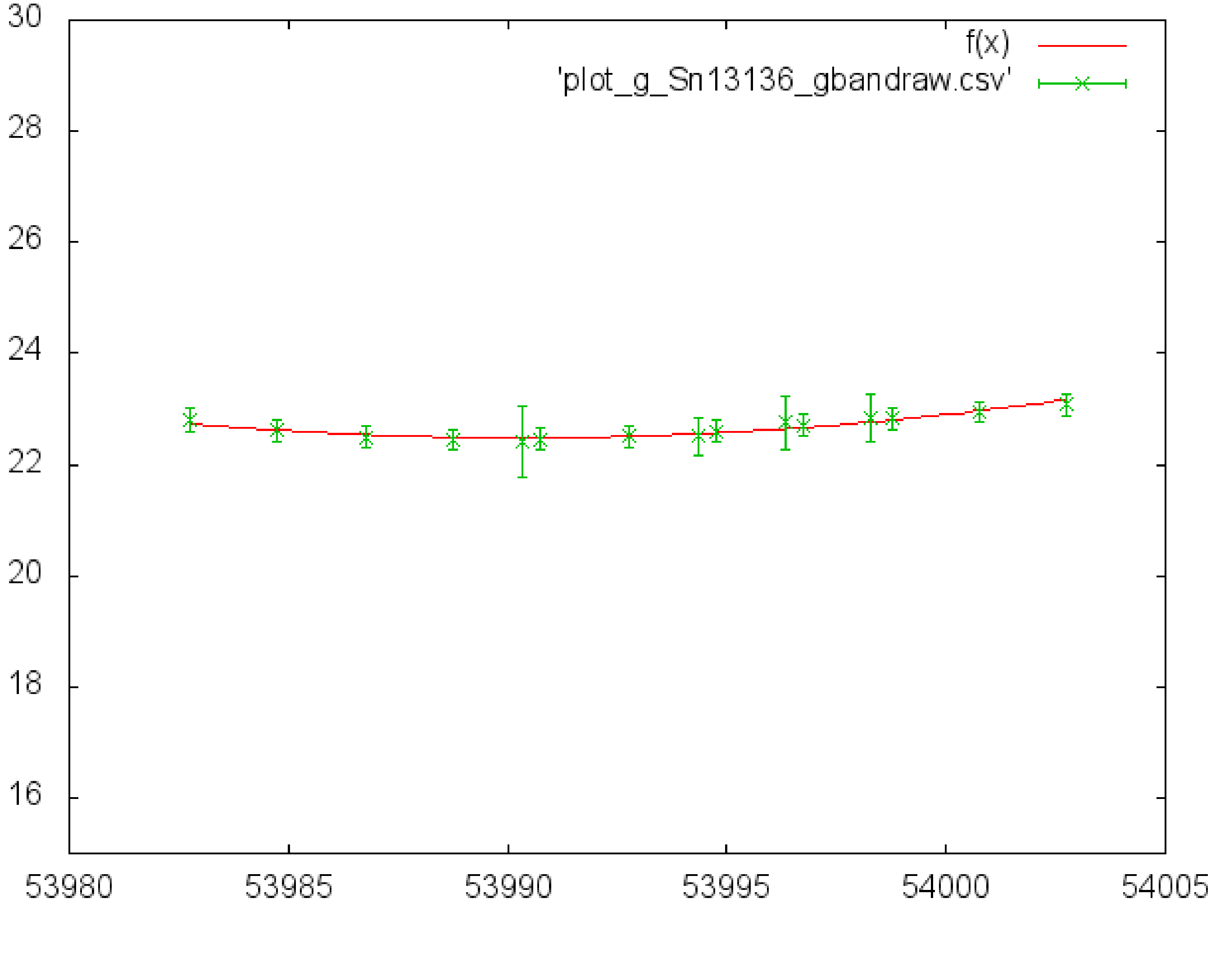
f(x)
'plot_g_Sn13136_gbandraw.csv'
30
28
26
24
22
20
18
16
53980
53985
53990
53995
54000
54005

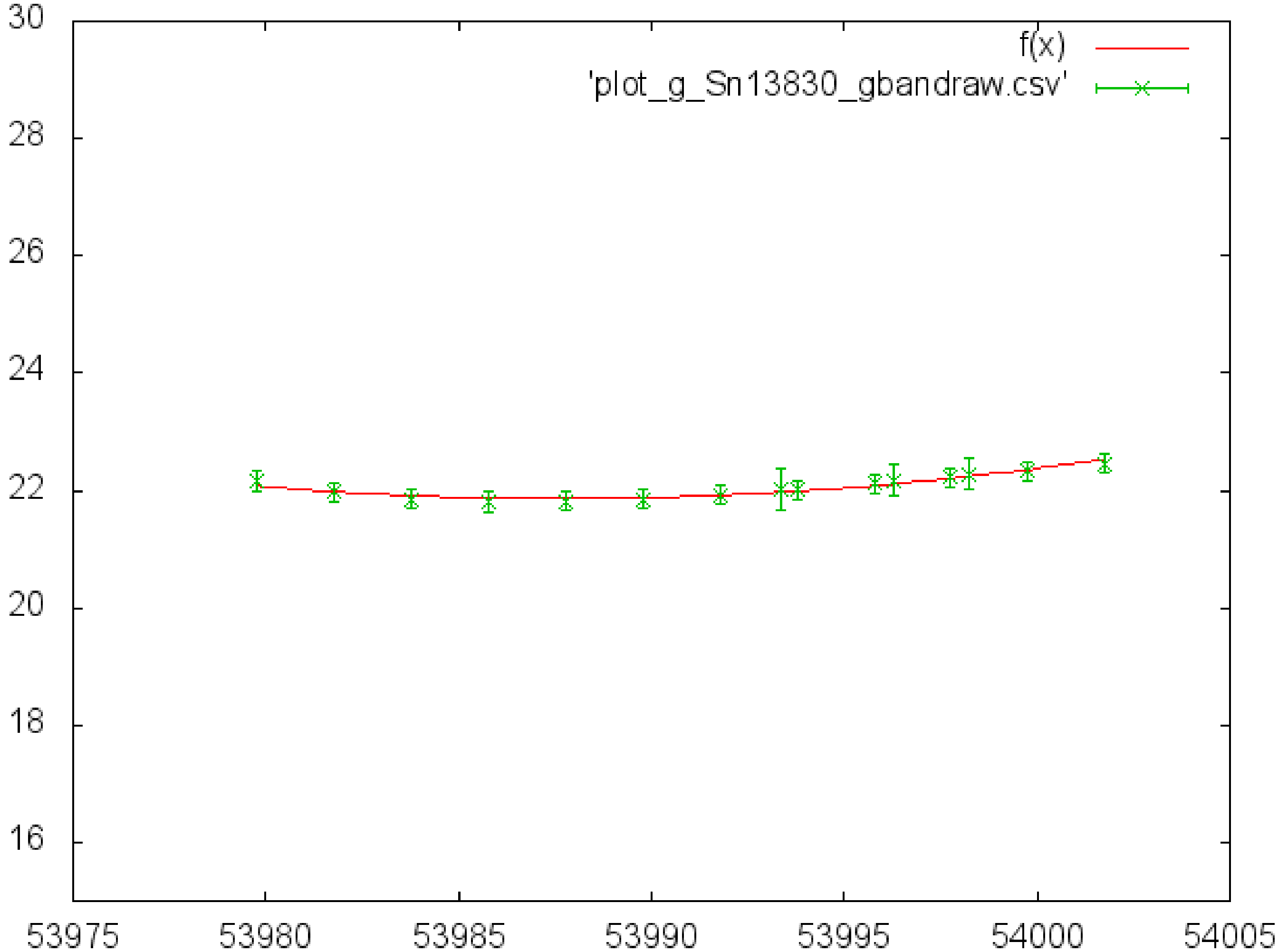

f(x)
'plot_g_Sn13830_gbandraw.csv'
30
28
26
24
22
20
18
16
53975
53980
53985
53990
53995
54000
54005

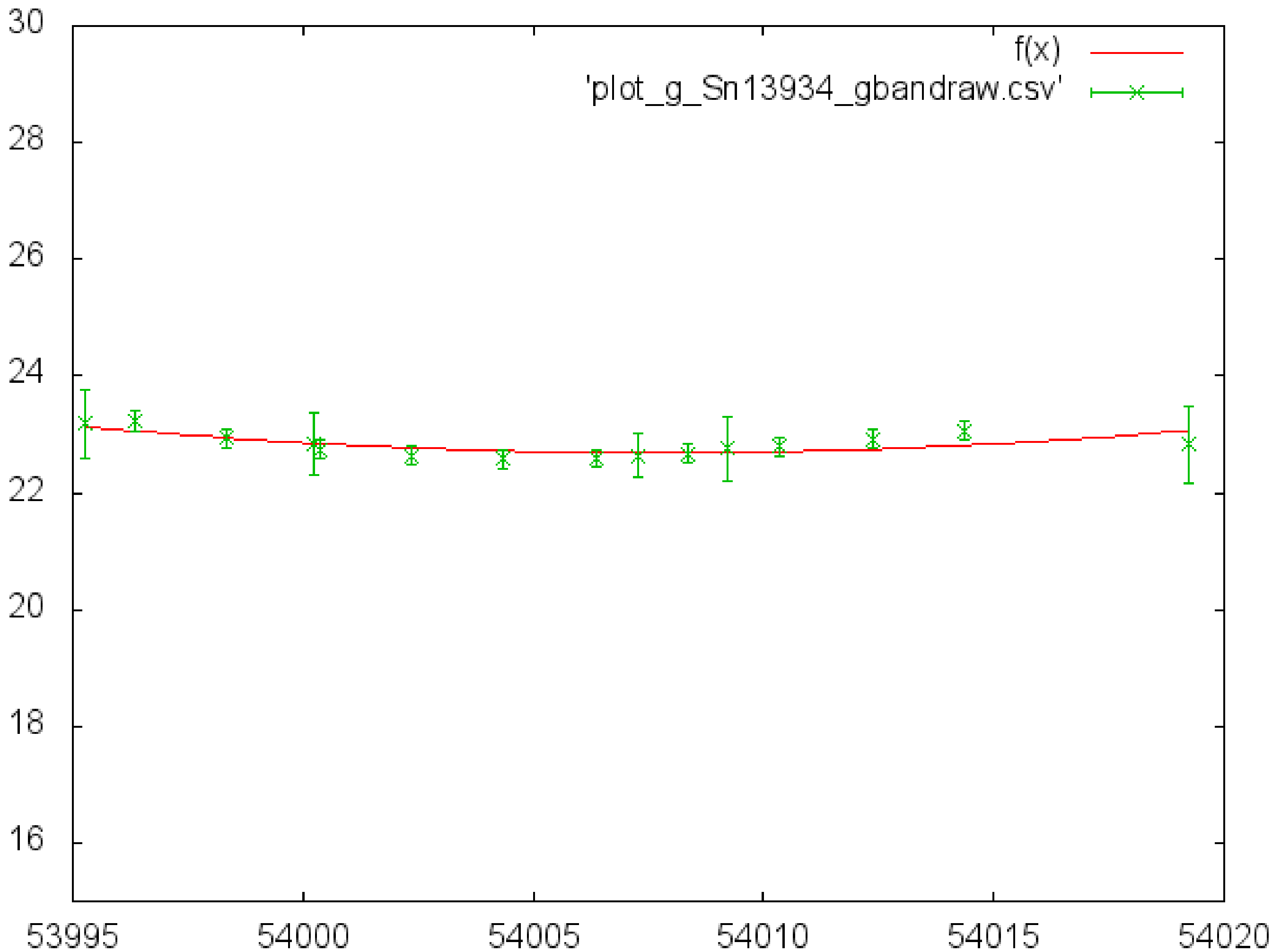
f(x)
'plot_g_Sn13934_gbandraw.csv'
30
28
26
24
22
20
18
16
53995
54000
54005
54010
54015
54020

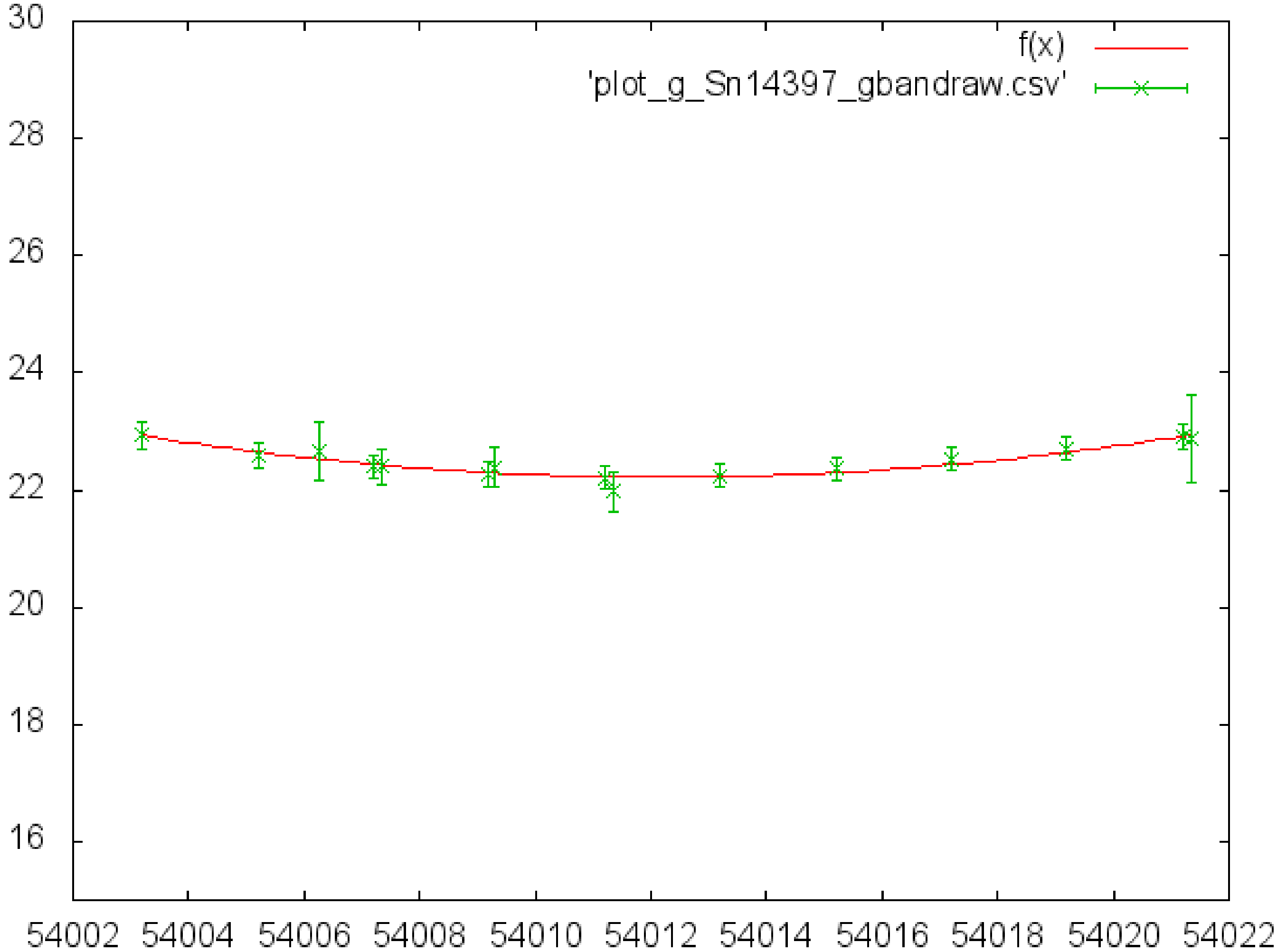

f(x)
'plot_g_Sn14397_gbandraw.csv'
30
28
26
24
22
20
18
16
54002
54004
54006
54008
54010
54012
54014
54016
54018
54020
54022

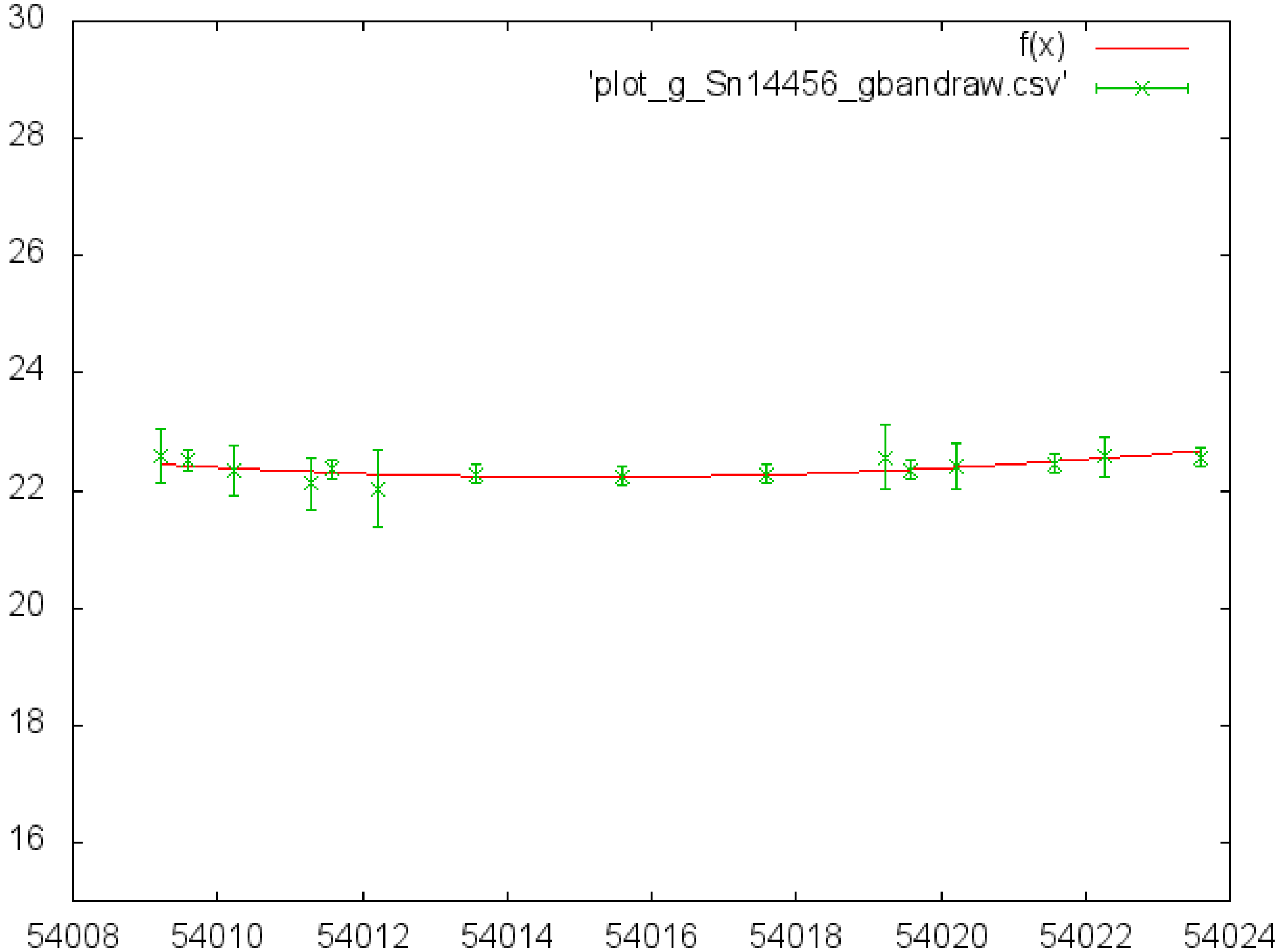

f(x)
'plot_g_Sn14456_gbandraw.csv'
30
28
26
24
22
20
18
16
54008
54010
54012
54014
54016
54018
54020
54022
54024

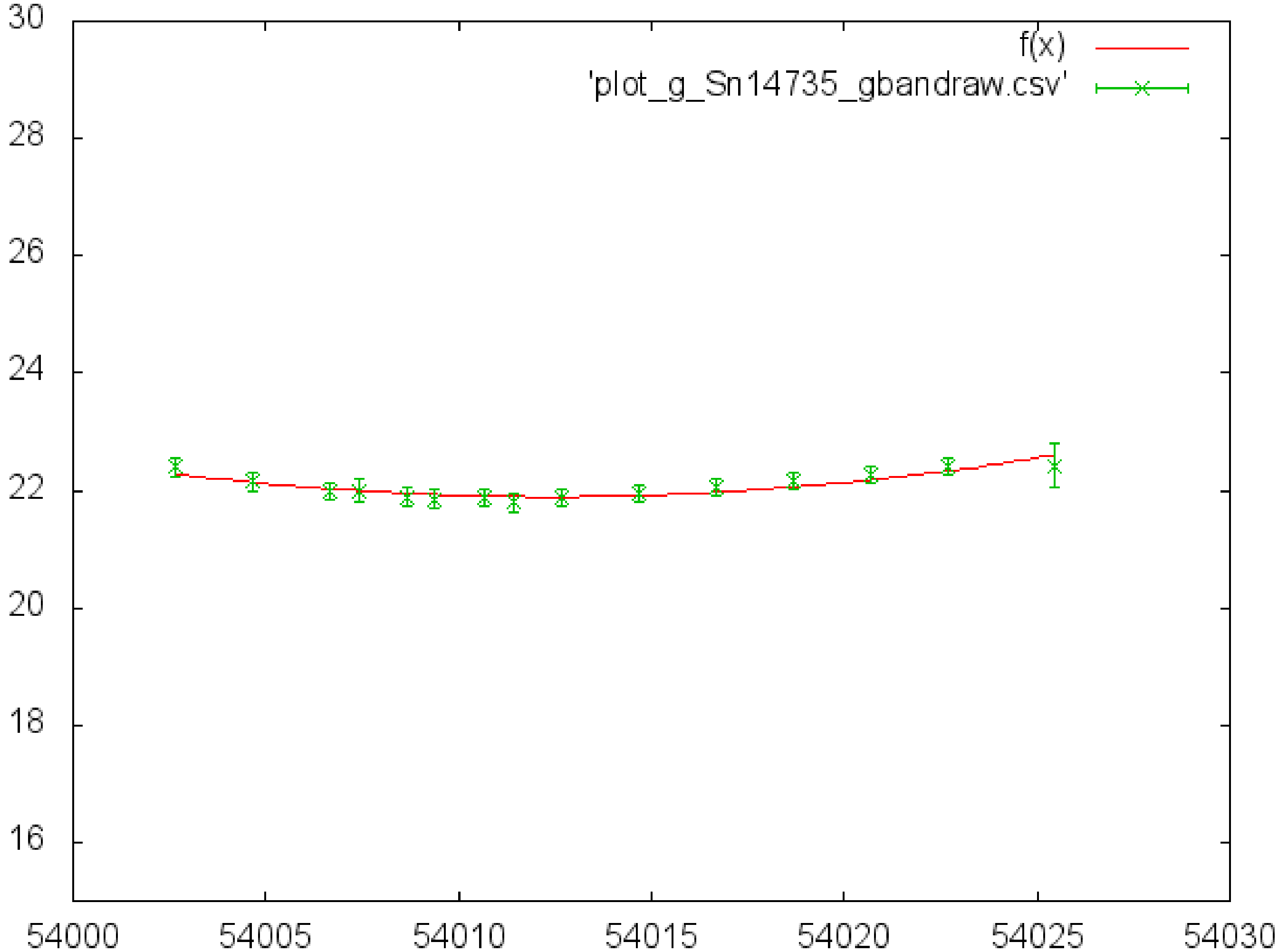

f(x)
'plot_g_Sn14735_gbandraw.csv'
30
28
26
24
22
20
18
16
54000
54005
54010
54015
54020
54025
54030

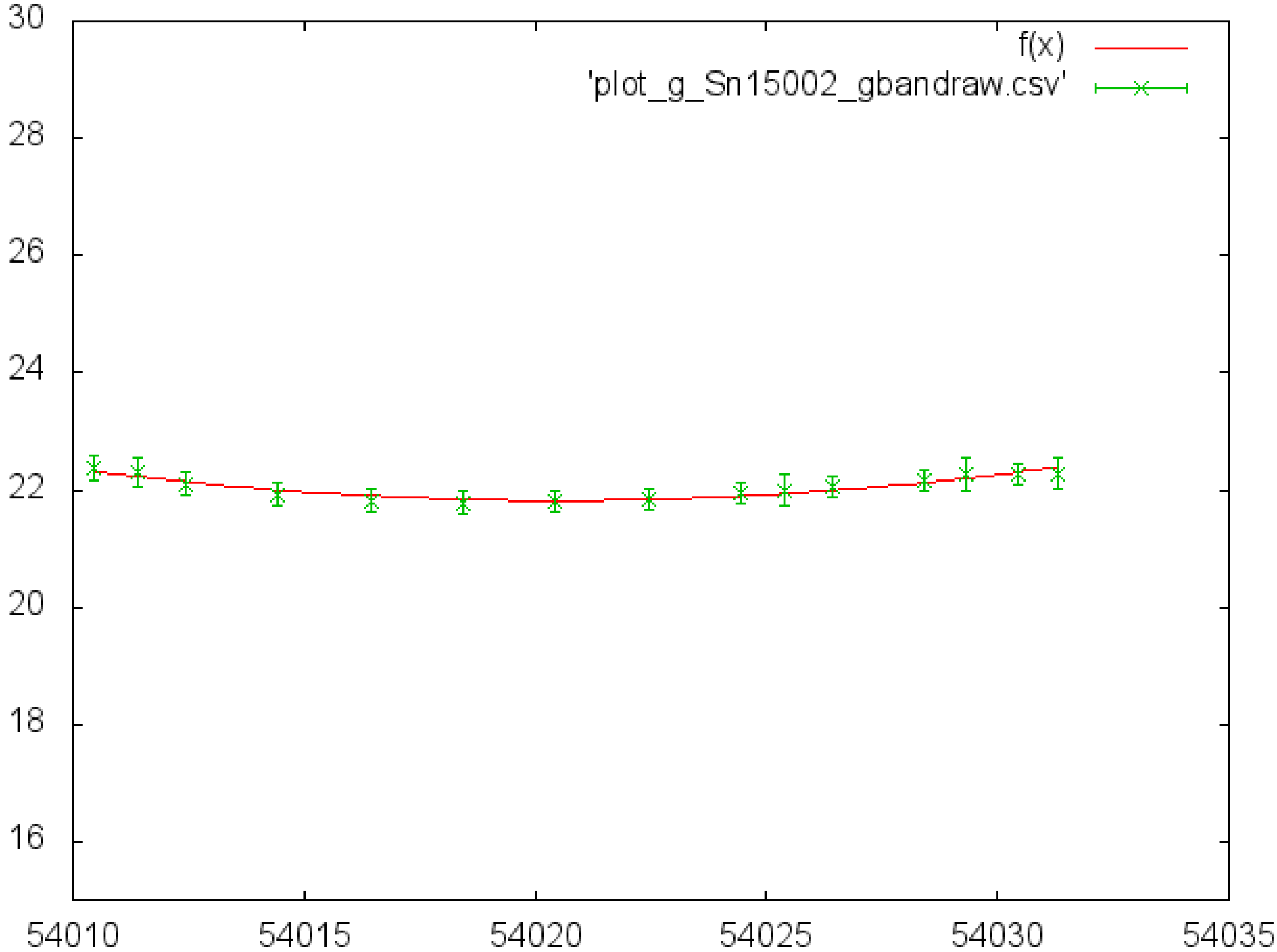

f(x)
'plot_g_Sn15002_gbandraw.csv'
30
28
26
24
22
20
18
16
54010
54015
54020
54025
54030
54035

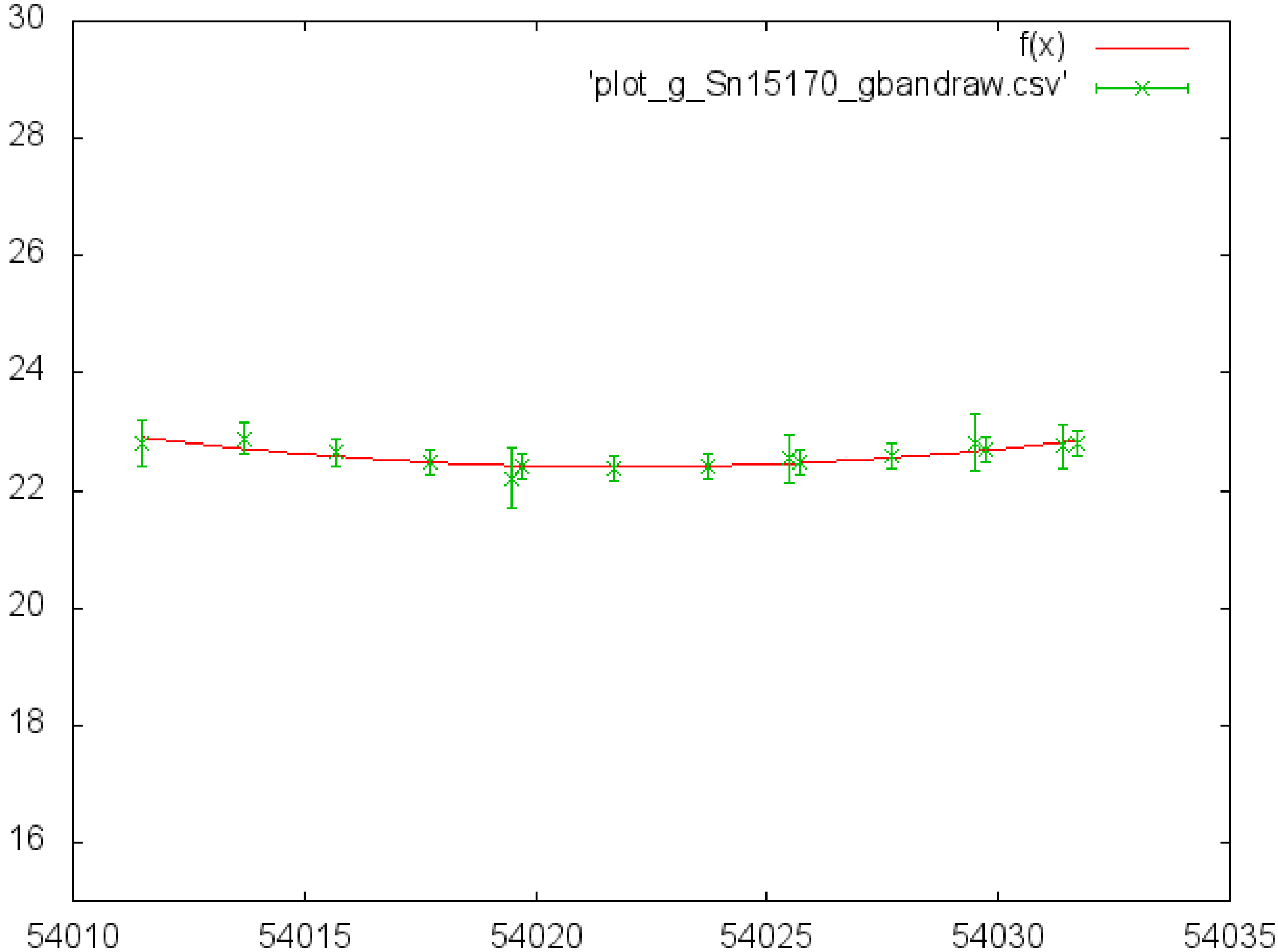

f(x)
'plot_g_Sn15170_gbandraw.csv'
30
28
26
24
22
20
18
16
54010
54015
54020
54025
54030
54035

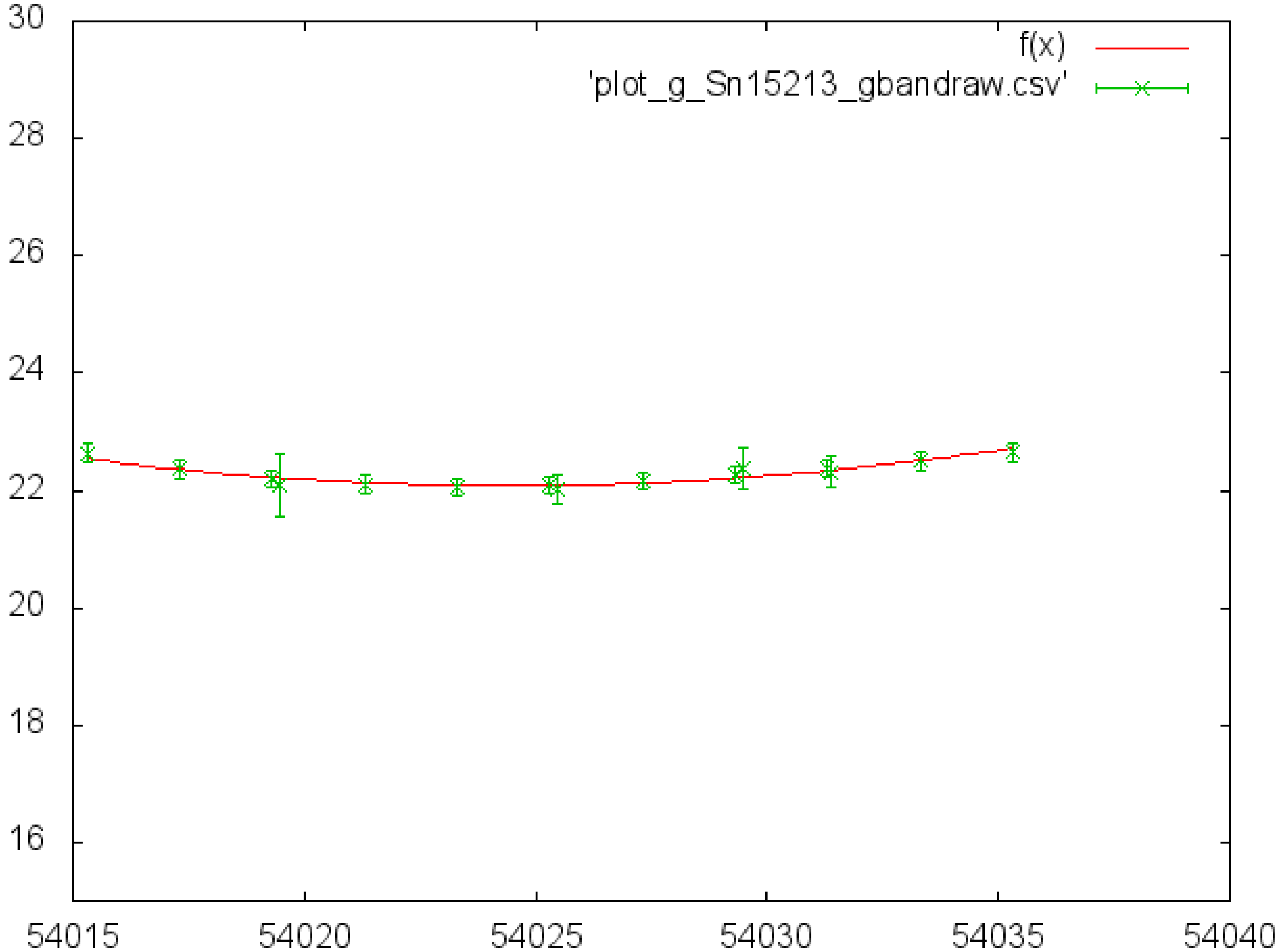
f(x)
'plot_g_Sn15213_gbandraw.csv'
30
28
26
24
22
20
18
16
54015
54020
54025
54030
54035
54040

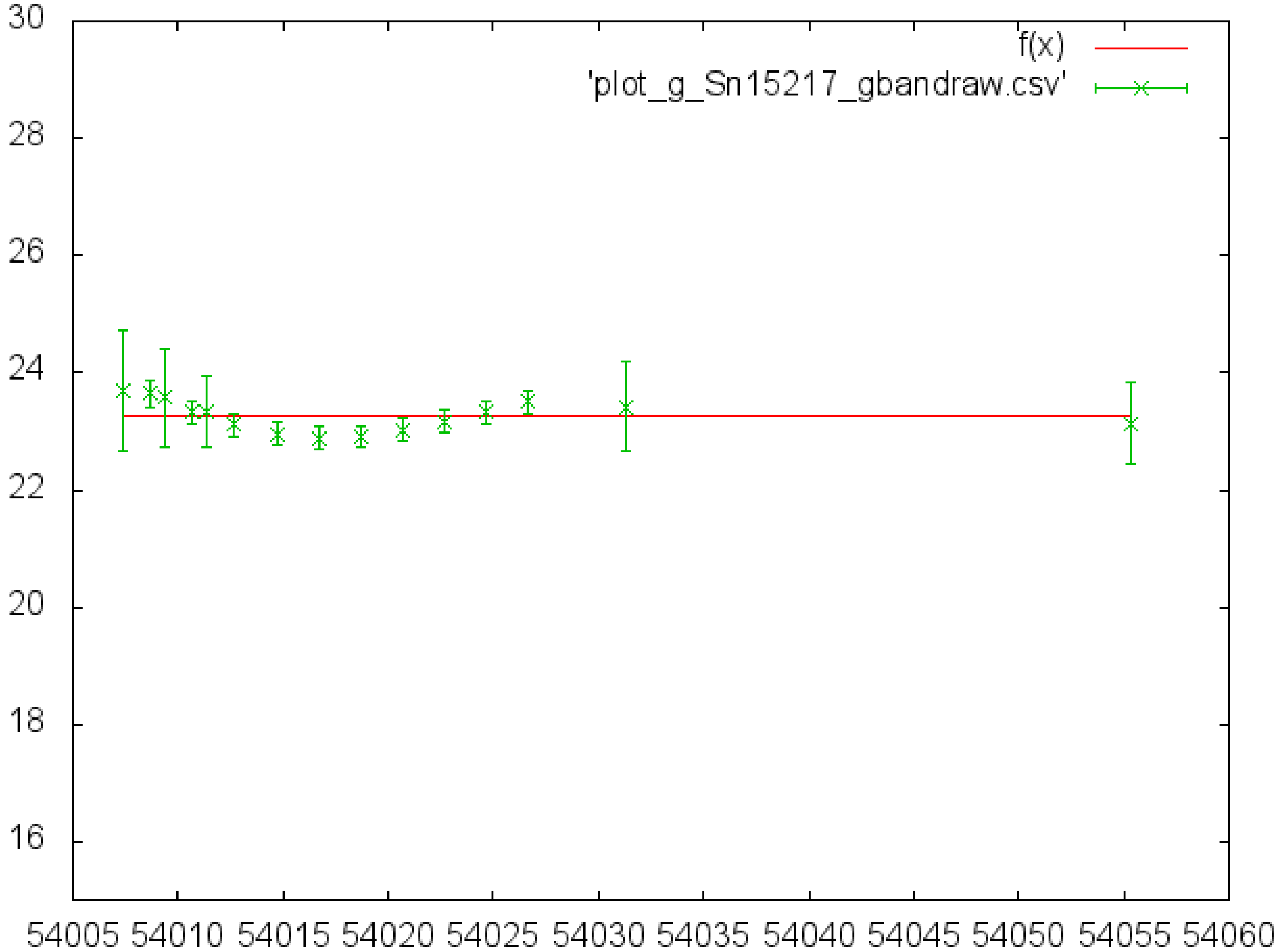

f(x)
'plot_g_Sn15217_gbandraw.csv'
30
28
26
24
22
20
18
16
54005 54010 54015 54020 54025 54030 54035 54040 54045 54050 54055 54060

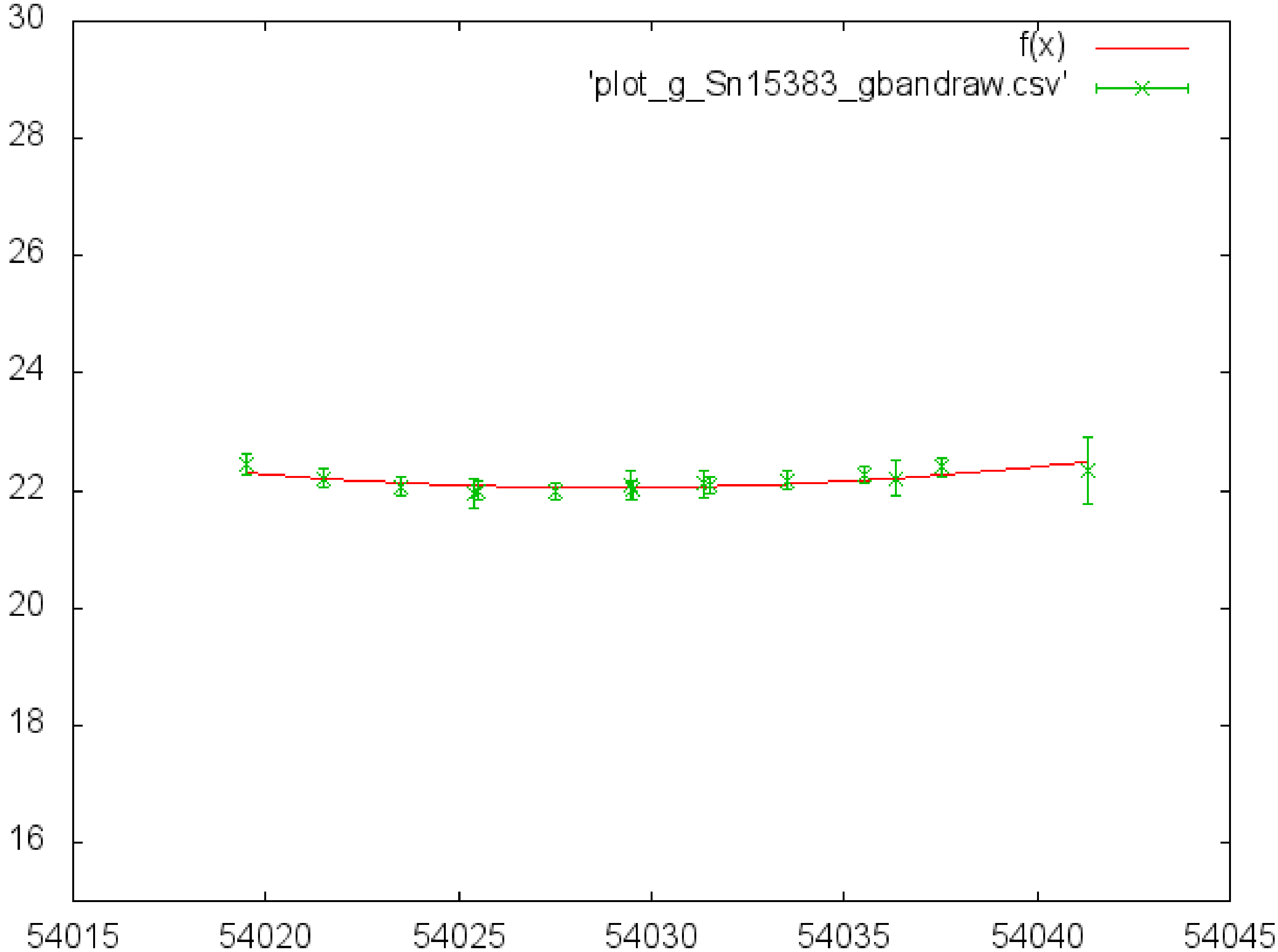
f(x)
'plot_g_Sn15383_gbandraw.csv'
30
28
26
24
22
20
18
16
54015
54020
54025
54030
54035
54040
54045

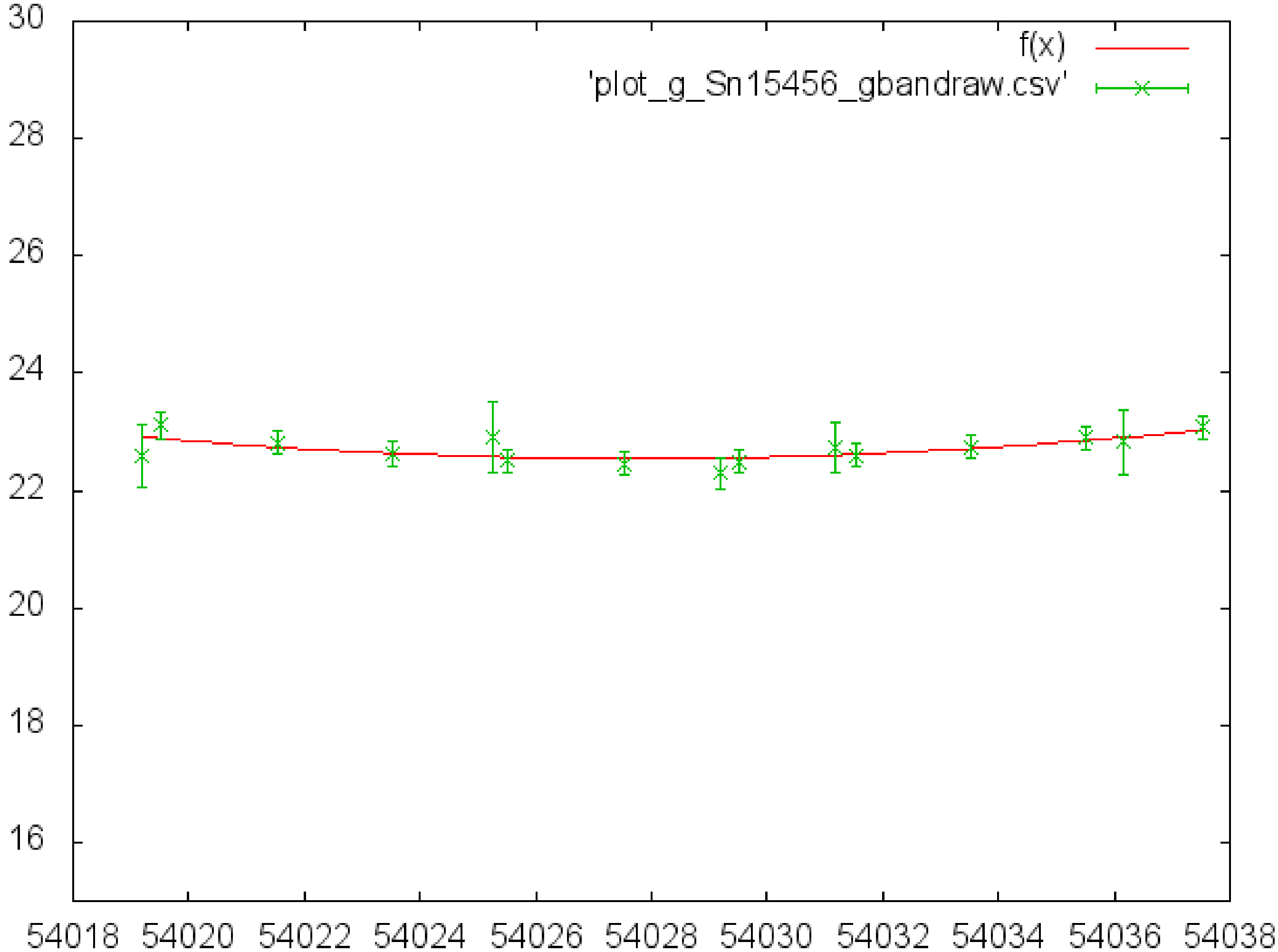
f(x)
'plot_g_Sn15456_gbandraw.csv'
30
28
26
24
22
20
18
16
54018
54020
54022
54024
54026
54028
54030
54032
54034
54036
54038

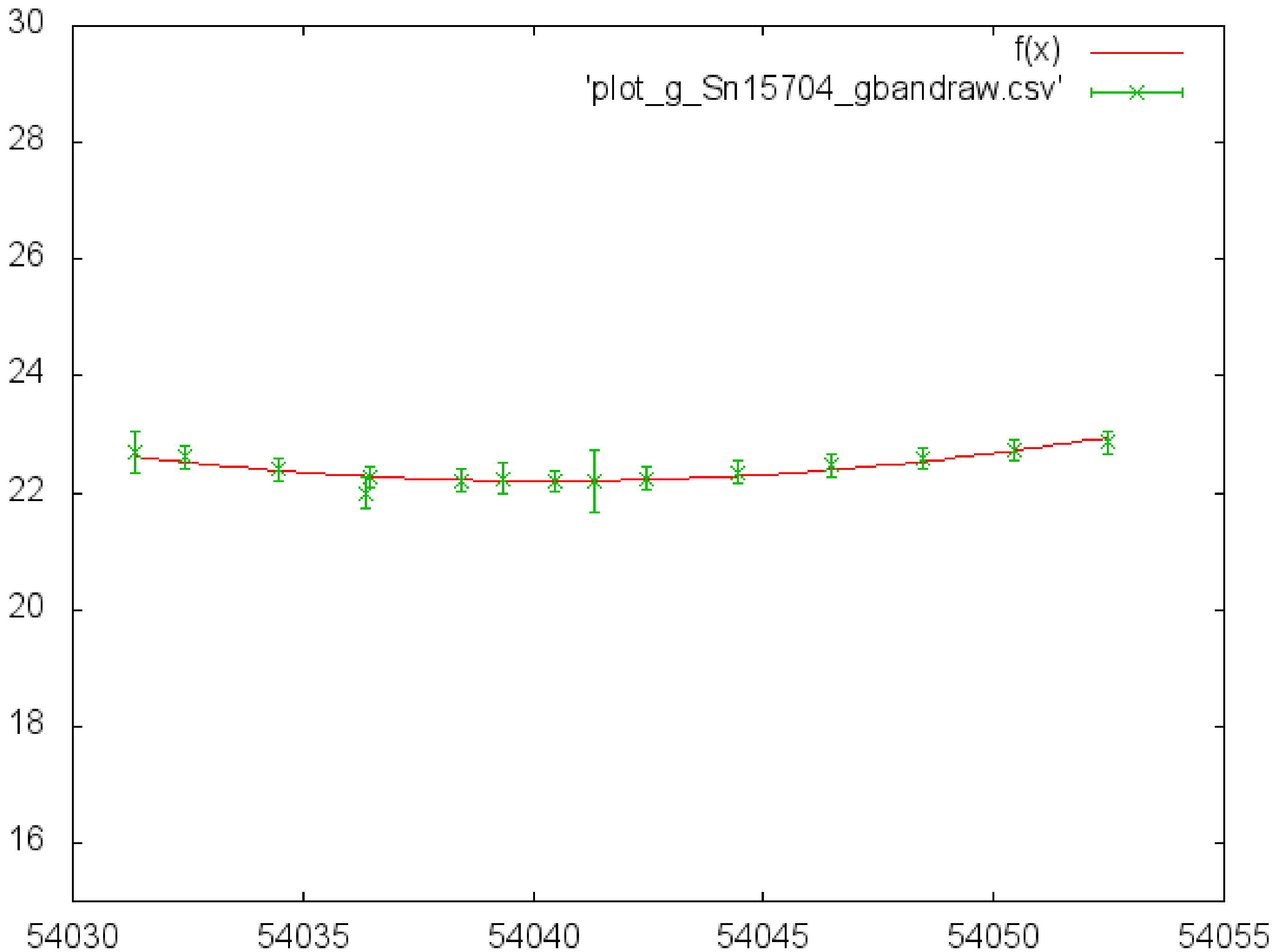

f(x)
'plot_g_Sn15704_gbandraw.csv'
30
28
26
24
22
20
18
16
54030
54035
54040
54045
54050
54055

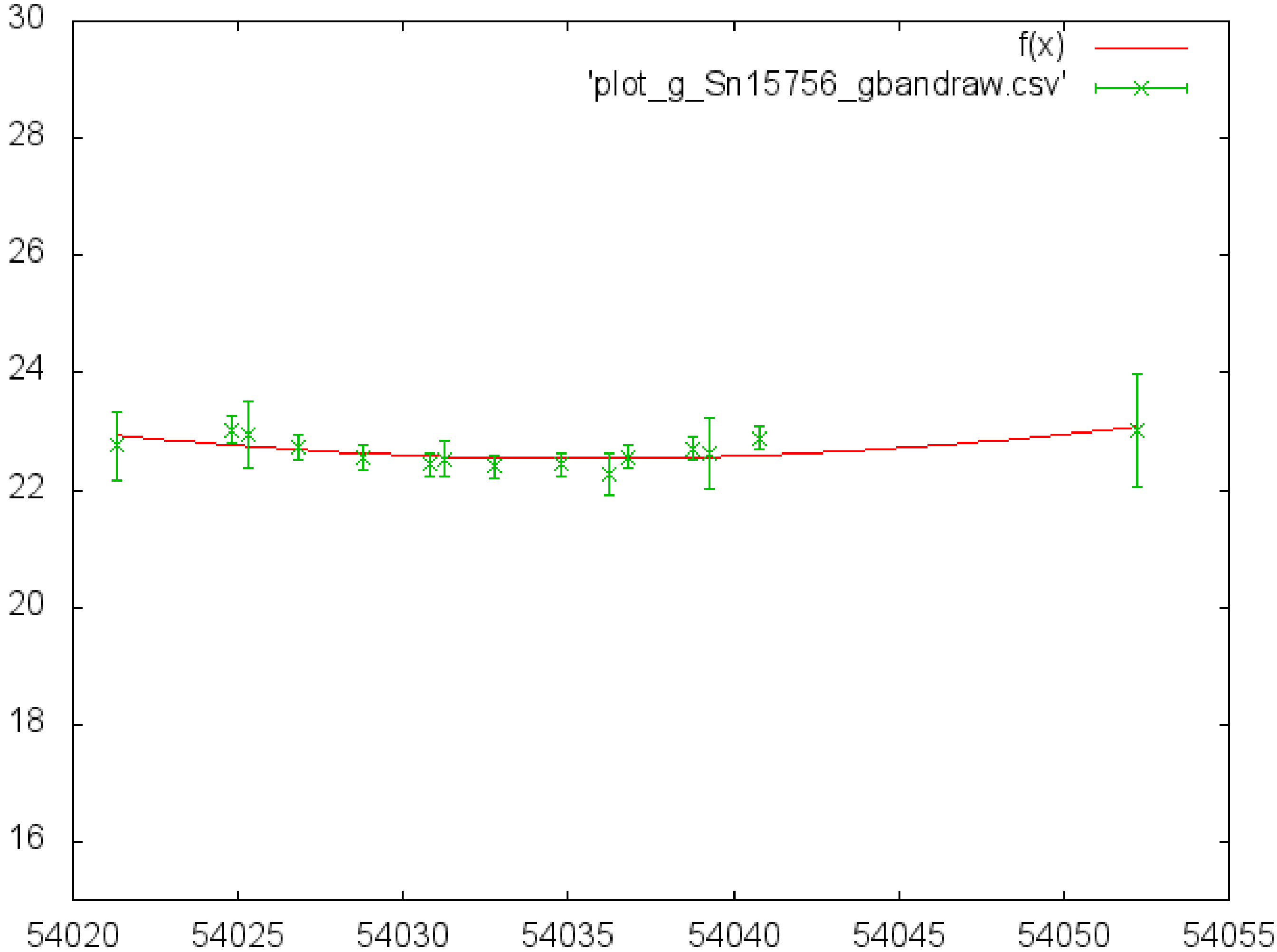

f(x)
'plot_g_Sn15756_gbandraw.csv'
30
28
26
24
22
20
18
16
54020
54025
54030
54035
54040
54045
54050
54055

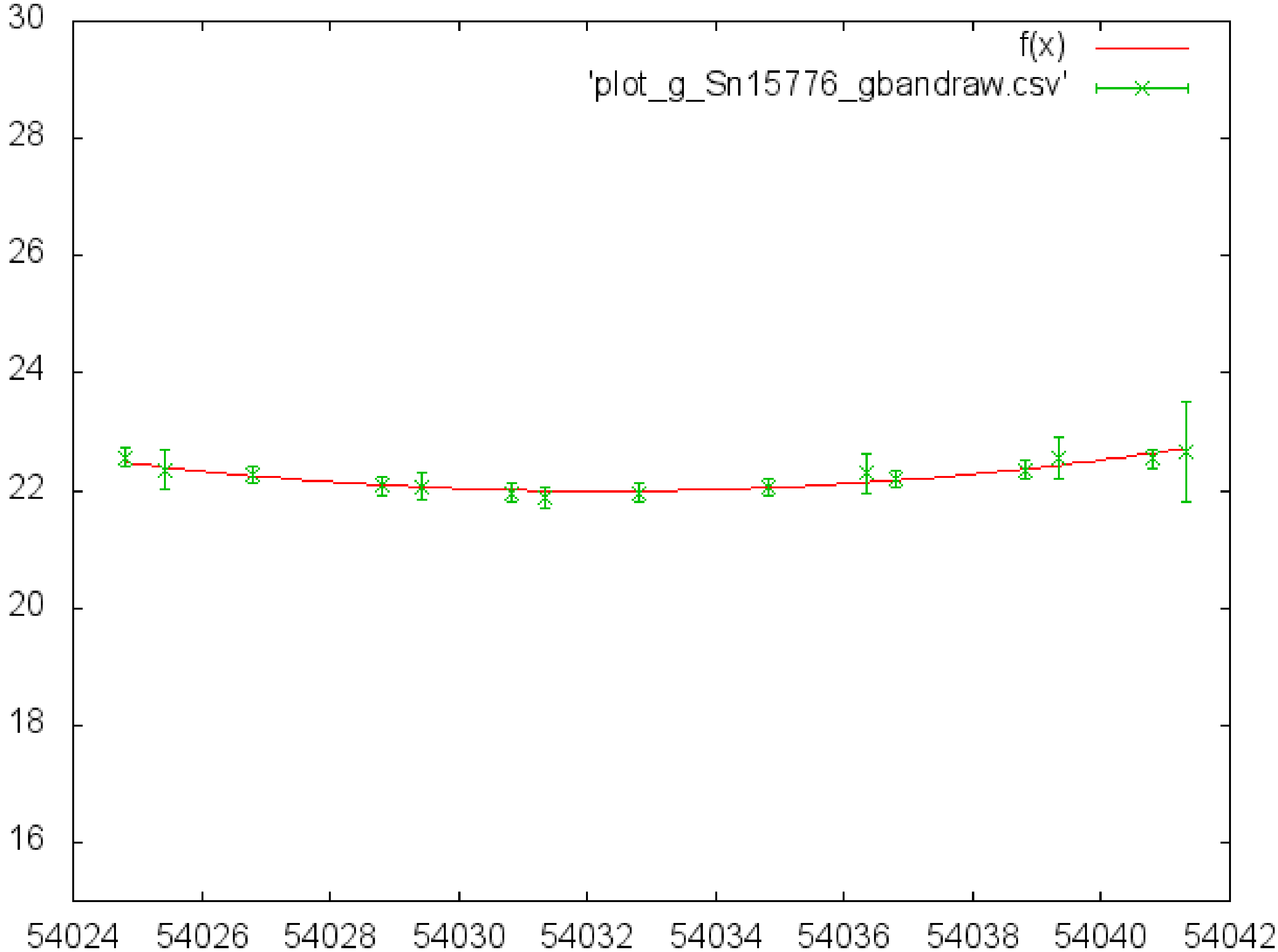

f(x)
'plot_g_Sn15776_gbandraw.csv'
30
28
26
24
22
20
18
16
54024
54026
54028
54030
54032
54034
54036
54038
54040
54042

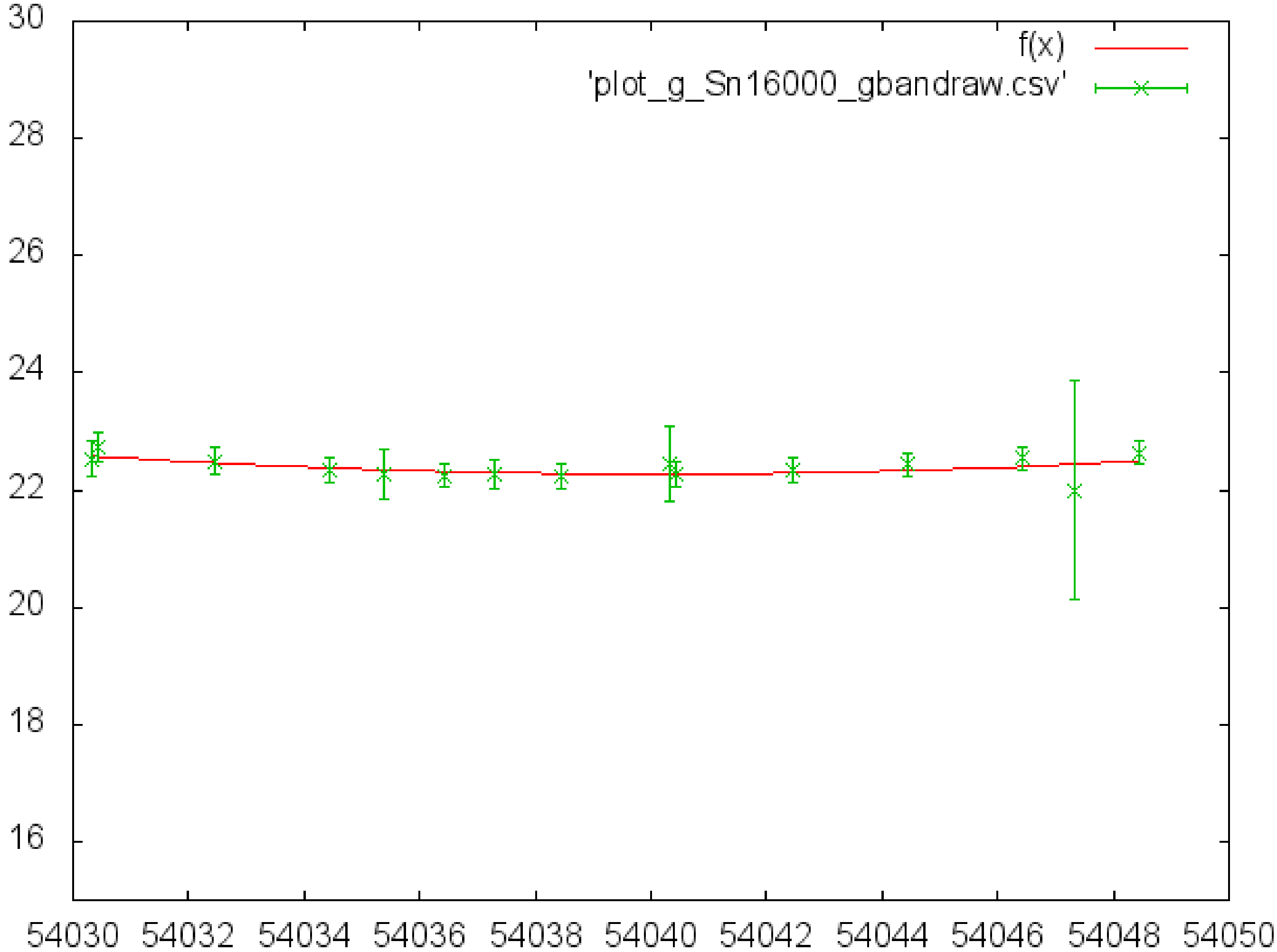

30
28
26
24
22
20
18
16
54030 54032 54034 54036 54038 54040 54042 54044 54046 54048 54050
f(x)
'plot_g_Sn16000_gbandraw.csv'

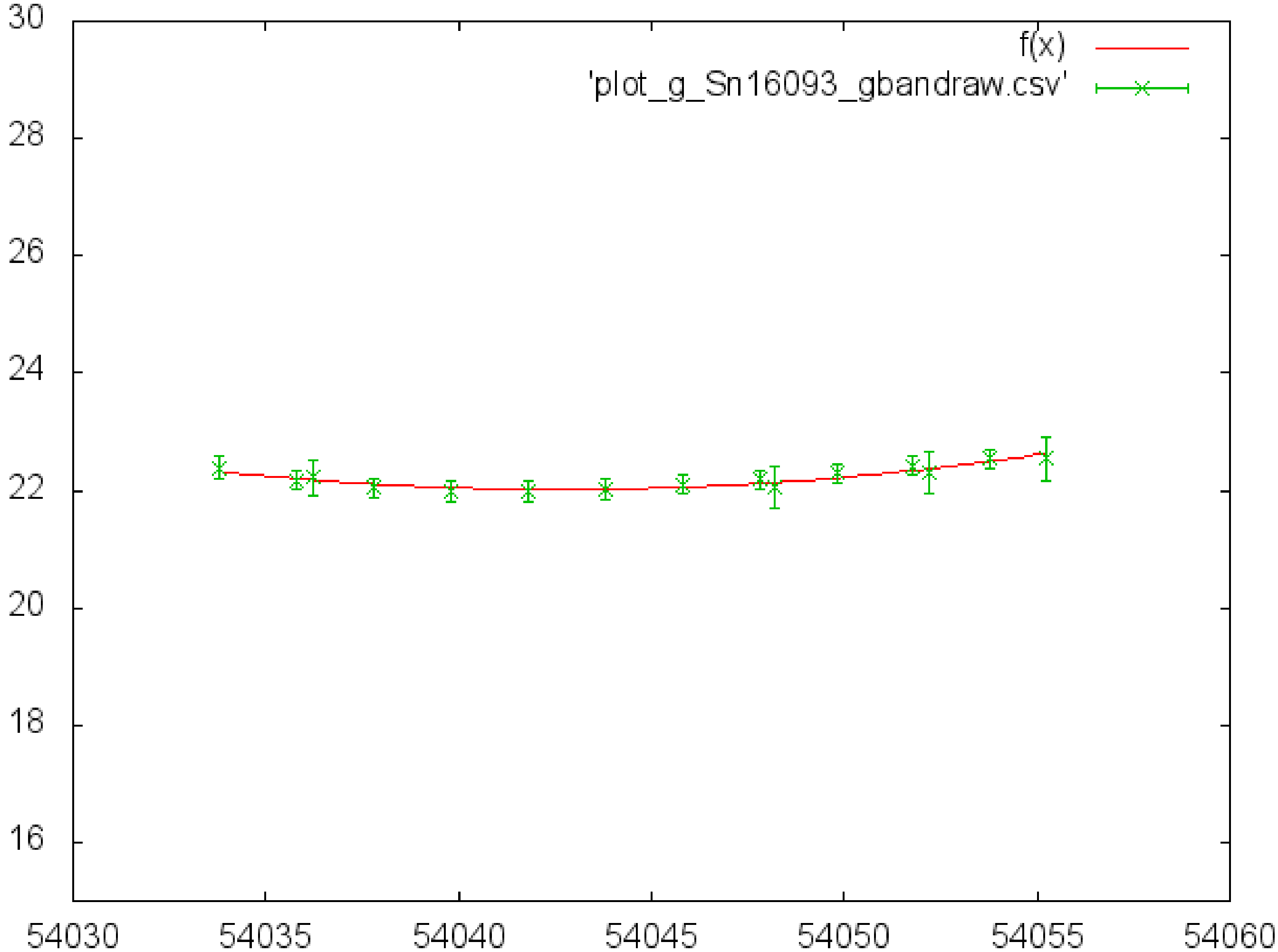

30
28
26
24
22
20
18
16
54030
54035
54040
54045
54050
54055
54060
f(x)
'plot_g_Sn16093_gbandraw.csv'

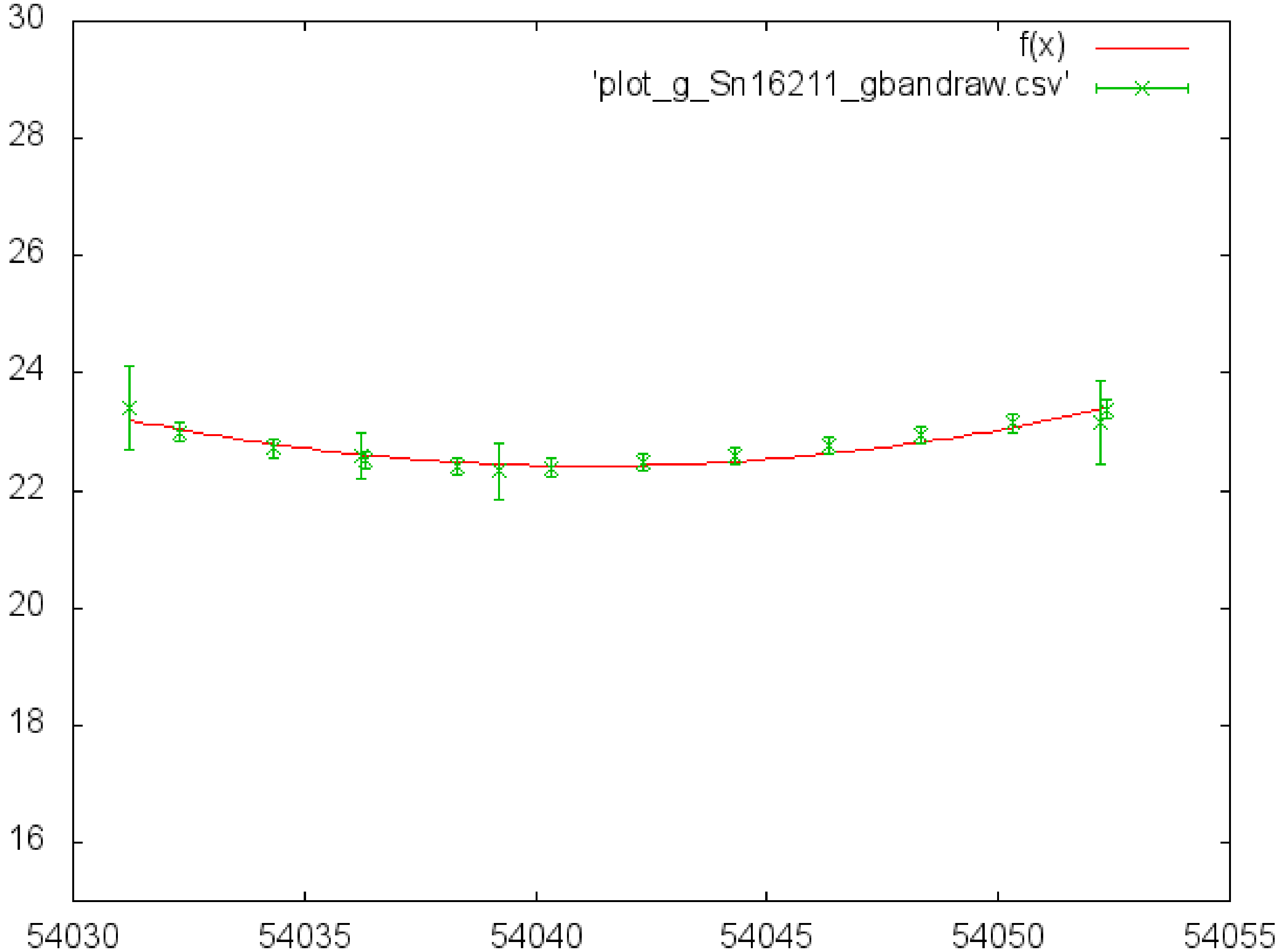
f(x)
'plot_g_Sn16211_gbandraw.csv'
30
28
26
24
22
20
18
16
54030
54035
54040
54045
54050
54055

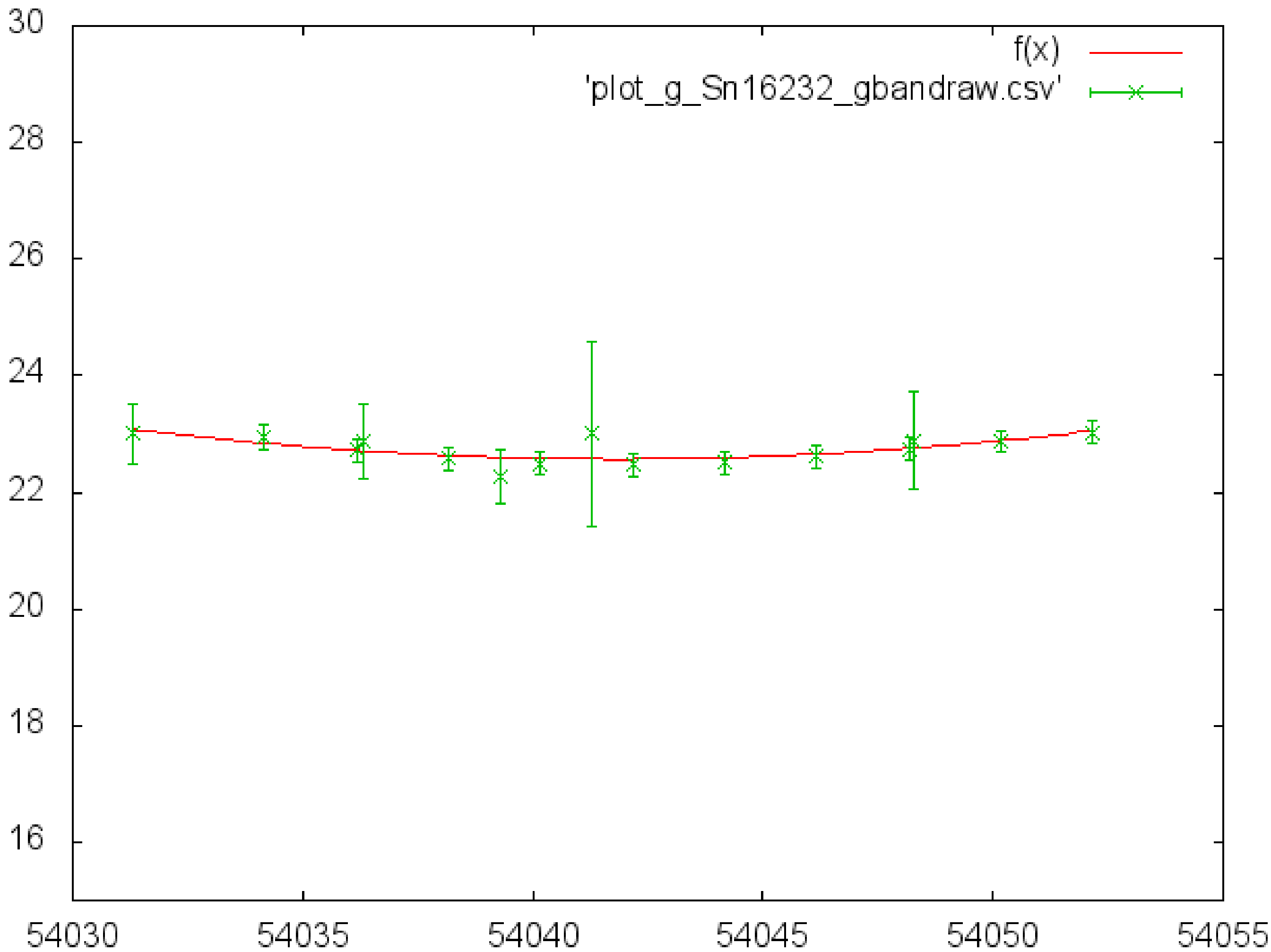
f(x)
'plot_g_Sn16232_gbandraw.csv'
30
28
26
24
22
20
18
16
54030
54035
54040
54045
54050
54055

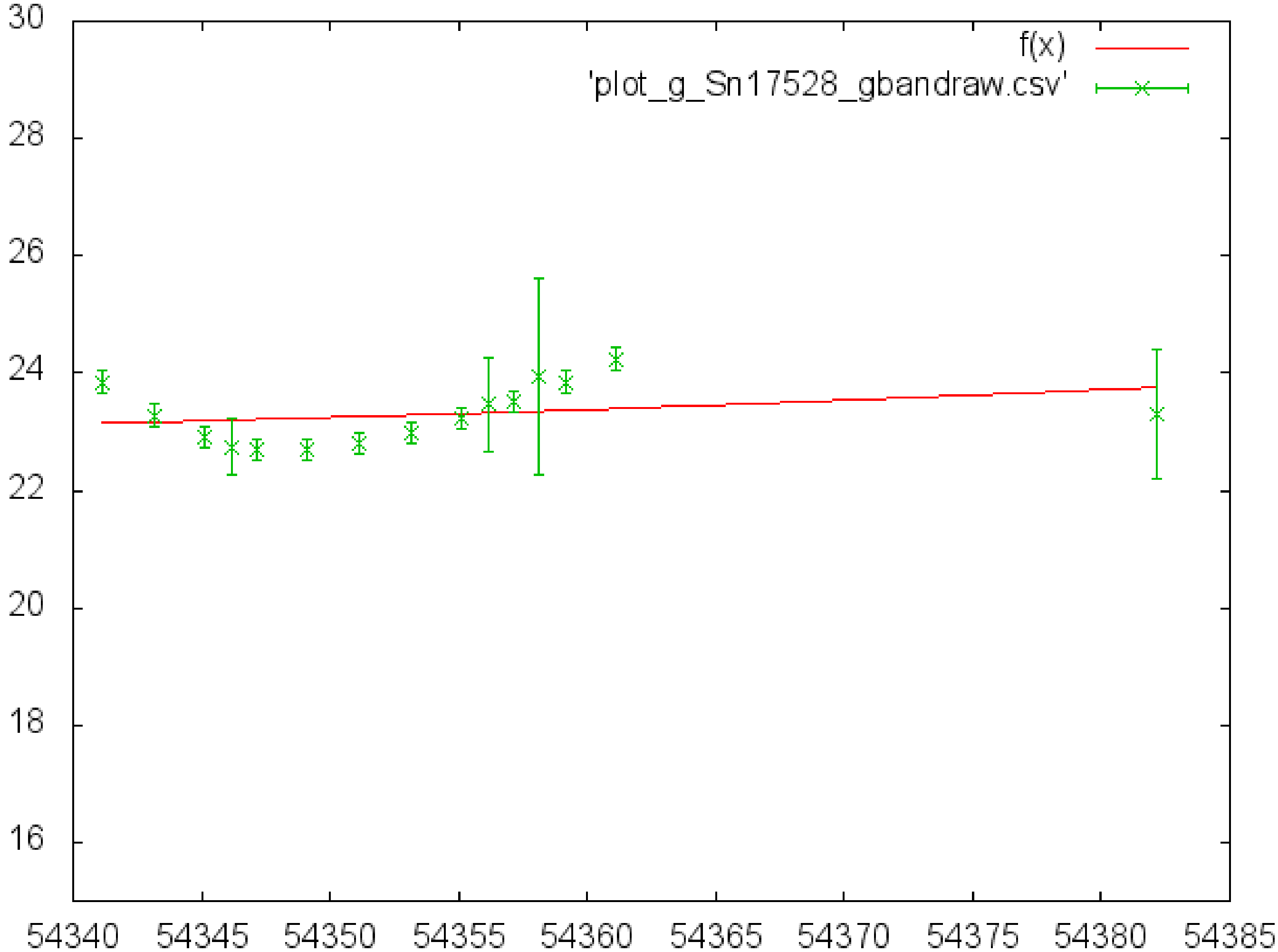

f(x)
'plot_g_Sn17528_gbandraw.csv'
30
28
26
24
22
20
18
16
54340
54345
54350
54355
54360
54365
54370
54375
54380
54385

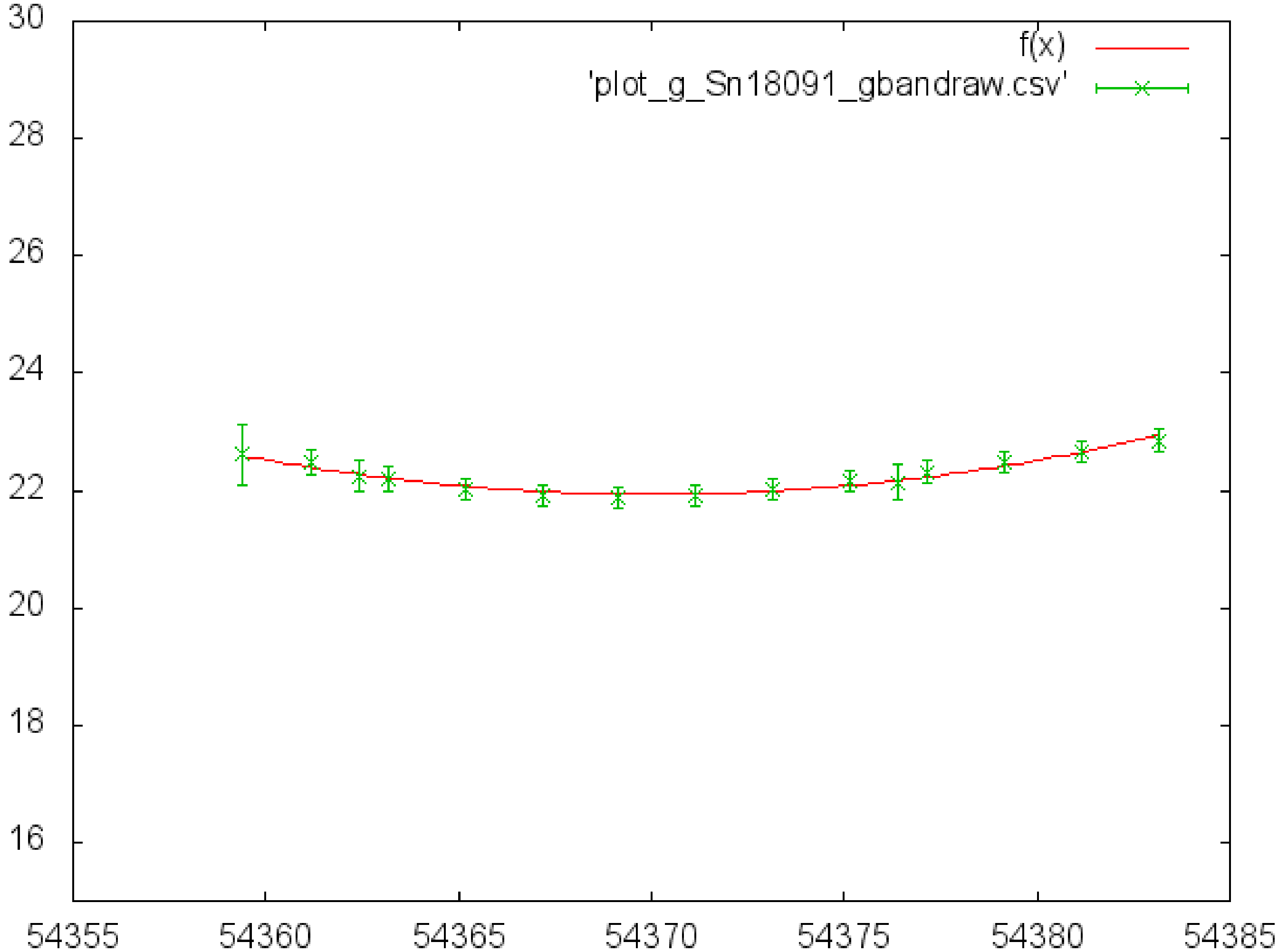
30
28
26
24
22
20
18
16
54355
54360
54365
54370
54375
54380
54385
f(x)
'plot_g_Sn18091_gbandraw.csv'

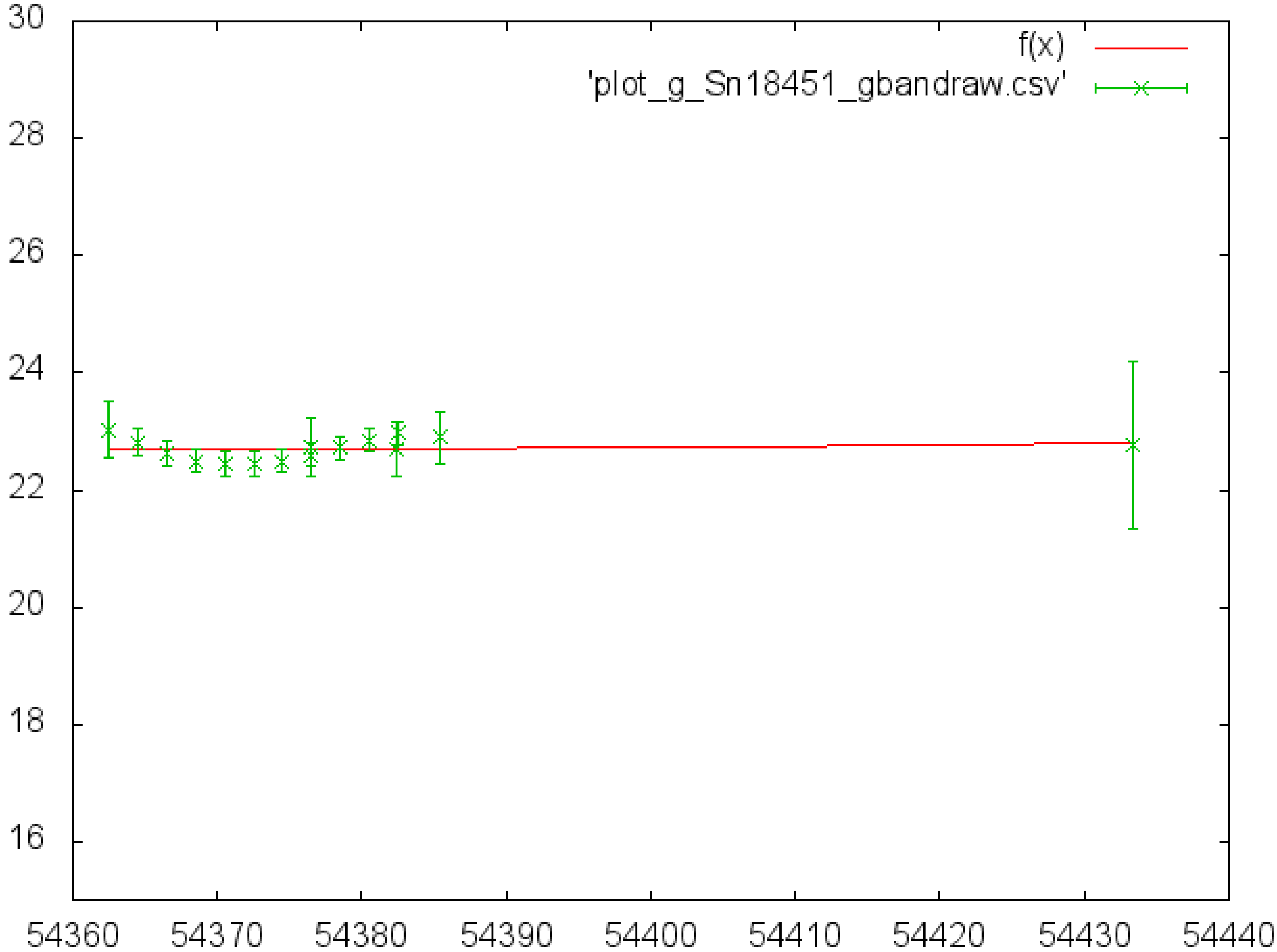

30
28
26
24
22
20
18
16
54360
54370
54380
54390
54400
54410
54420
54430
54440
f(x)
'plot_g_Sn18451_gbandraw.csv'

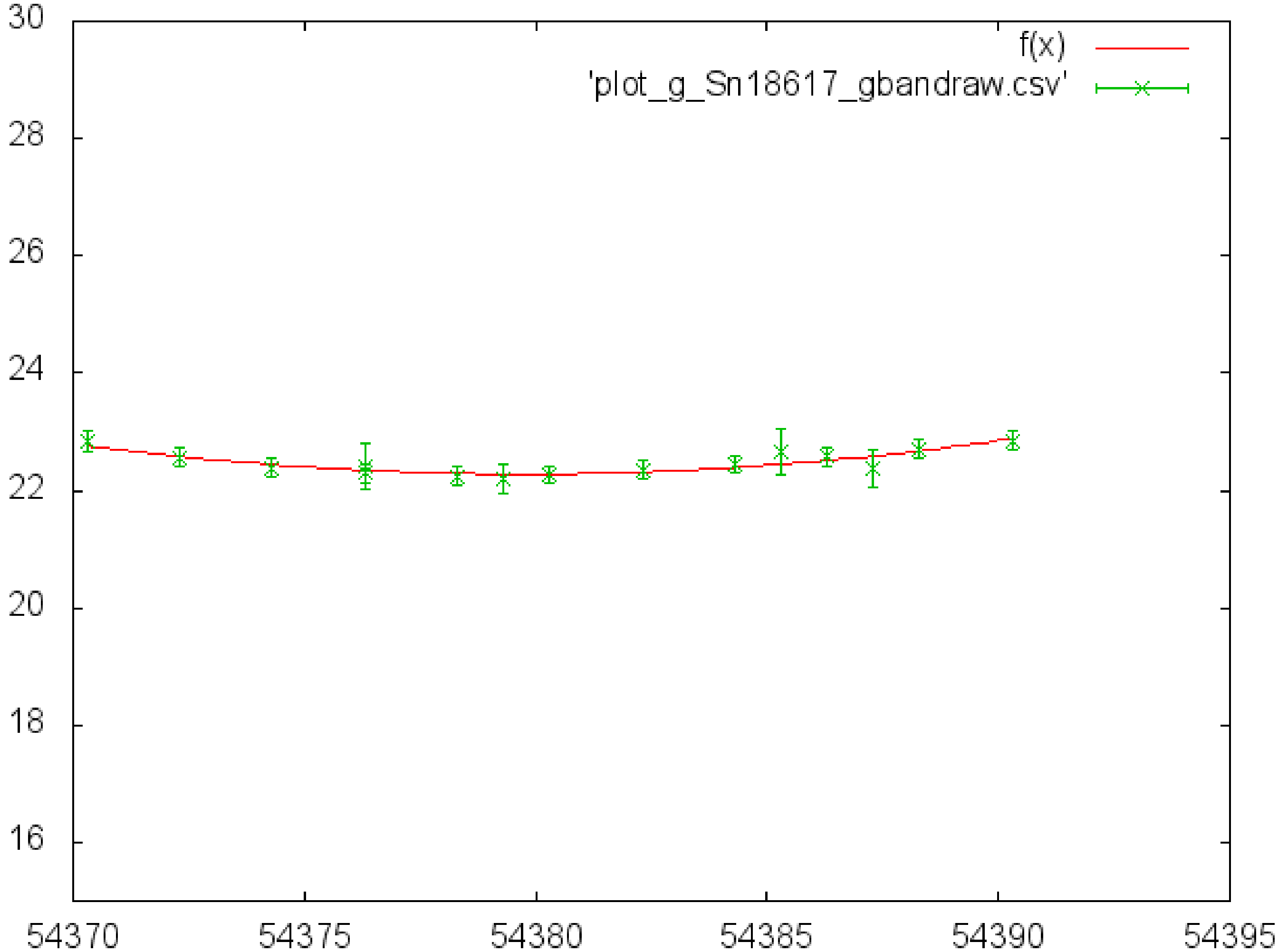
f(x)
'plot_g_Sn18617_gbandraw.csv'
30
28
26
24
22
20
18
16
54370
54375
54380
54385
54390
54395

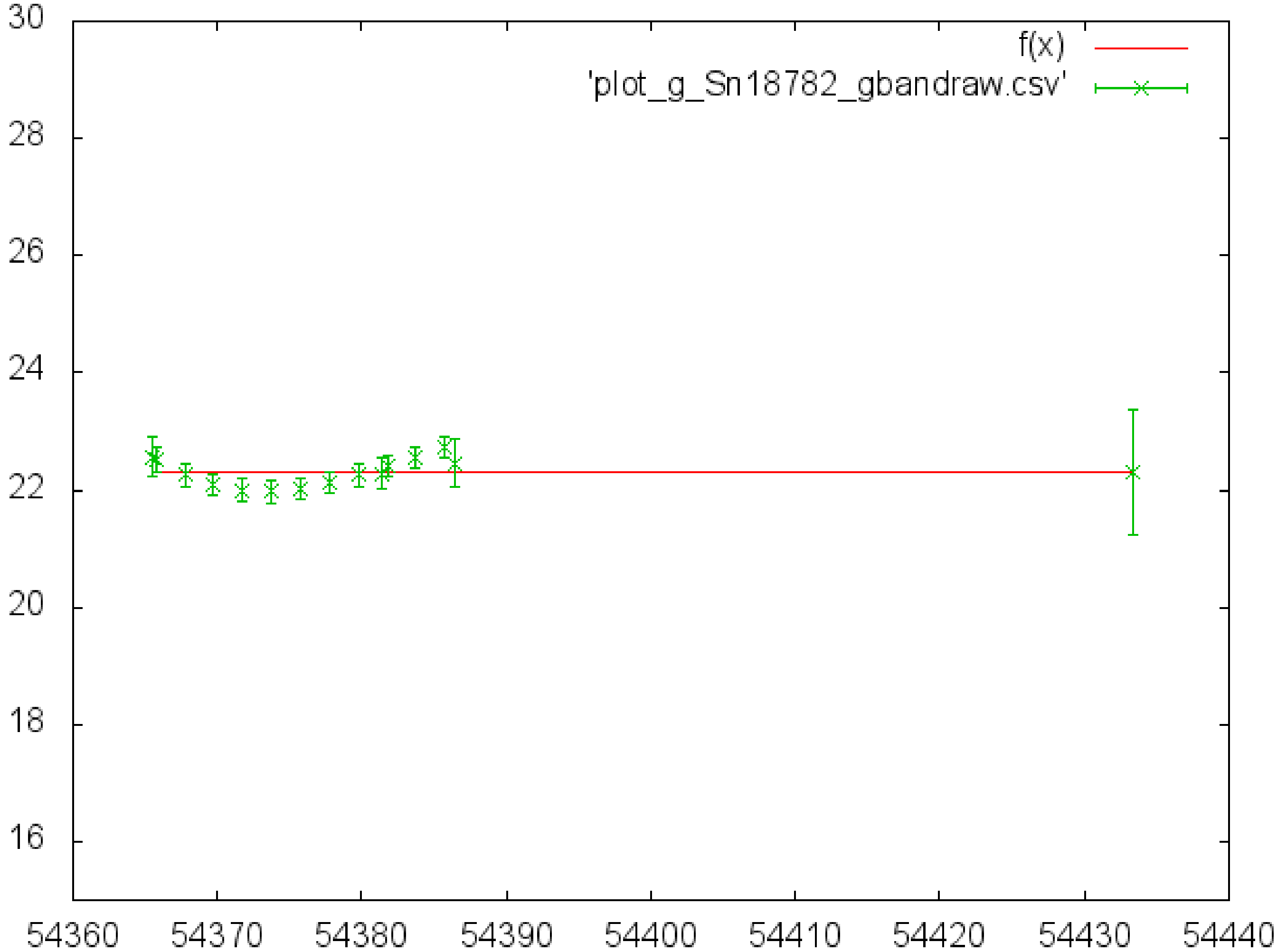

f(x)
'plot_g_Sn18782_gbandraw.csv'
30
28
26
24
22
20
18
16
54360
54370
54380
54390
54400
54410
54420
54430
54440

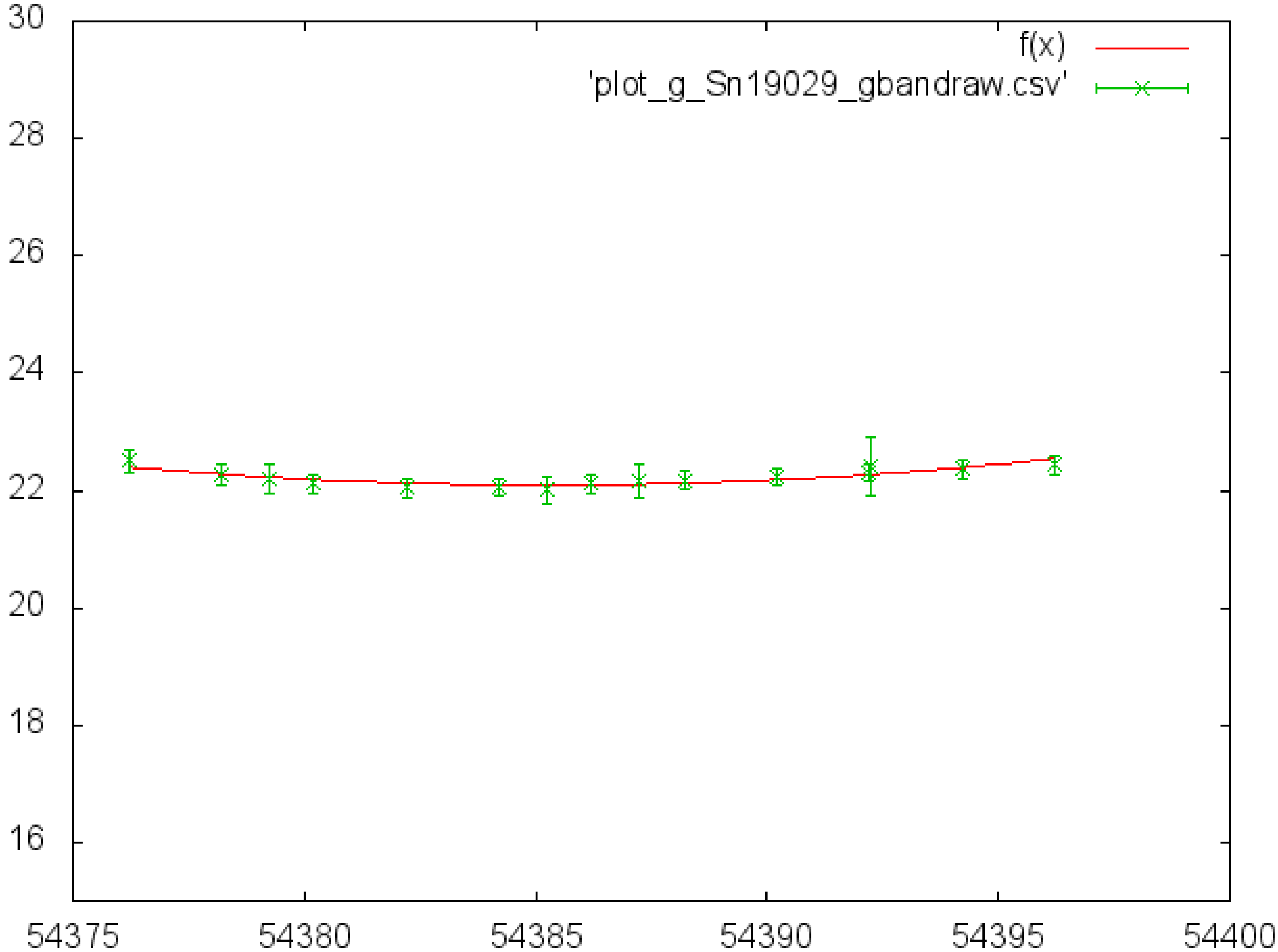
30
28
26
24
22
20
18
16
54375
54380
54385
54390
54395
54400
f(x)
'plot_g_Sn19029_gbandraw.csv'

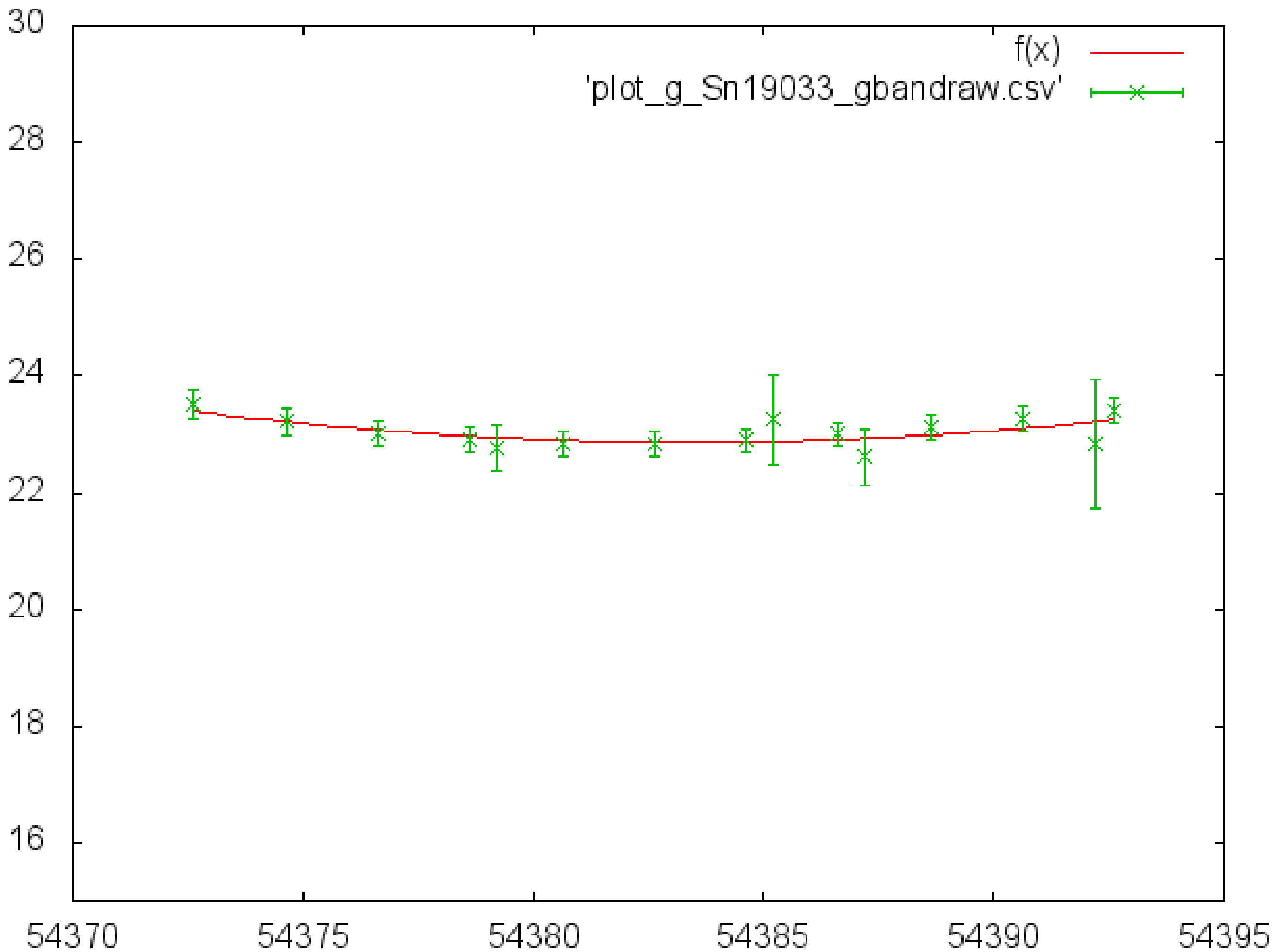

f(x)
'plot_g_Sn19033_gbandraw.csv'
30
28
26
24
22
20
18
16
54370
54375
54380
54385
54390
54395

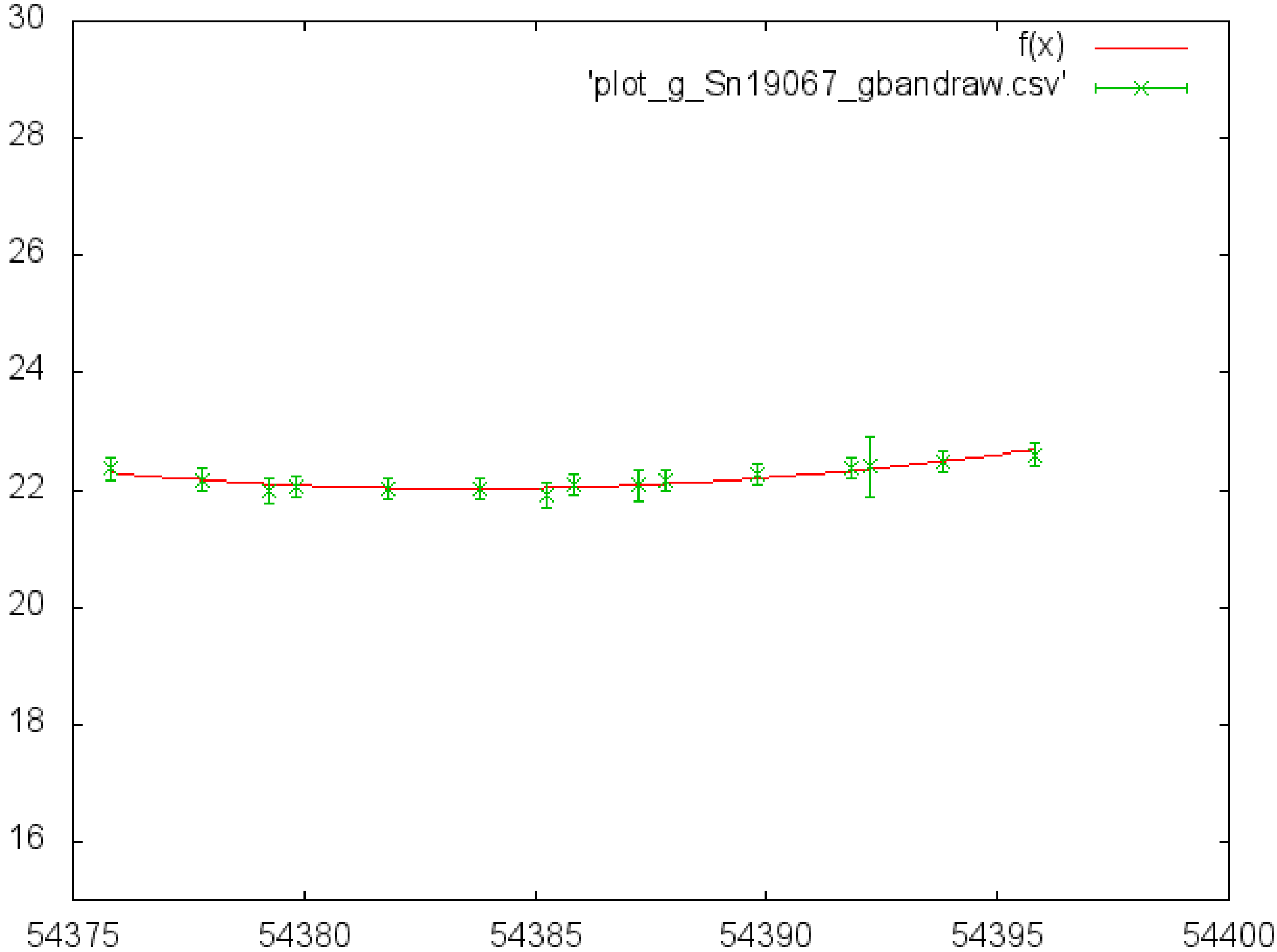

30
28
26
24
22
20
18
16
54375
54380
54385
54390
54395
54400
f(x)
'plot_g_Sn19067_gbandraw.csv'

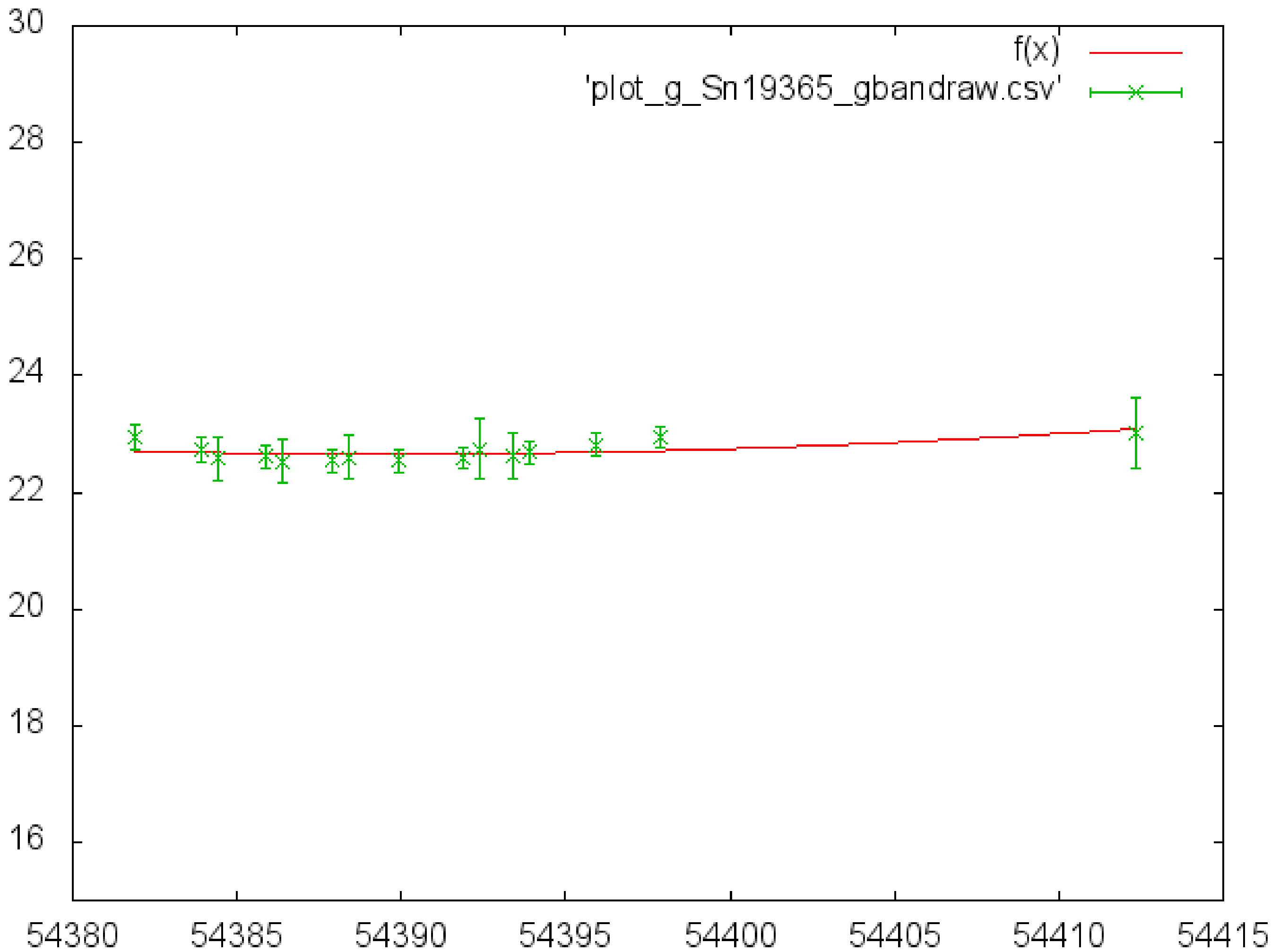

f(x)
'plot_g_Sn19365_gbandraw.csv'
30
28
26
24
22
20
18
16
54380
54385
54390
54395
54400
54405
54410
54415

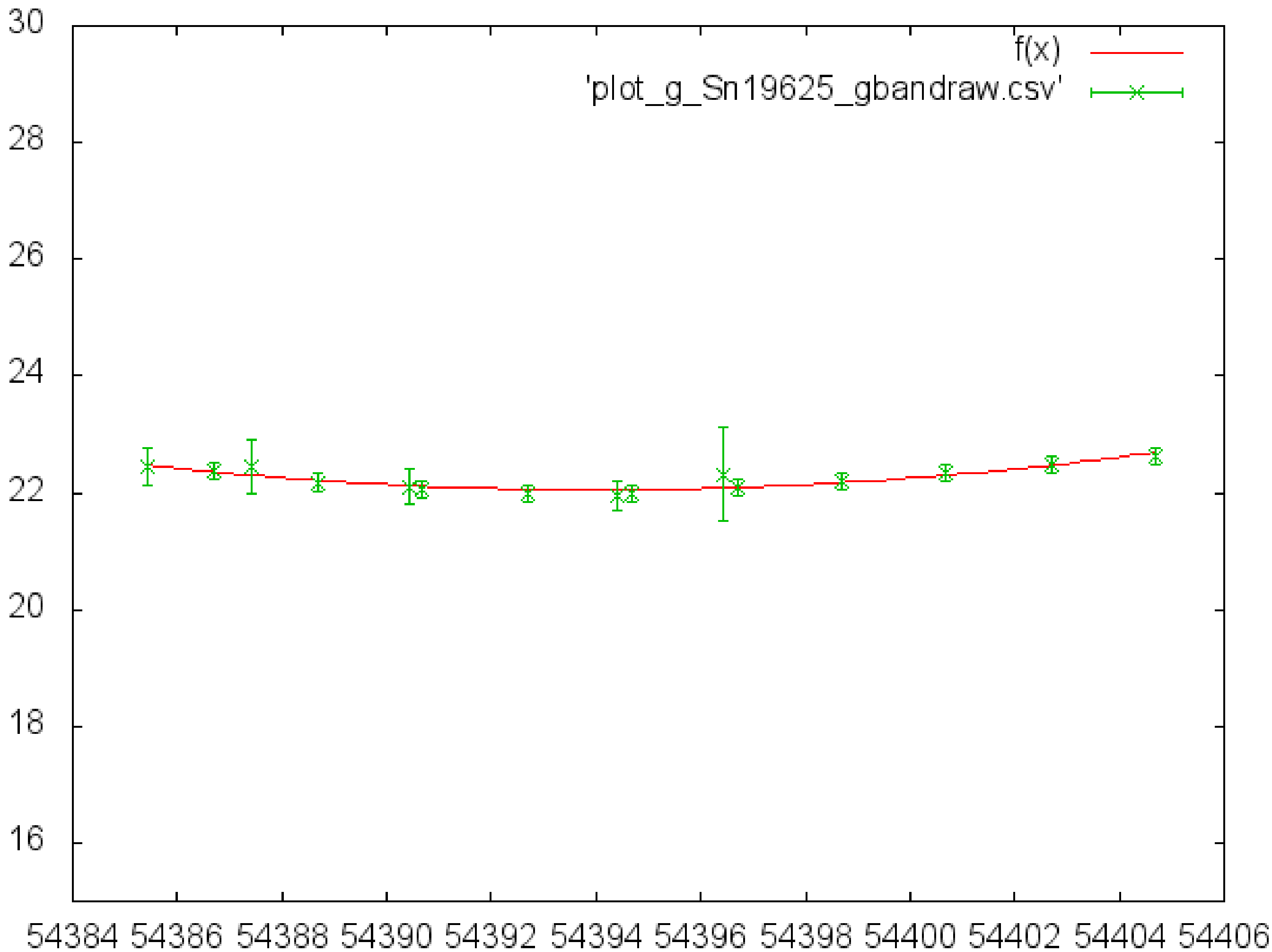

30
28
26
24
22
20
18
16
54384
54386
54388
54390
54392
54394
54396
54398
54400
54402
54404
54406
f(x)
'plot_g_Sn19625_gbandraw.csv'

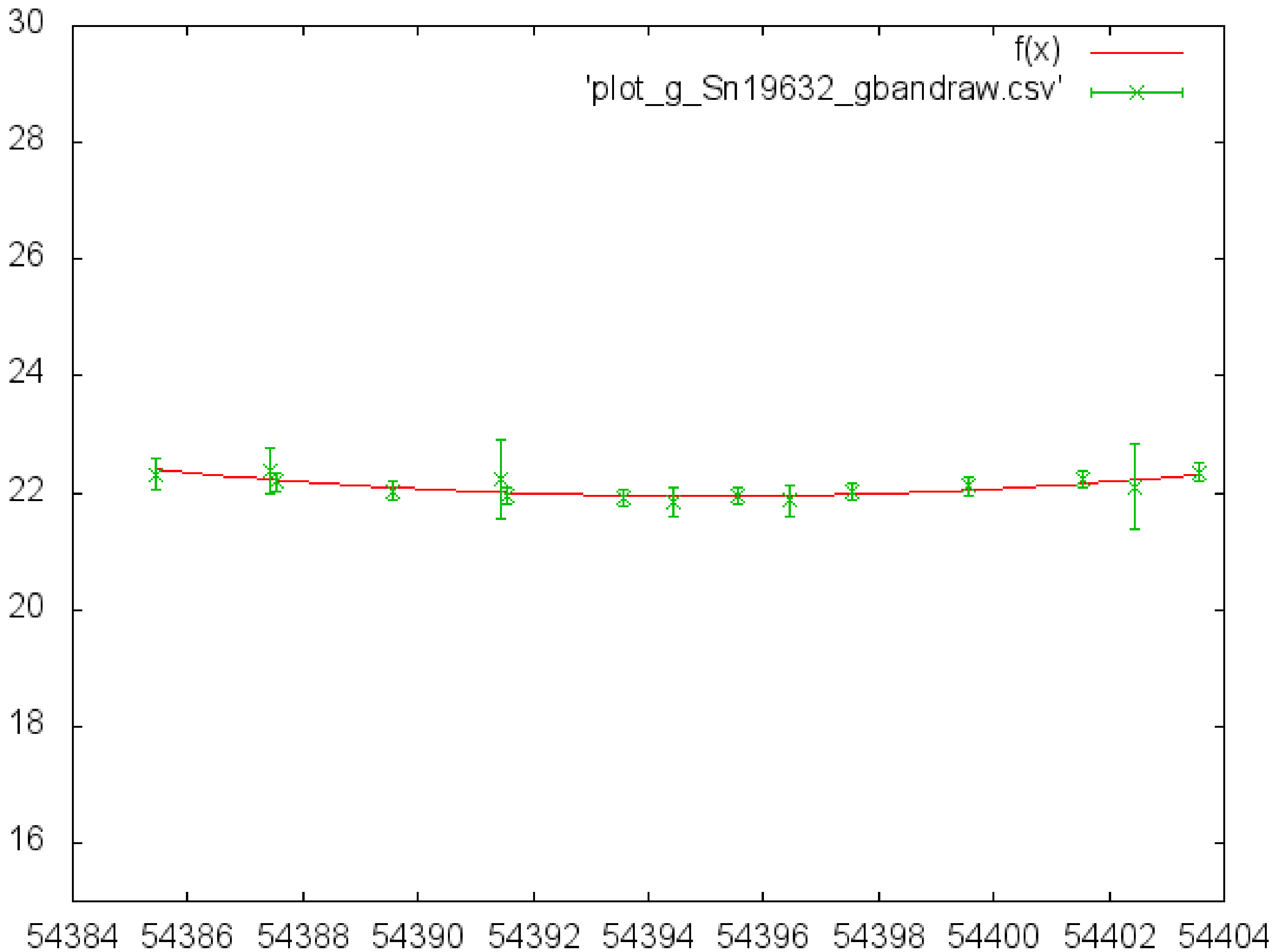

30
28
26
24
22
20
18
16
54384
54386
54388
54390
54392
54394
54396
54398
54400
54402
54404
f(x)
'plot_g_Sn19632_gbandraw.csv'

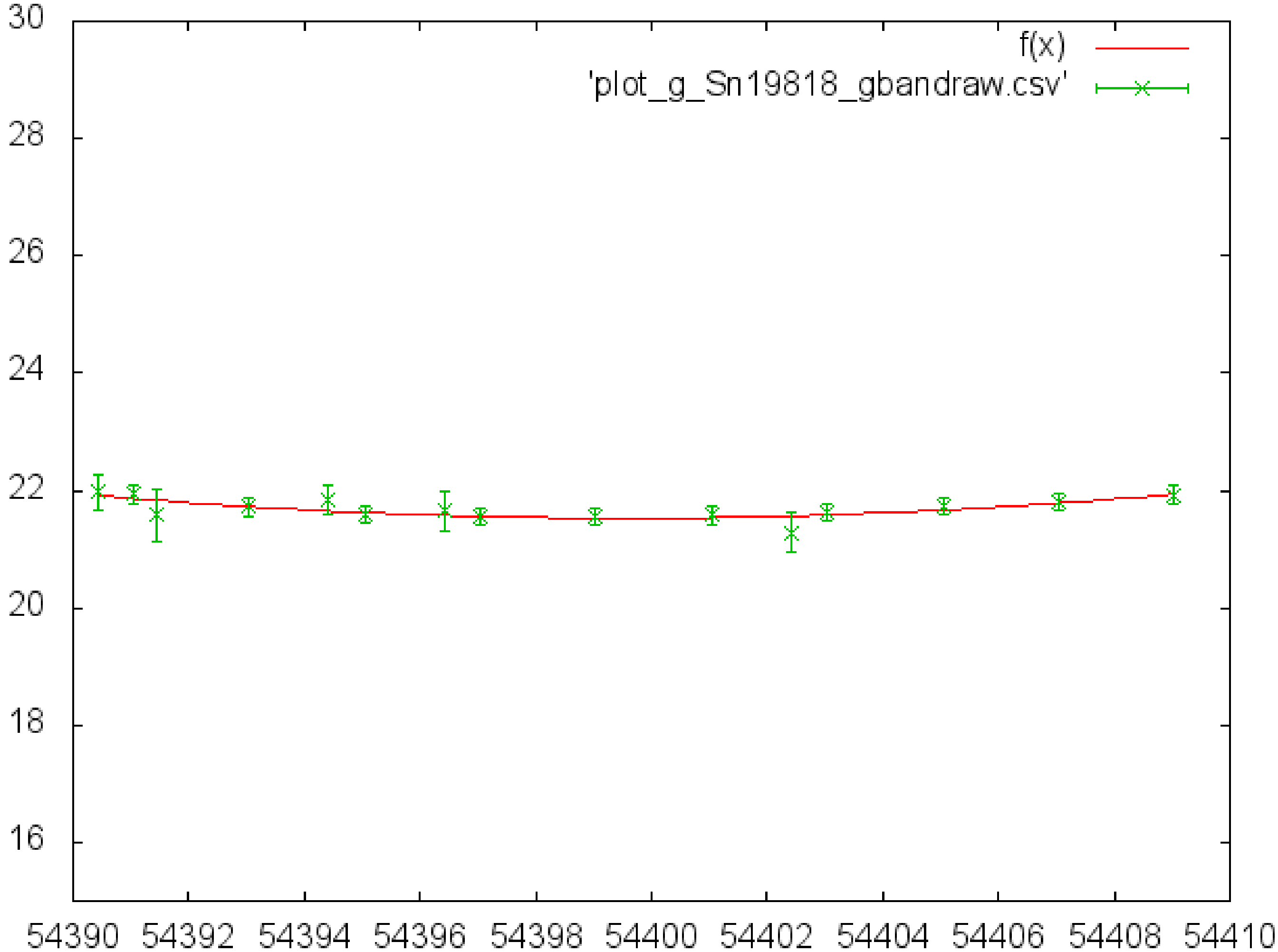

f(x)
'plot_g_Sn19818_gbandraw.csv'
30
28
26
24
22
20
18
16
54390
54392
54394
54396
54398
54400
54402
54404
54406
54408
54410

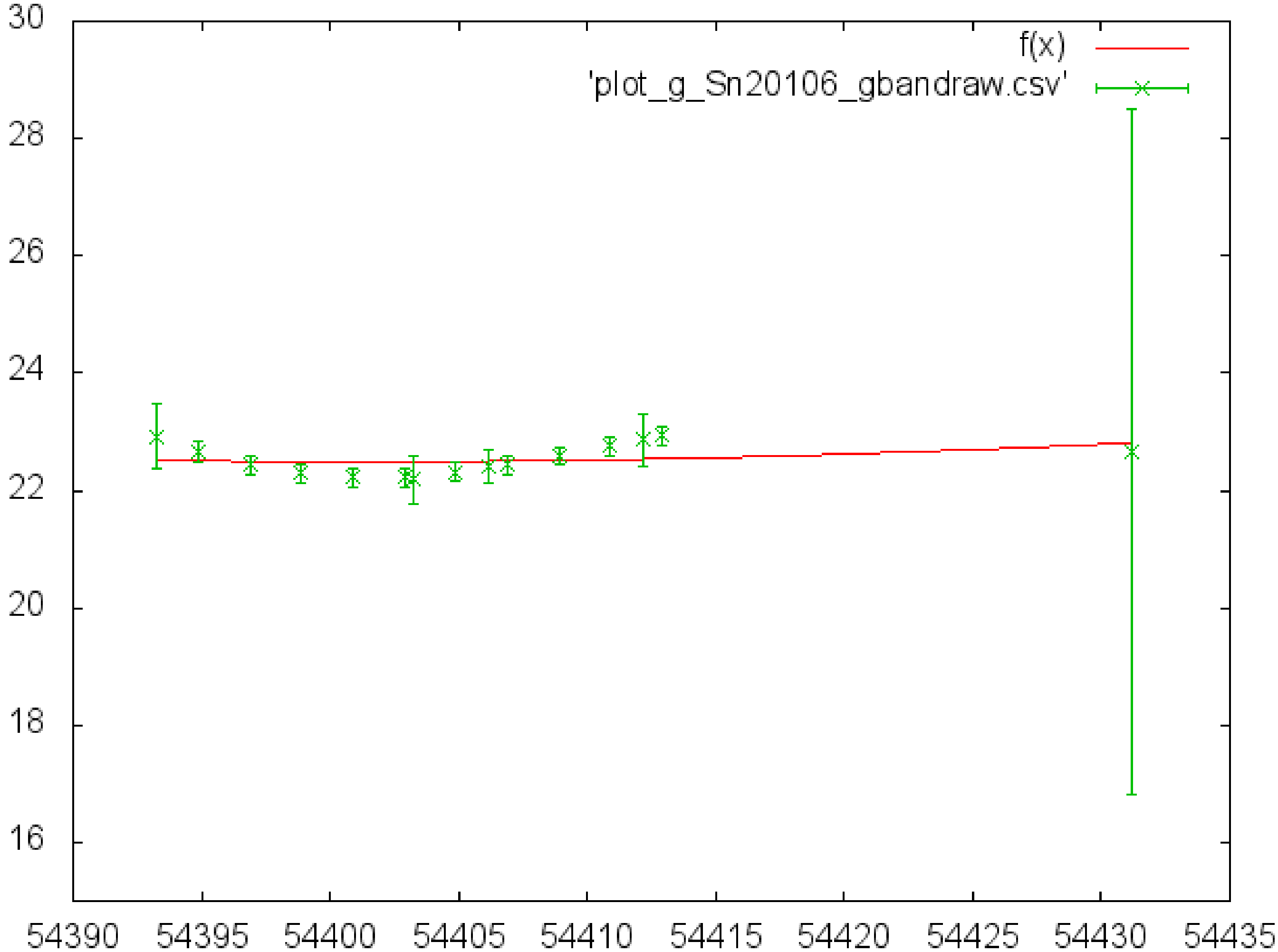

30
28
26
24
22
20
18
16
54390
54395
54400
54405
54410
54415
54420
54425
54430
54435
f(x)
'plot_g_Sn20106_gbandraw.csv'

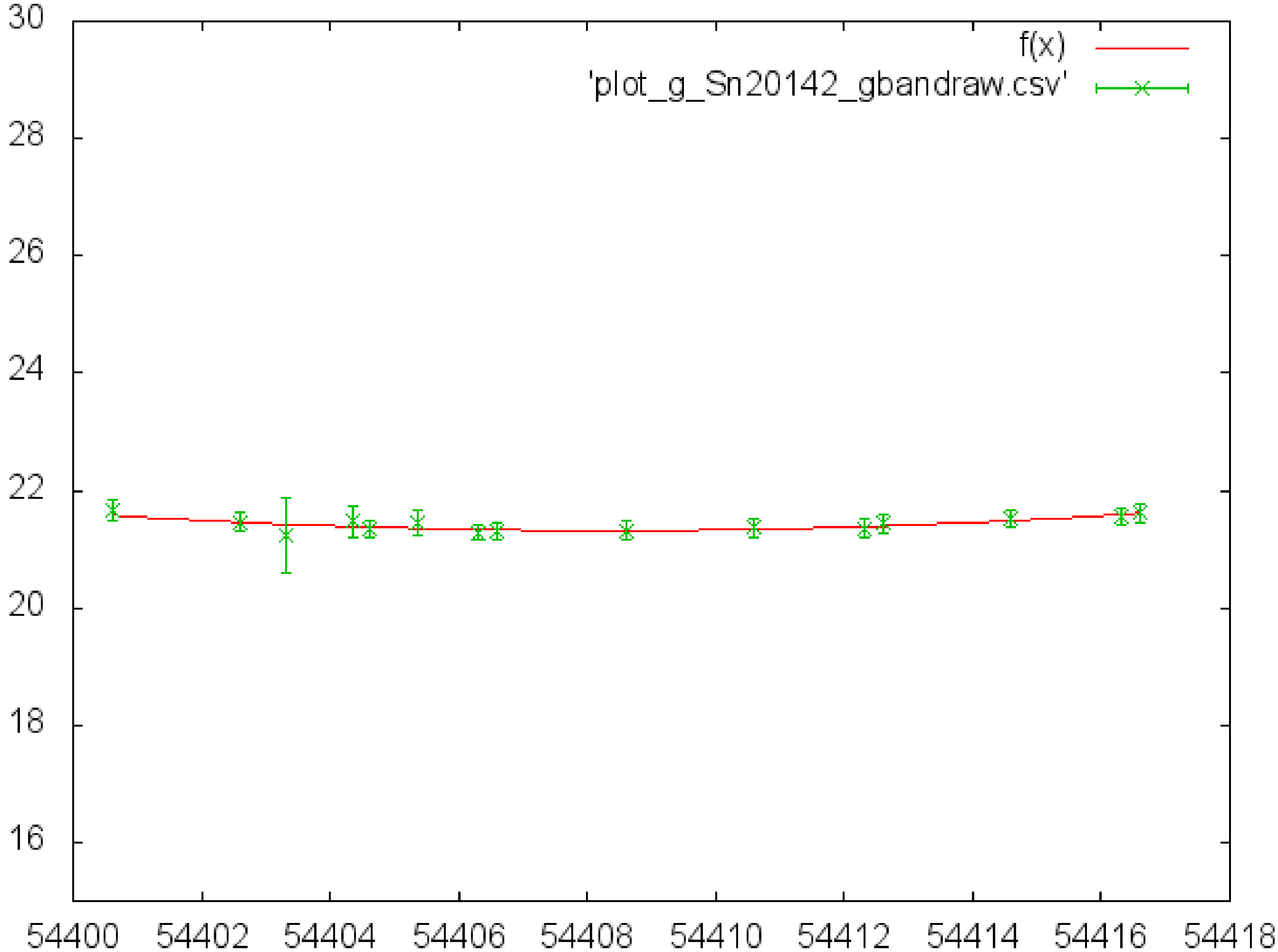

f(x)
'plot_g_Sn20142_gbandraw.csv'
30
28
26
24
22
20
18
16
54400
54402
54404
54406
54408
54410
54412
54414
54416
54418

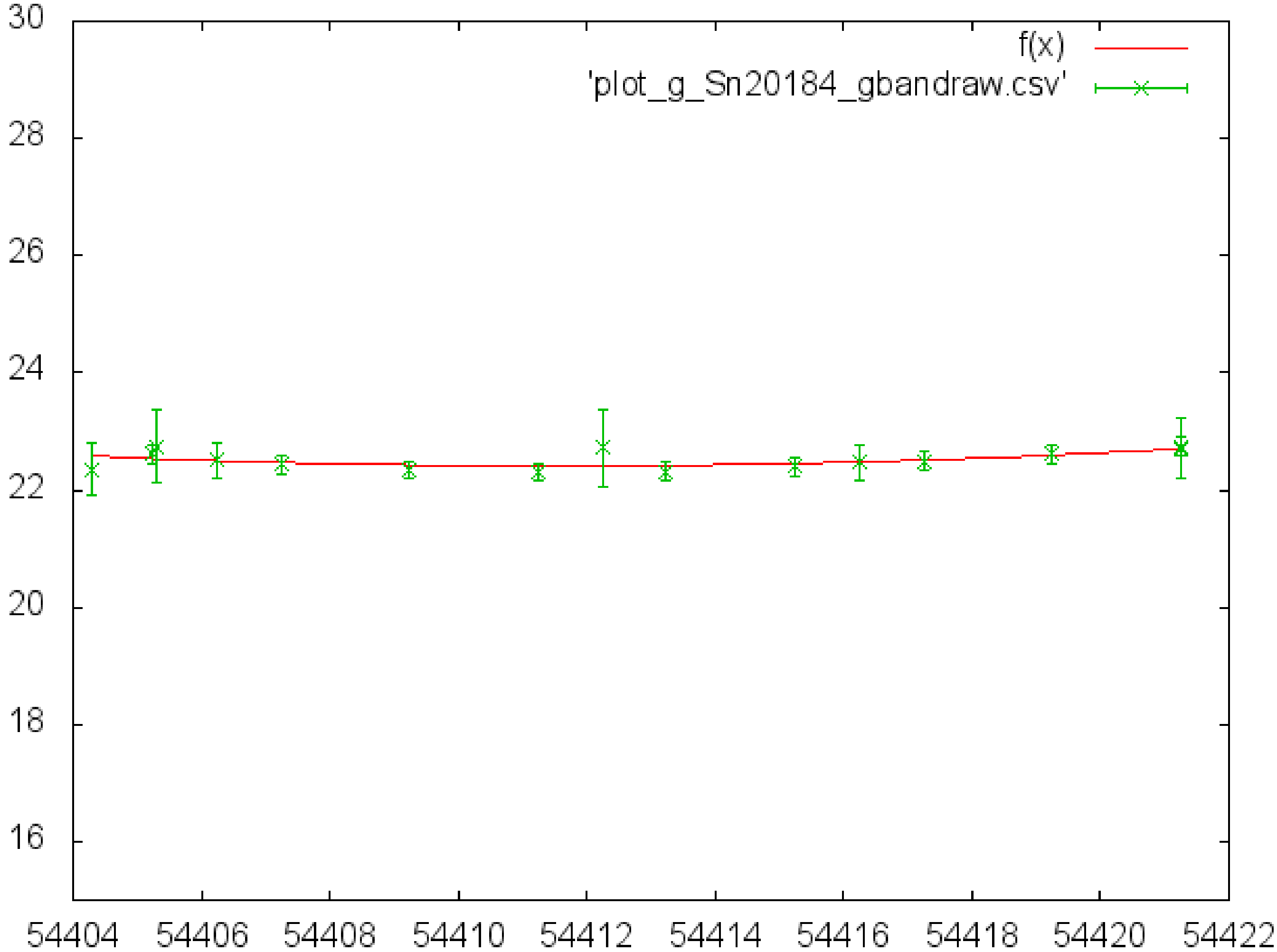

f(x)
'plot_g_Sn20184_gbandraw.csv'
30
28
26
24
22
20
18
16
54404
54406
54408
54410
54412
54414
54416
54418
54420
54422

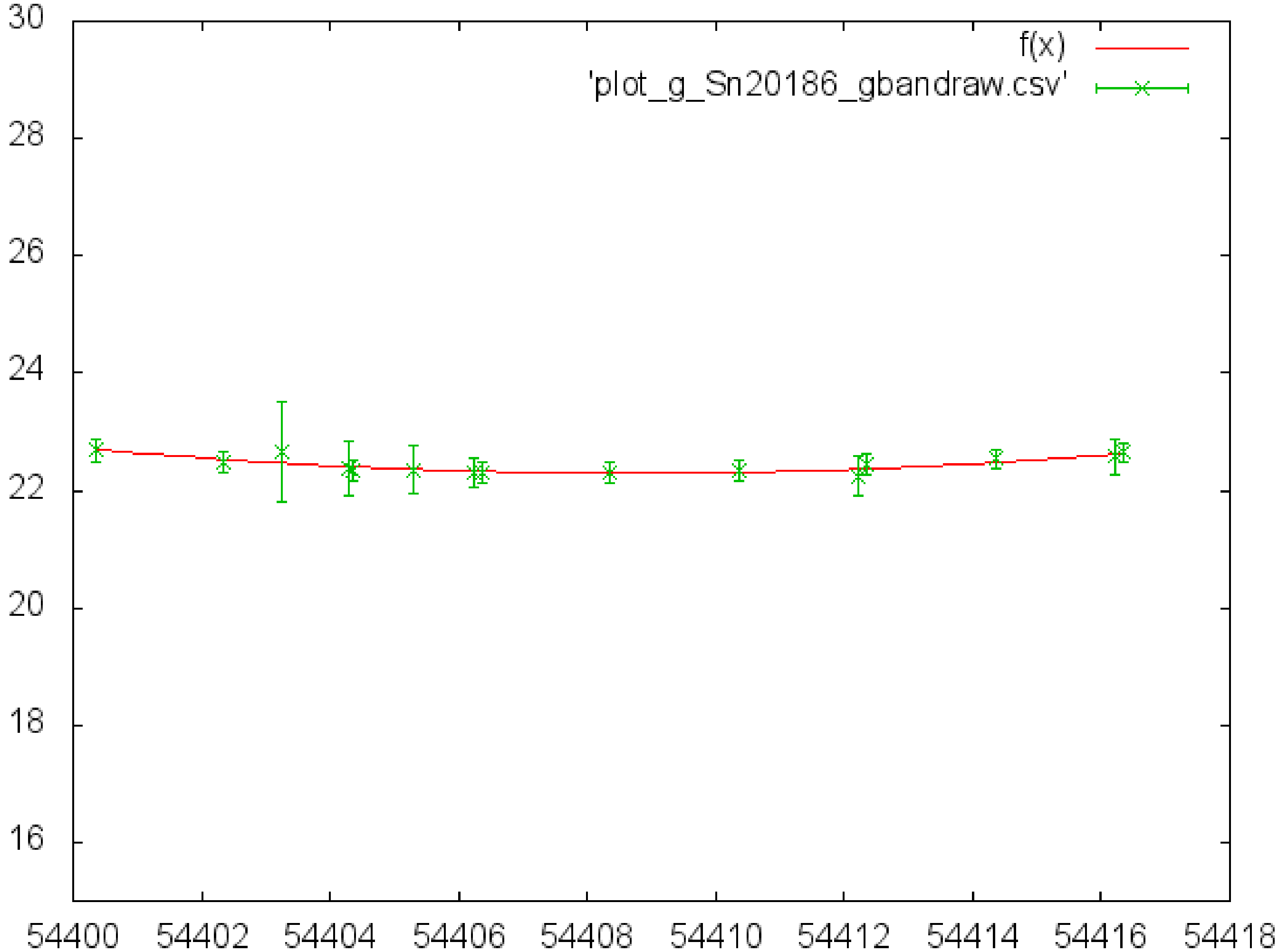
30
28
26
24
22
20
18
16
f(x)
'plot_g_Sn20186_gbandraw.csv'
54400
54402
54404
54406
54408
54410
54412
54414
54416
54418

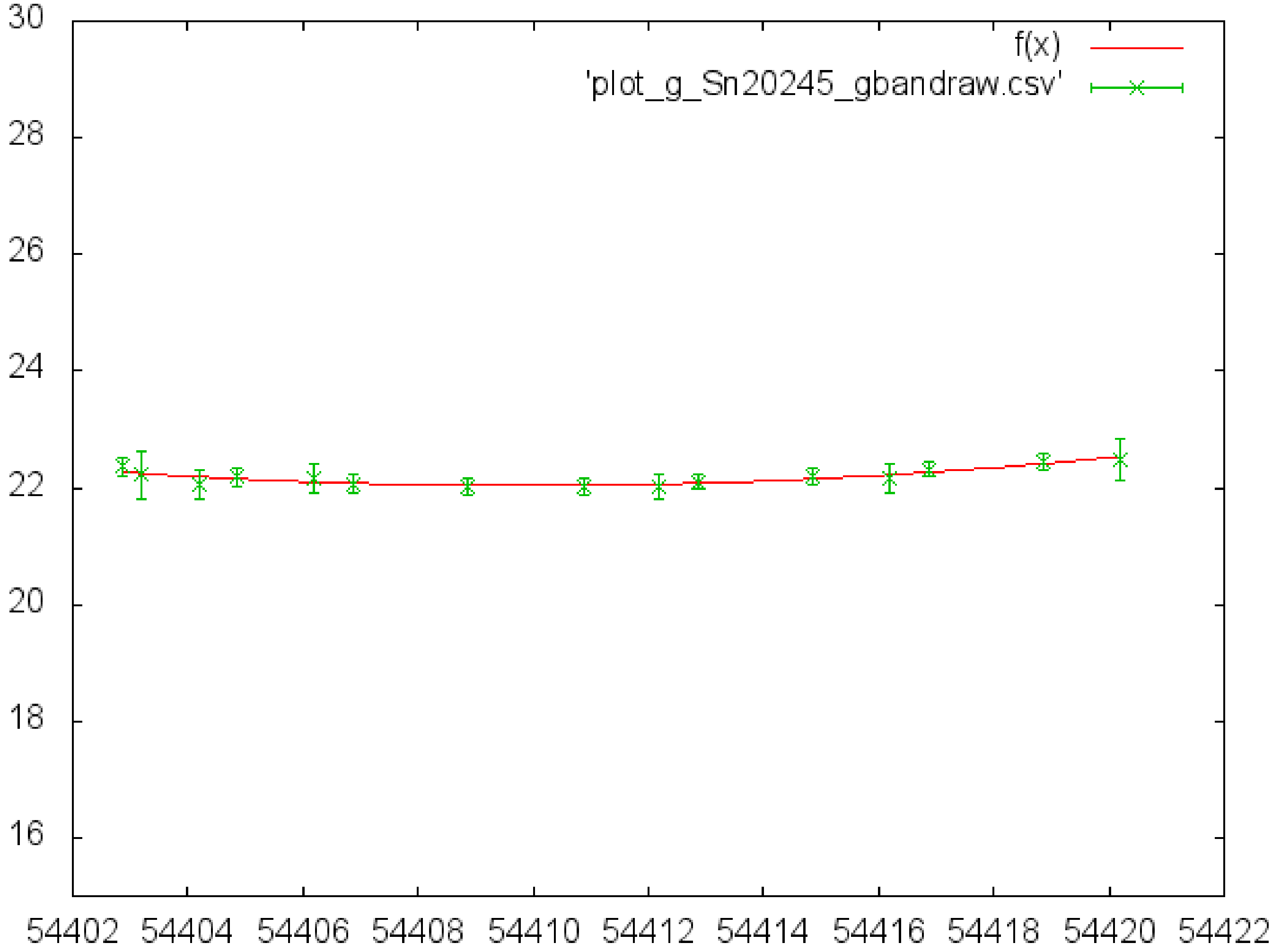

f(x)
'plot_g_Sn20245_gbandraw.csv'
30
28
26
24
22
20
18
16
54402
54404
54406
54408
54410
54412
54414
54416
54418
54420
54422

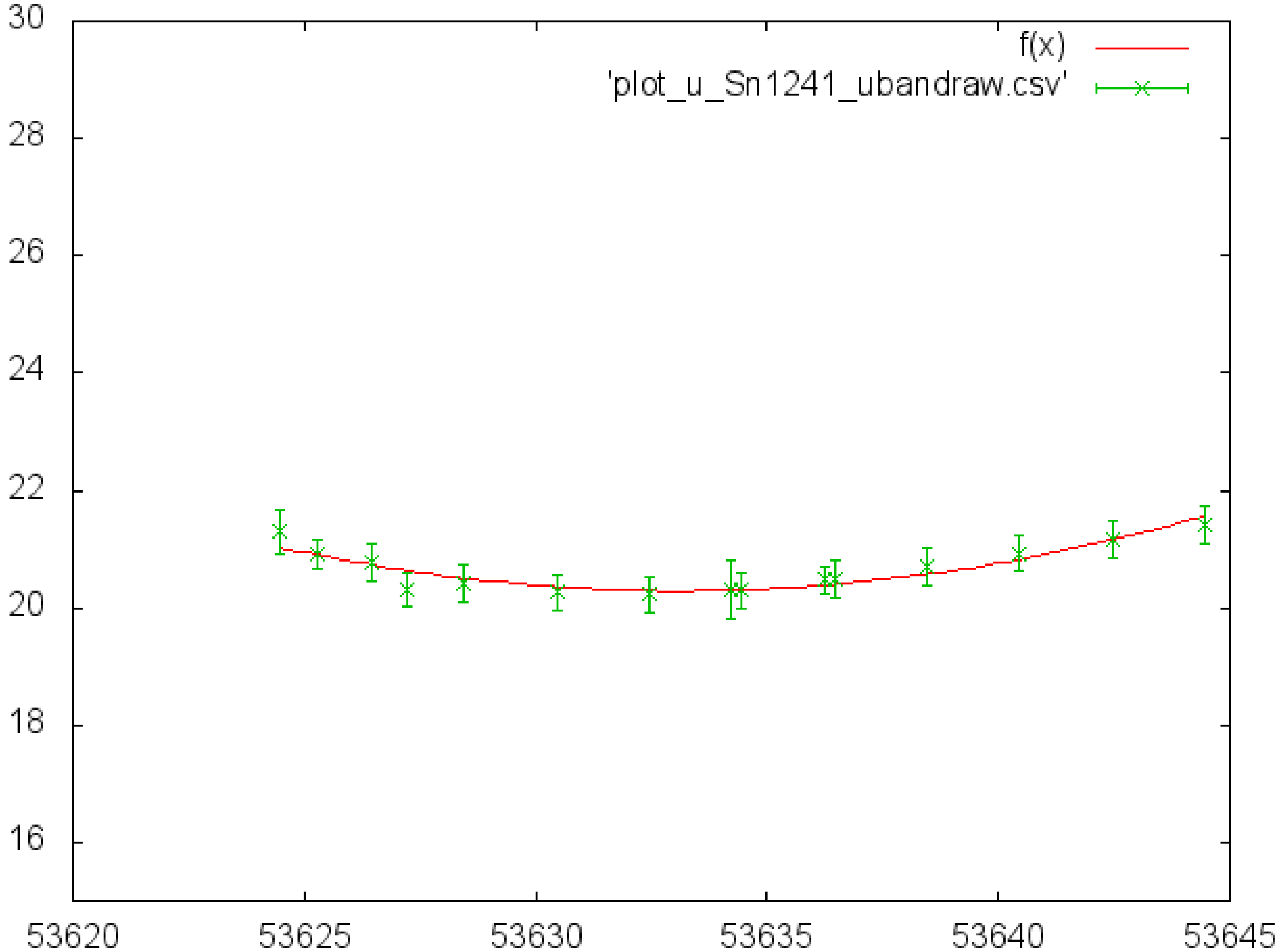

f(x)
'plot_u_Sn1241_ubandraw.csv'
30
28
26
24
22
20
18
16
53620
53625
53630
53635
53640
53645

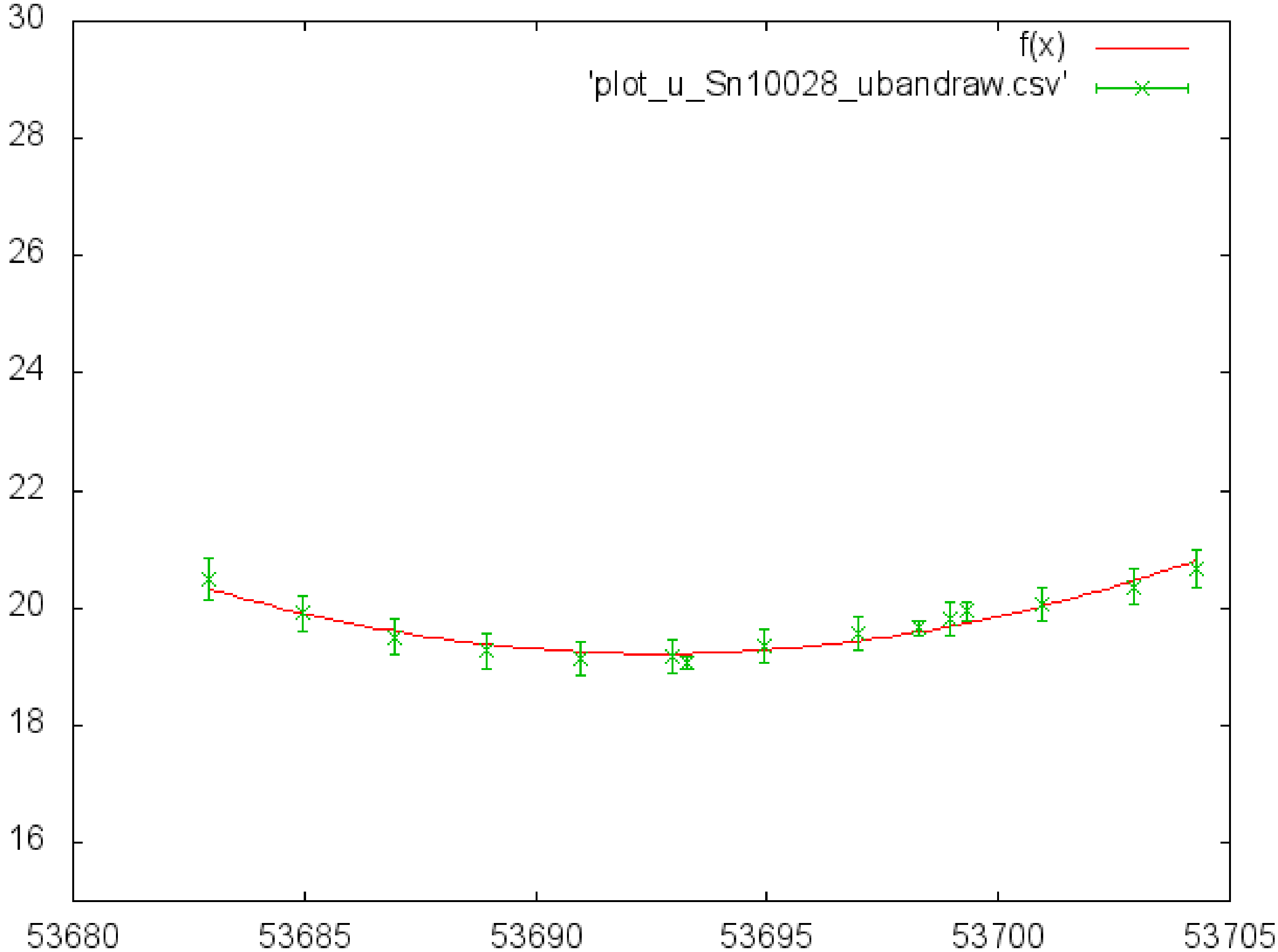

f(x)
'plot_u_Sn10028_ubandraw.csv'
30
28
26
24
22
20
18
16
53680
53685
53690
53695
53700
53705

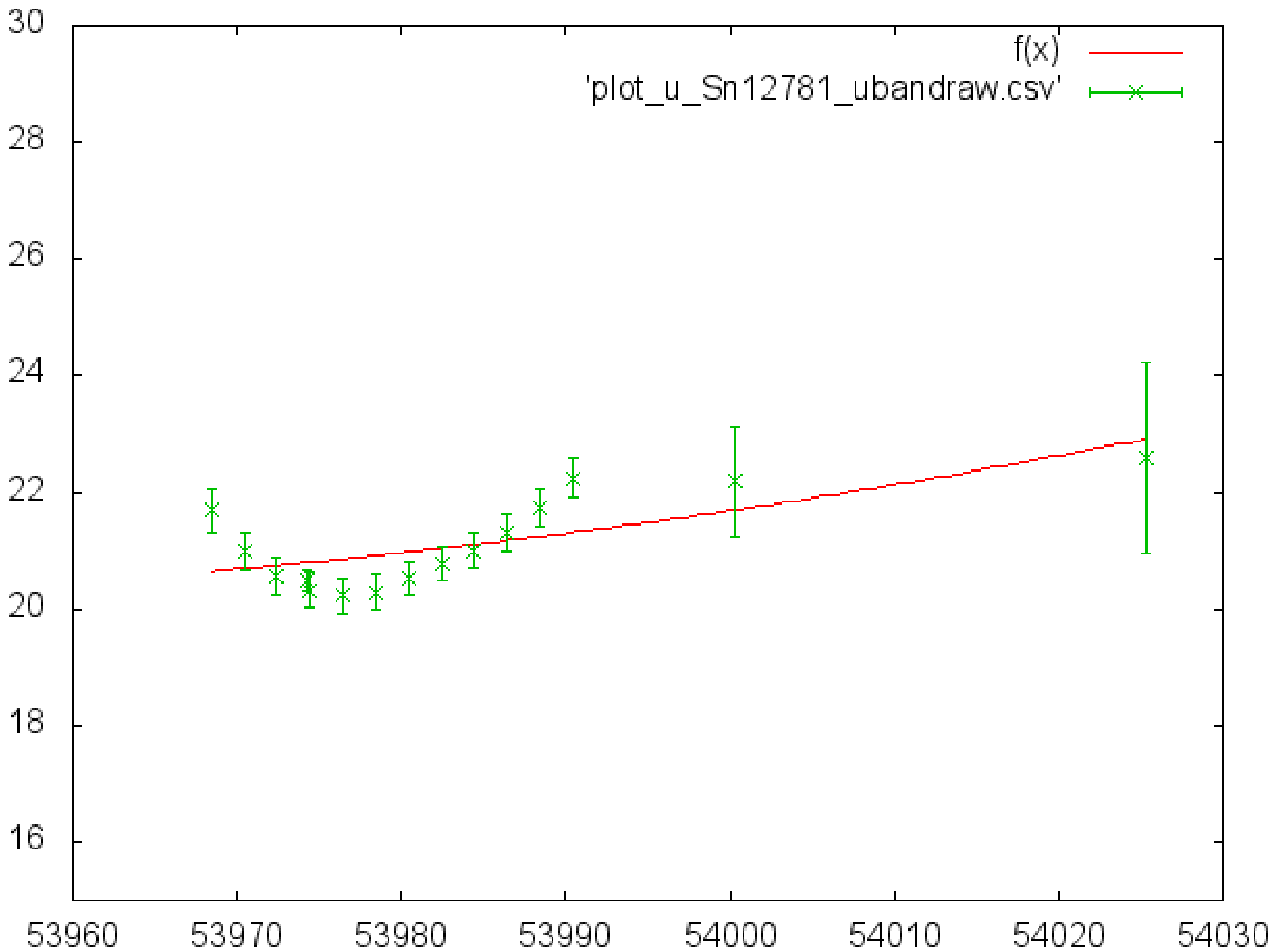

f(x)
'plot_u_Sn12781_ubandraw.csv'
30
28
26
24
22
20
18
16
53960
53970
53980
53990
54000
54010
54020
54030

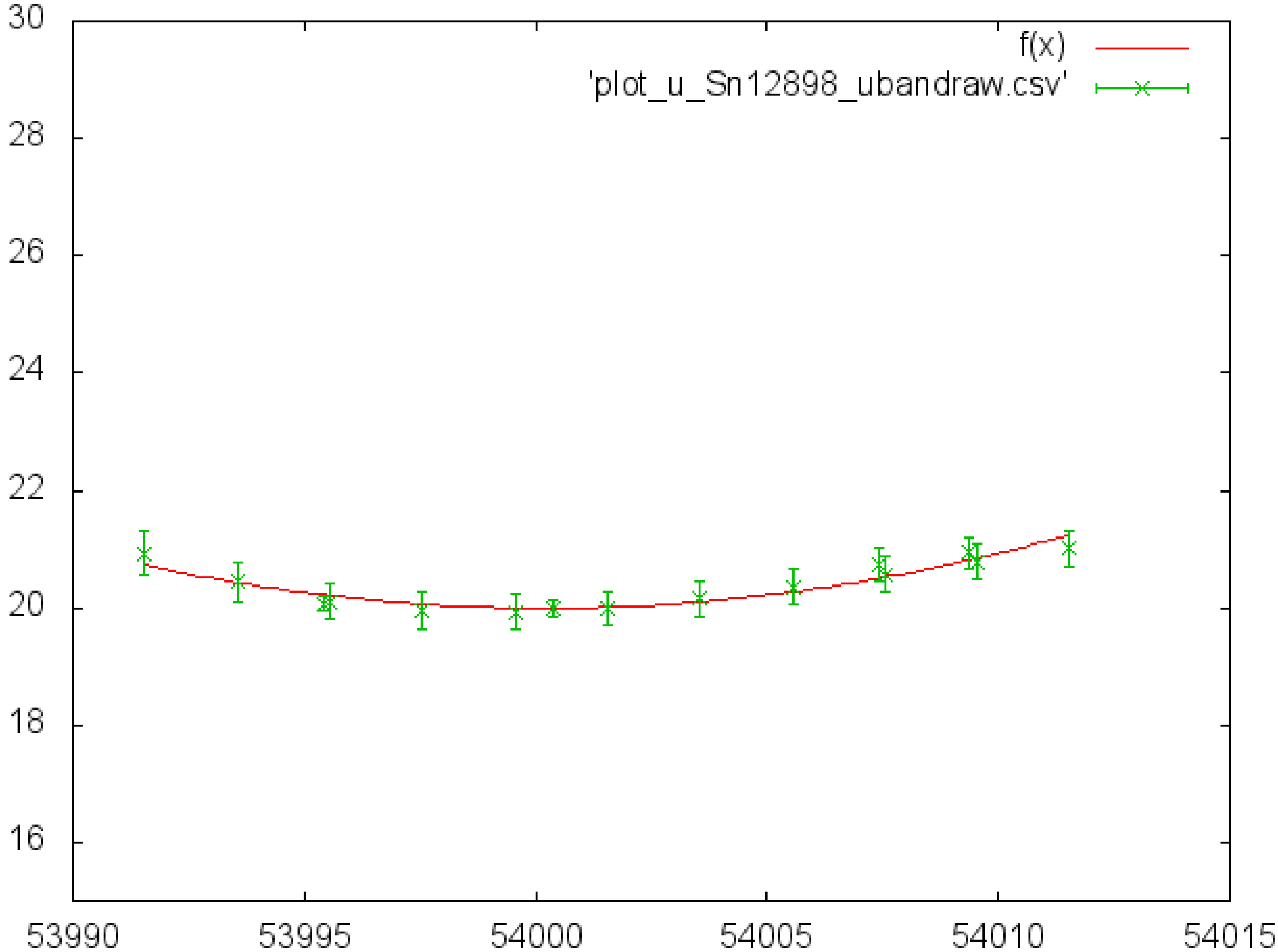

30
28
26
24
22
20
18
16
53990
53995
54000
54005
54010
54015
f(x)
'plot_u_Sn12898_ubandraw.csv'

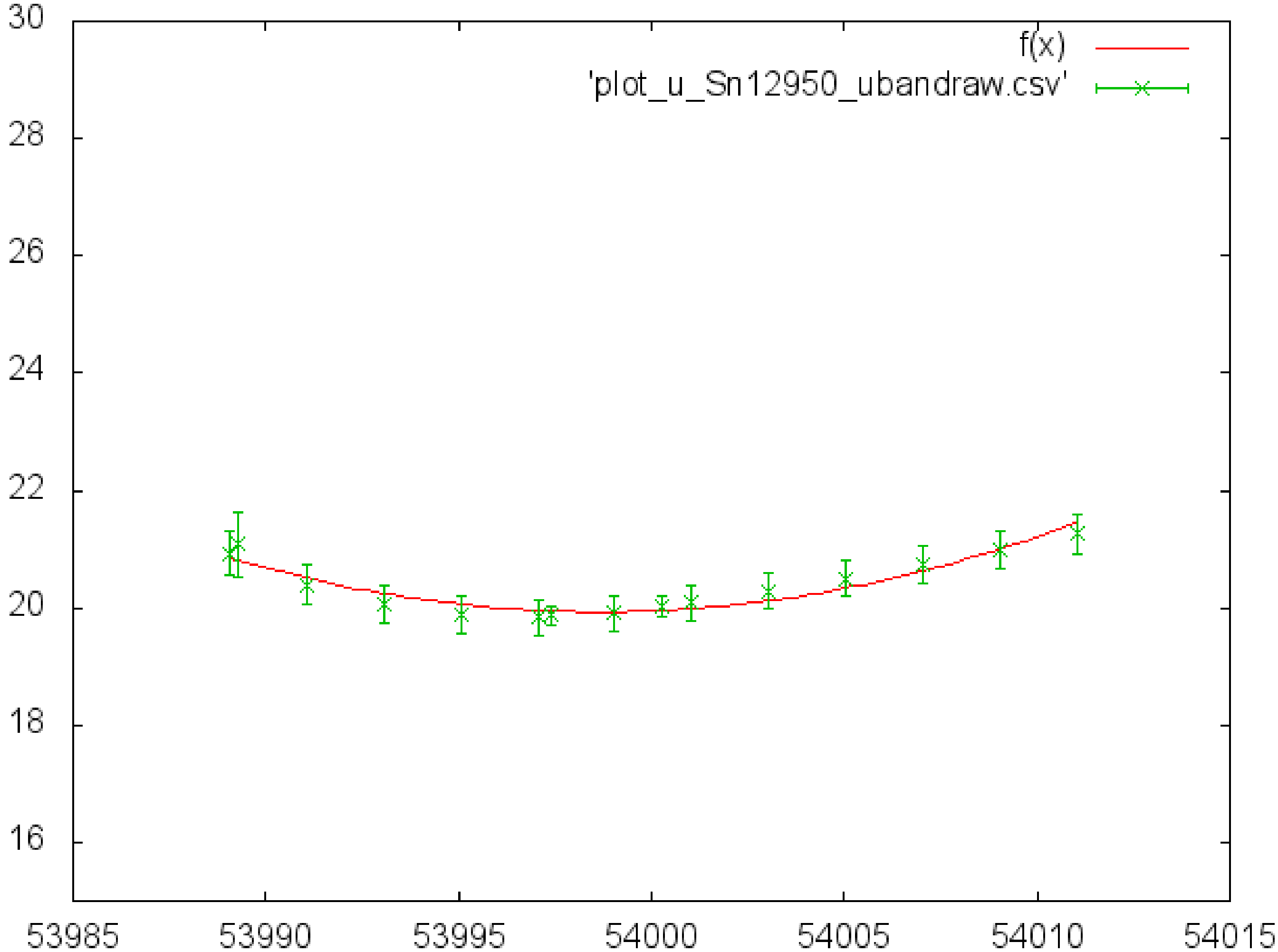
f(x)
'plot_u_Sn12950_ubandraw.csv'
30
28
26
24
22
20
18
16
53985
53990
53995
54000
54005
54010
54015

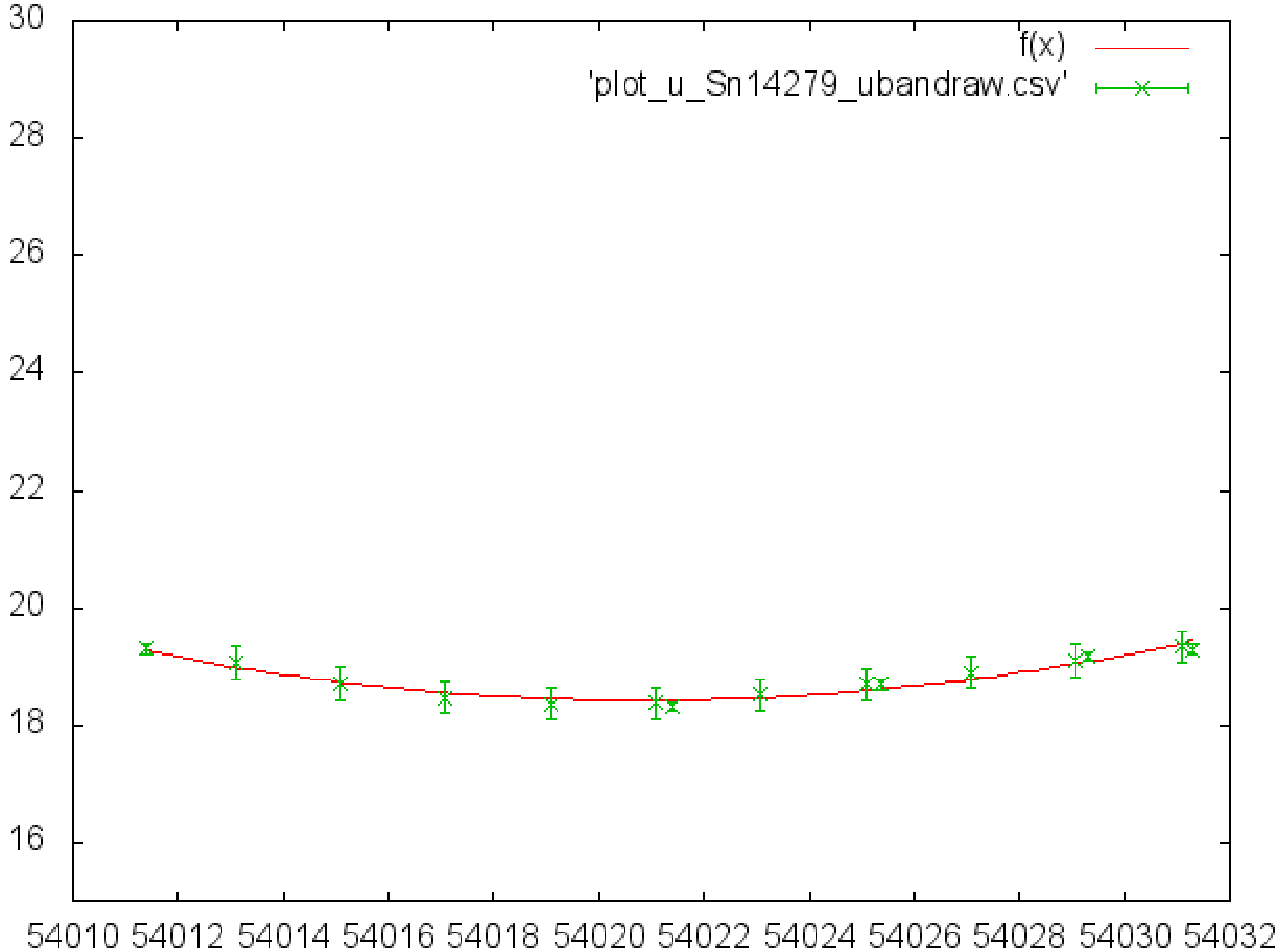

f(x)
'plot_u_Sn14279_ubandraw.csv'
30
28
26
24
22
20
18
16
54010 54012 54014 54016 54018 54020 54022 54024 54026 54028 54030 54032

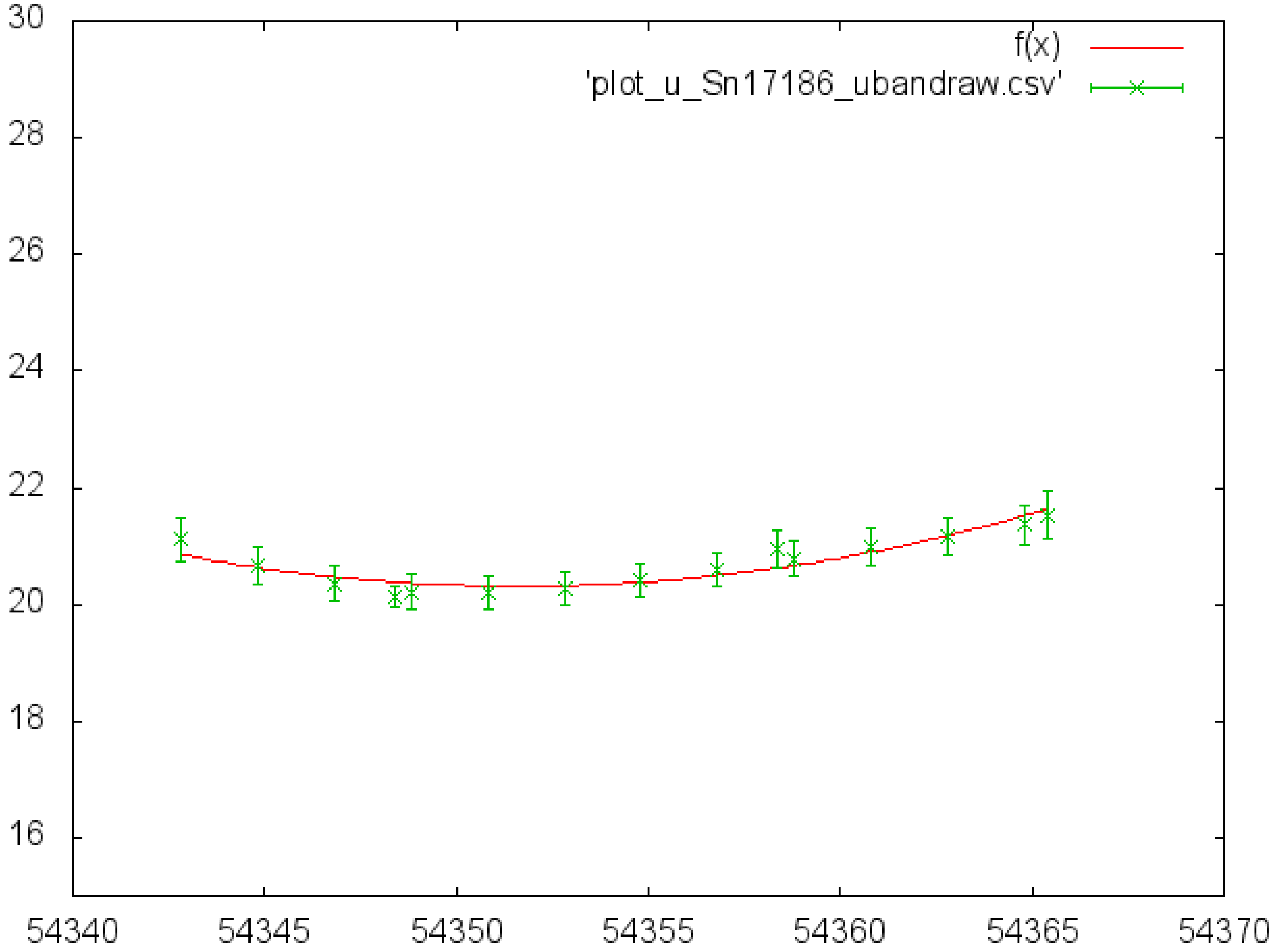
f(x)
'plot_u_Sn17186_ubandraw.csv'
30
28
26
24
22
20
18
16
54340
54345
54350
54355
54360
54365
54370

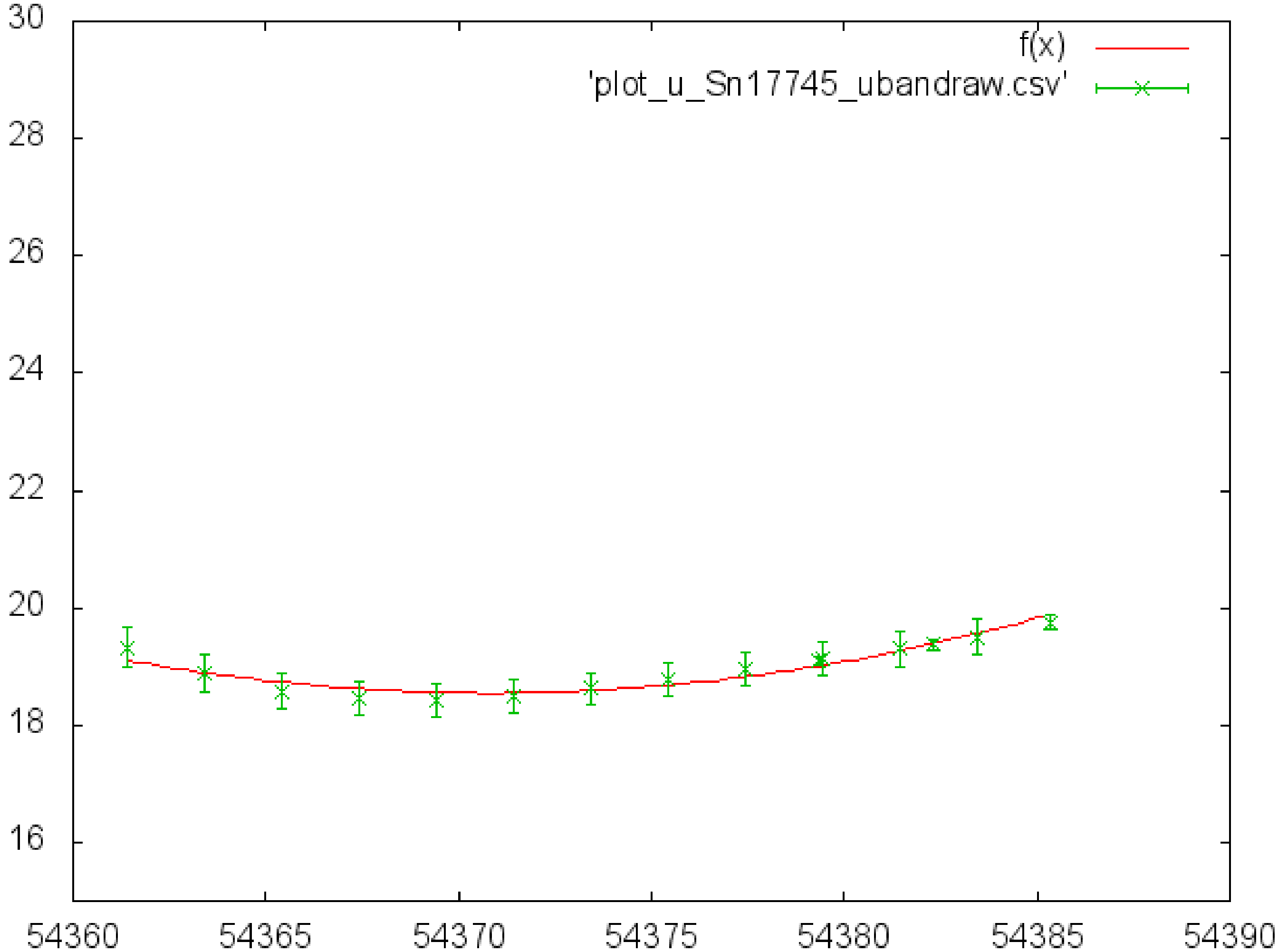
f(x)
'plot_u_Sn17745_ubandraw.csv'
30
28
26
24
22
20
18
16
54360
54365
54370
54375
54380
54385
54390

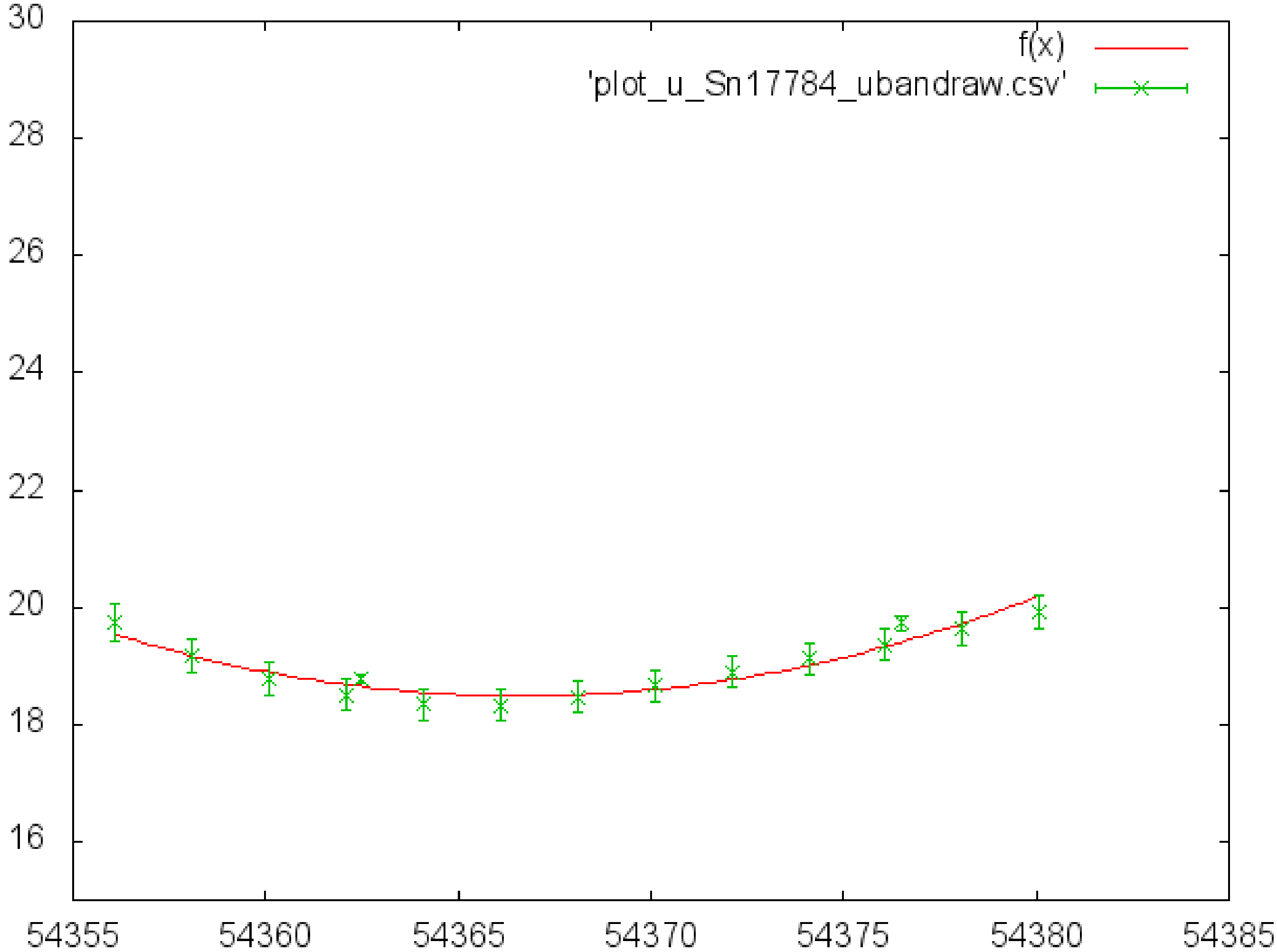
30
28
26
24
22
20
18
16
54355
54360
54365
54370
54375
54380
54385
f(x)
'plot_u_Sn17784_ubandraw.csv'

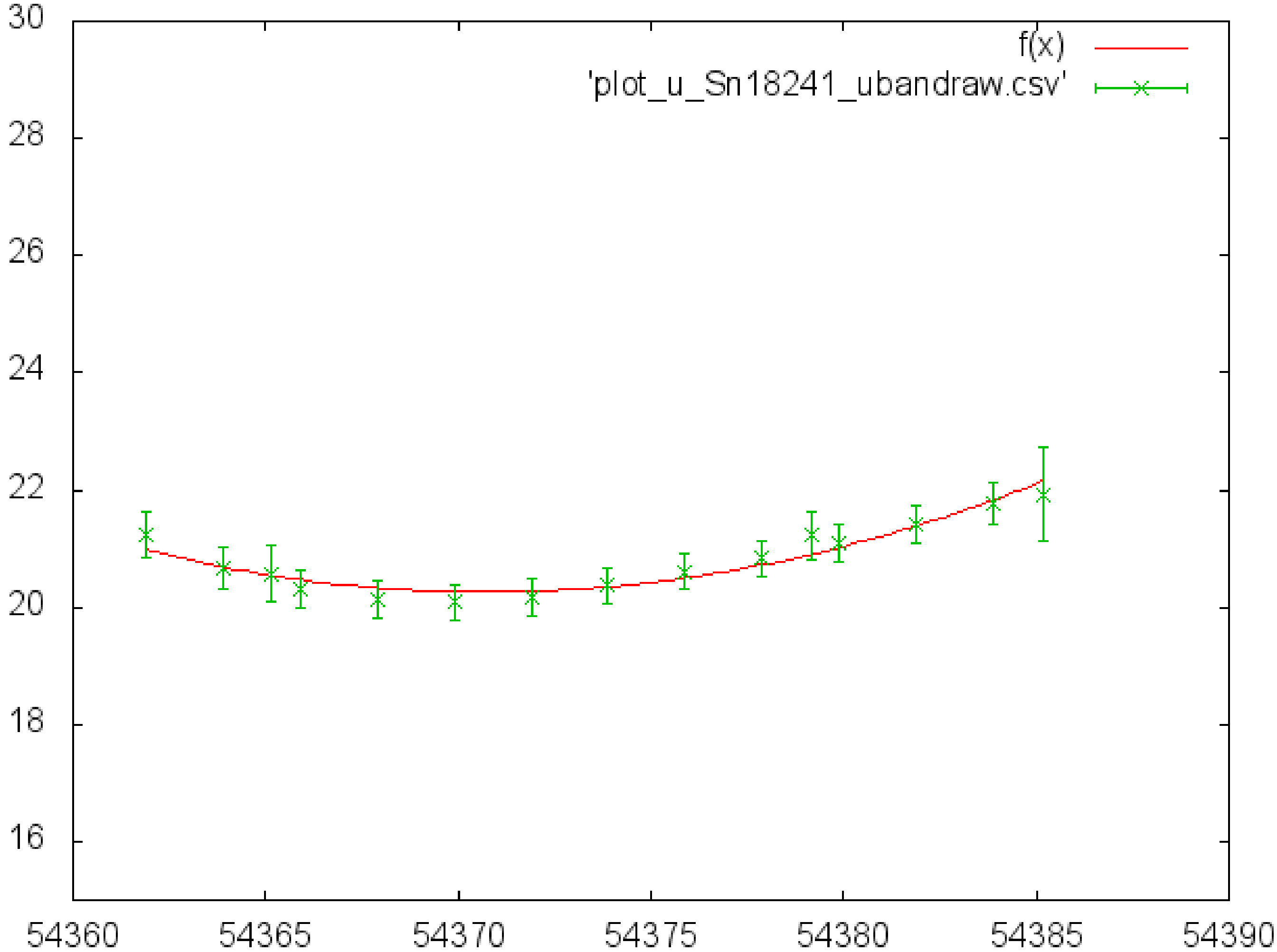

30
28
26
24
22
20
18
16
54360
54365
54370
54375
54380
54385
54390
f(x)
'plot_u_Sn18241_ubandraw.csv'

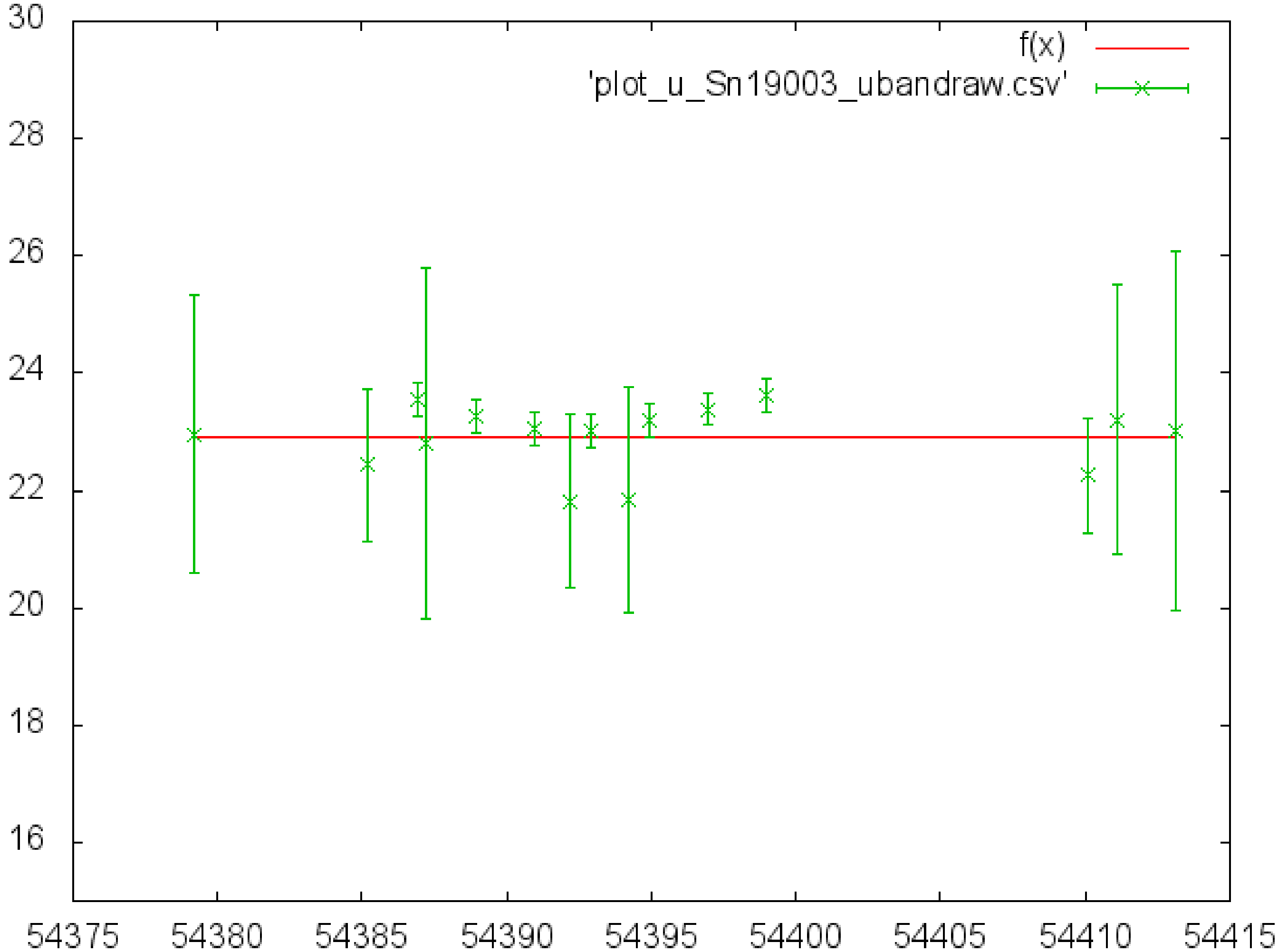
30
28
26
24
22
20
18
16
54375
54380
54385
54390
54395
54400
54405
54410
54415
f(x)
'plot_u_Sn19003_ubandraw.csv'

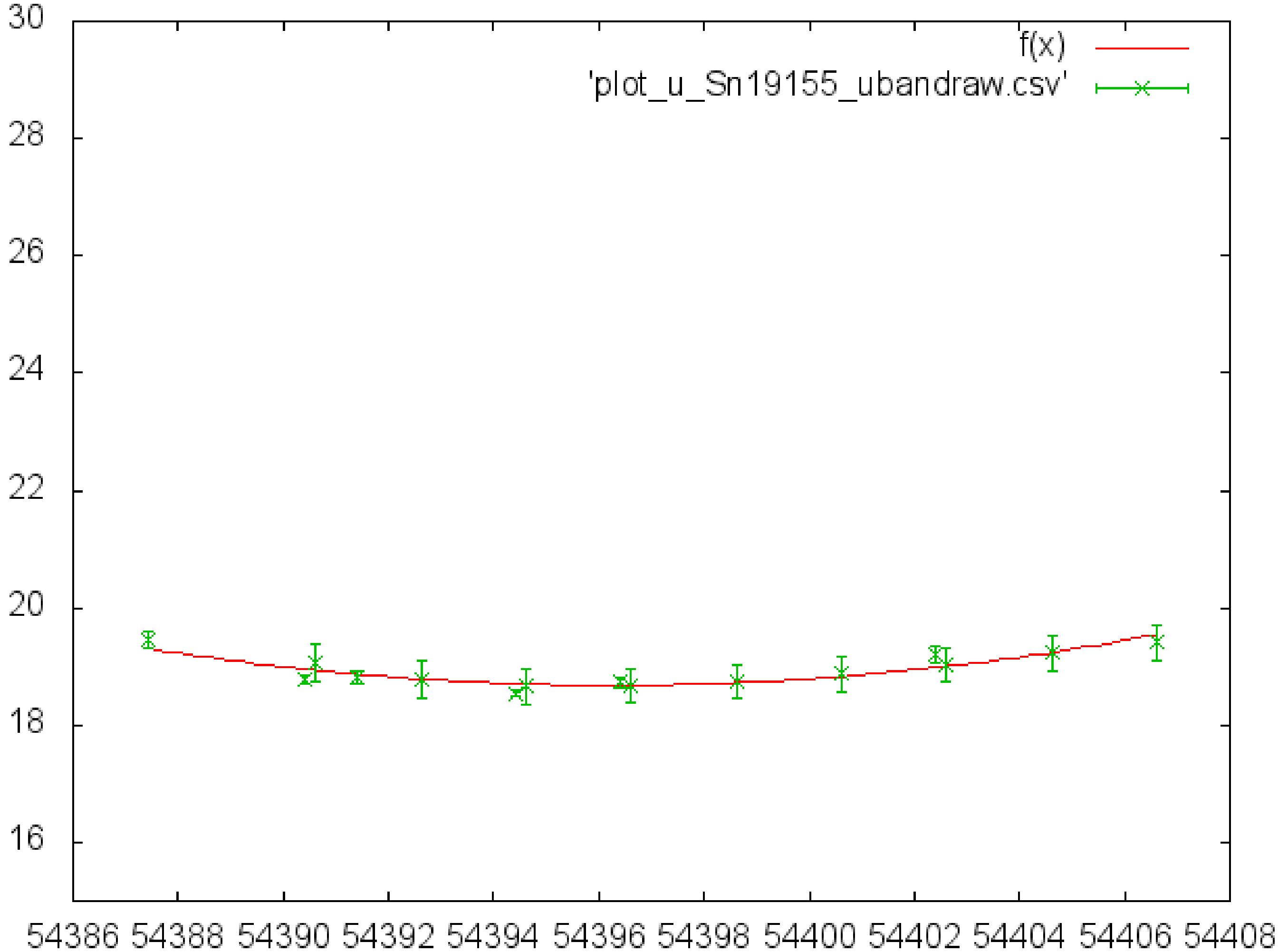

f(x)
'plot_u_Sn19155_ubandraw.csv'
30
28
26
24
22
20
18
16
54386 54388 54390 54392 54394 54396 54398 54400 54402 54404 54406 54408

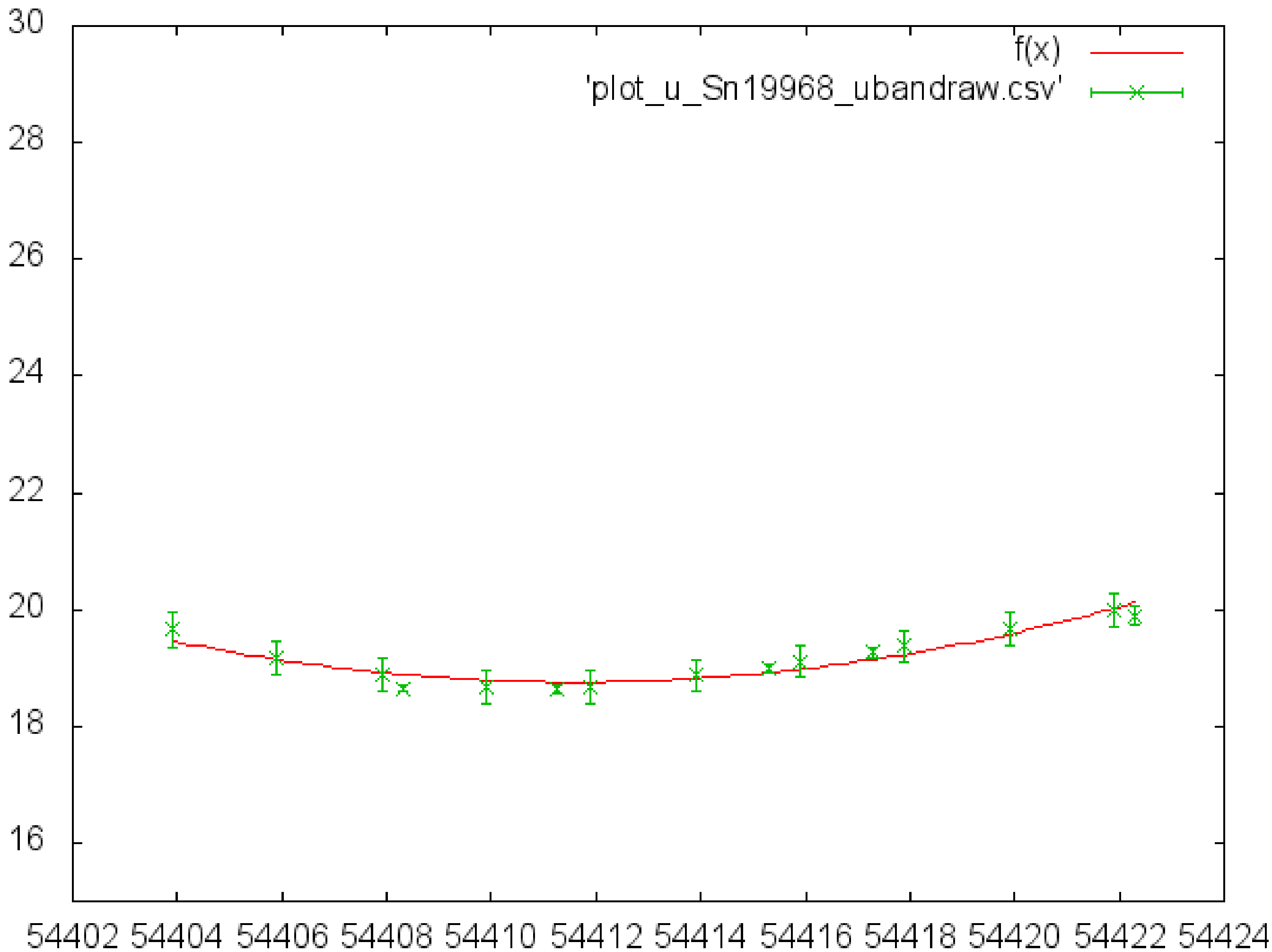
30
28
26
24
22
20
18
16
f(x)
'plot_u_Sn19968_ubandraw.csv'
54402 54404 54406 54408 54410 54412 54414 54416 54418 54420 54422 54424